But that man who sets himself the task of singling out the thread of order from the tapestry will by the decision alone have taken charge of the world and it is only by such taking charge that he will effect a way to dictate the terms of his own fate.

— Cormac McCarthy, Blood Meridian, or the Evening Redness in the West

Okay, well, sometimes science is more art than science, Morty.

— Rick, *Rick and Morty*, "Rick Potion #9"

Promoters

Prof. dr. ir. Korneel Rabaey

Department of Biochemical and Microbial Technology, Faculty of Bioscience Engineering, Ghent University, Gent, Belgium

Dr. Xochitl Dominguez-Benetton

Flemish Institute for Technological Research / Vlaamse Instelling voor Technologisch Onderzoek (VITO), Mol, Belgium

Members of the examination committee

Prof. dr. Colin Janssen
Chairman
Faculty of Bioscience Engineering, Ghent University; Belgium

Prof. dr. ir. Arne Verliefde
Secretary
Faculty of Bioscience Engineering, Ghent University; Belgium

Prof. dr. ir. Eveline Volcke
Faculty of Bioscience Engineering, Ghent University; Belgium

Prof. Bruce Logan
Department of Civil and Envrionmental Engineering, The Pennsylvania State University; The United States

Prof. dr. Ir. Cees Buisman
Wetsus & Department of Agrotechnology and Food Sciences,Wageningen University; The Netherlands

Dean:

Prof. dr. ir. Marc Van Meirvenne

Rector:

Prof. dr. Anne De Paepe

Electrochemical extraction, recovery and valorization of carboxylic acids from biorefineries

Stephen John Andersen

Thesis submitted in fulfillment of the requirements for the degree of Doctor (PhD) in Applied Biological Sciences

Department of Biochemical and Microbial Technology,
Faculty of Bioscience Engineering, Ghent University, Ghent, Belgium

Cover illustration by Alessia Landi

Titel van het doctoraat in het Nederlands:

Elektrochemische extractie, recuperatie en valorisatie van carbonzuren van bioraffinaderijen

Andersen SJ, Electrochemical extraction, recovery and valorization of carboxylic acids from biorefineries, PhD thesis, **2016**, Ghent University, Belgium

ISBN: 978-90-5989-936-0

This work was supported by the European Union Framework Programme 7 project "ProEthanol 2G" and the Ghent University Multidisciplinary Research Partnership (MRP)—Biotechnology for a sustainable economy (01 MRA 510 W)

Dedicated to my father

Abbreviations

AD	Anaerobic Digestion
AEM	Anion Exchange Membrane
-CoA	-coenzyme A, *e.g.* Acetyl-CoA, a common metabolic intermediate
COD/sCOD/tCOD	chemical oxygen demand / soluble - / total -
CPE	constant phase element
Cx to Cy	VFA carbon chain length, *e.g.* C2 = acetic acid, C6 = hexanoic acid
DDGS	Dried Distillers Grains & Solubles
EDL	electric double layer
EIS	Electrochemical Impedance Spectroscopy
gC	grams of carbon, *i.e.* 1 mol of Caproic (C6) Acid = 116.16 g = 6 × 12.01 gC = 72.06 gC
HRT	Hydraulic Retention Time
Ir MMO	Iridium mixed metal oxide
NAD^+/NADH	The oxidized/ reduced form of Nicotinamide Adenine Dinucleotide
OECD	The Organisation for Economic Co-operation and Development
OTU	Operational Taxonomic Unit
PCA	Principal co-ordinate analysis
PCR	Polymerase chain reaction
RDA	Redundancy Discriminant Analysis
SRT	Solids Retention Time

Notation Index & Terminology.

SCFA / MCFA	Short Chain Fatty Acids: linear, C1 to C5 saturated carboxylic acids; and Mid Chain Fatty Acids: linear, C6 to C10 saturated carboxylic acids
TSS	Total Suspended Solids
VFA*	Volatile Fatty Acids: linear saturated carboxylic acids

Notes:

*VFA is usually synonymous with SCFA, but this term is used in this thesis to encompass both SCFA and MCFA.

In this thesis the MCFA are expressed by the IUPAC name to avoid confusion between caproic, caprylic and capric acids, while the common name is used for the SCFA.

Electrochemical Impedance Spectroscopy terms

- Im (Z)	imaginary component of the impedance response, Ω
Re (Z)	real component of the impedance response, Ω
N	molar flux, mol m^{-2}
D	diffusion coefficient, m^2 s^{-1}
C	concentration, mol m^{-3}
z	charge number
μ_{mobi}	ionic mobility, s m^2 kg^{-1}
ϕ_l	electrolyte potential, V
u	fluid velocity vector, m s^{-1}
F	Faraday's constant, 96 485.3399 s A mol^{-1}
j	current density, A m^{-2}

Notation Index & Terminology.

j_{lim}	limiting current density, A m^{-2}
σ_l	electrolyte conductivity, S m^{-1}
t_i	transport number, dimensionless fraction of current carried by ions relative to total ions
δ	diffusion boundary layer thickness, m
U_{Tot}	total cell potential, V
R	gas constant, 8.3145 J mol^{-1} K^{-1}
Z_{Tot}	total impedance of the system, Ω
Z_{dif}	impedance (resistance) due to diffusion, Ω
Z_{ohm}	impedence (resistance) due to electrolyte diffusion, Ω
Z_{mig}	impedance (resistance) due to migration, Ω
Z_P	membrane polarization resistance, Ω
α	constant phase element parameter where $\alpha = 0$ is perfect resistor, and $\alpha = 1$ is a capacitor
Q	constant phase element parameter that represents the differential capacitance of the interface
ω	Angular frenquency, Hz
f	Frequency, Hz

Chain elongation equivalents calculation

Chain elongation equivalents: the grams of carbon (gC) required to convert C2 to C4 or longer, or C3 to C5 or longer on a simplified stoichiometric basis. For a compound C*x*, assumes C*n* + C2 → C(*n*+2), iterated until $n = x$, starting from n = 2 or 3.

i.e. 7.2 gC of C6 = 2.4 gC C2 + (2 × 2.4 gC), ∴ 4.8 gC of chain elongation equivalents

Table of Contents

Table of Contents

Table of Contents

Table of Contents

CHAPTER 1

Introduction

Adapted from:

Stephen J Andersen, Tom Hennebel, Sylvia Gildemyn, Marta Coma, Joachim Desloover, Jan Berton, Junko Tsukamoto, Christian Stevens and Korneel Rabaey, Electrolytic Membrane Extraction Enables Production of Fine Chemicals from Biorefinery Sidestreams; *Environmental Science & Technology,* **2014**; 48 (12), pp 7135–7142; DOI: 10.1021/es500483w

Stephen J Andersen, Pieter Candry, Thais Basadre, Way Cern Khor, Hugo Roume, Emma Hernandez Sanabria, Marta Coma and Korneel Rabaey, Electrolytic extraction drives volatile fatty acid chain elongation through lactic acid and replaces chemical pH control in thin stillage fermentation; *Biotechnology for Biofuels* **2015**, 8:221 DOI: 10.1186/s13068-015-0396-7

Andrea Schievano, Tommu Pepé Sciarria, Korolien Vanbroekhoven, Heleen De Wever, Sebastia Puig., **Stephen J. Andersen,** Korneel Rabaey, Deepak Pant, D. Electro-fermentation - Merging electrochemistry with fermentation in industrial applications. *Trends in Biotechnology*, **2016,** pii: S0167-7799(16)30026-9. DOI: 10.1016/j.tibtech.2016.04.007

1.0 Of carbon, chemicals and current

In our carbon based economy, energy is invested in the transformation of carbon into a myriad of chemicals, materials and fuels. This energy largely comes from the same source as the carbon, from oil and gas, from petrochemistry. The chemicals industry used approximately 135 million TJ (1 terajoule = 10^{24} joules) of energy in OECD nations in 2012, and petrochemical feedstocks consisted of approximately 81 million TJ, or roughly 60 % of the total. This does not include the energy involved in the refining of petrochemical fuels, which accounts for another 10 million TJ (EIA 2016).

Carbon, chemicals and energy are as interlinked in biology as in chemistry. Plants invest energy harvested from the sun through photosynthesis in the building of complex carbohydrates, which they use as both fuel and carbon source. The chemical sector has long been guided by biology, utilizing the complex carbon molecules built by plants, yeasts and bacteria to generate an ever-increasing cache of chemicals. Wood, biomass and biogas can all be used as an energy source, however biology alone cannot meet the extensive energy demands of chemical industry. There is an opportunity to take advantage of the growth of renewable energy to utilize effective, efficient and sustainable energy sources if the industry moves towards electricity driven processes.

Renewable electricity is projected to grow globally at a rate of 2.9 % per year over the coming quarter century. By 2020, wind generated electricity is anticipated to generate an additional 790 million kWh and from solar and additional 340 million kWh. Renewable energy is projected to be the fastest growing energy resource, and there is an opportunity to direct some of this burgeoning resource towards the production of sustainable bio-chemicals (EIA 2016).

The work of this thesis centers around a novel electrochemical extraction technology tailored to the bio-production of carboxylic acids chemicals used extensively in petrochemistry, to improve both the sustainability and economic prospects of these chemicals.

1.1 Conversion, production and recovery in renewable chemistry

The chemical industry requires a broad range of carbon-based building blocks and platform chemicals, many of which can be generated sustainably through microbial conversions from sugar, lignocellulosic biomass, and carbon dioxide (Gavrilescu and Chisti 2005; Rabaey and Rozendal 2010; Deloitte 2014; Wagemann 2014). Anaerobic microbial conversions increasingly contribute to the production of sustainable, non-fuel chemicals. In chemistry, greater value is associated with more reactive functional groups (Wagemann 2014) and non-fuel compounds, on average, are priced fifteen times higher per ton than fuels (Deloitte 2014). Most biotechnology success stories to date are those of drop-in bulk bio-fuels such as biogas and alcohols, chemicals generally recovered simply by gas separation or with petrochemical era separation technologies such as distillation and solvent extraction. Such technologies are mature and well developed for a broad range of chemicals, but they are not broadly suited to biologically constrained titers in complex broths, particularly where extensive dewatering is required. The high energy and capital investment often fatally weakens the economics and sustainability of bulk biochemical production. This issue is compounded when production is constrained by a complex substrate, such as agro-industrial sidestreams and waste.

Conversion, production and recovery are intimately connected in bio-production due to the functional boundaries of the working organisms. Conversion here refers to the processing, biological or otherwise, required for optimum utility of the substrate (e.g. pre-treatments like enzymatic hydrolysis), production refers to the biological (pure culture or consortium) transformation of the substrate into the target product (e.g. glucose to ethanol) and recovery refers to the extraction and purification unit operations required to bring the product to the desired quality (e.g. distillation). A sugar based production tends to require the most intensive conversion processes, as a sugar product needs to be refined from a sugar-rich crop, or a crop requires physicochemical pre-treatment to increase the availability of the sugar. This can include grinding, extrusion, steam-explosion, acid hydrolysis, and enzymatic hydrolysis (Maurya et al. 2015). Transforming a plant polymer can be energy and chemical intensive, particularly when one considers transport and invested energy for the substrate and the processing chemicals (*i.e.* acid, base, hydrolytic enzymes). Waste streams such as syngas, water based refuse and agricultural residues are often targeted for opportunistic production. Waste and side-stream conversions take advantage of the energy invested in the up-stream operation to minimize conversion costs,

though if the waste stream is being targeted for full conversion, additional unit operations that add energy and chemicals may be necessary. Single-stage conversion and production is fleetingly rare, and arguably only successfully achieved at the full scale in Anaerobic Digestion (AD) to biogas. AD takes advantage of a diverse microbial community to convert a broad range of organic substrates through a hydrolytic pathway to produce biogas and ultimately, heat or electricity. AD is predominantly used as a sludge reduction strategy rather than for bio-production of energy, as the value of methane is low and conversion to power adds only marginal value, often requiring government incentives for make for a sound economic argument (Edwards et al. 2015). As a conversion strategy, the process is sustainable with minimal added energy and chemicals, as mentioned, and the gaseous product conveniently leaves the reactor of its own accord.

Table 1.1 Summary of common physico-chemical treatments and biological conversion strategies (Brodeur et al. 2011, Chaturvedi and Verma 2013, Maurya et al. 2015). Treatments are listed in ascending order of least to most energy intensive.

Treatment	**Side products & process implications**
Biological	
Fungal degradation	Requires long residence time (10 to 30 days)
Digestion*	Sludge & methane side products, VFA inhibitors, long residence time
Enzyme	VFA side-products can inhibit hydrolysis, expensive
Physico-chemical	
Base	Low side products, limited increase in conversion without added heat
Acid	Lactic, acetic acid, furans, phenolic inhibitors, needs neutralizing & wash-out
Greens solvents	Expensive, fouled solvents need to be recovered
Steam explosion	Low generation of side products, high yields (+75%) with base or acid
Extrusion / Grinding	Low generation of side products
Ozonolysis	Expensive, high yields (90%) combined with extrusion

* Digestion here does not refer to the process of AD, which produces biogas from waste, rather the microbial processes of digesting complex substrates

1.2 Titer versus recovery, biology versus chemical engineering

Few chemicals conveniently leave the production broth as methane does, and often the conversion of the substrates to higher value, functional platform chemicals will be limited by product inhibition and microbial kinetics. Product titer in the fermentation broth impacts production economics, sustainability, and in many cases, conversion. Production in fermentation is restricted to bio-friendly conditions: an aqueous environment with low salts and a relatively neutral broth, and any species that perform out of these limits are either engineered or inoculated from extreme environments. The upper limit of productive product concentrations is varied, and again tolerance to extremes must be either engineered or selected (Zhang et al. 2009). In a mixed community, this is more complicated. Many volatile fatty acids (VFAs) at relatively low concentrations can be inhibitory to hydrolysis and fermentation, or can be toxic (Jönsson et al. 2013, Pratt et al. 2012). Mid-chain fatty acids (MCFA), such as hexanoic acid, have a pH dependent toxicity on a broad range of microorganisms due to detergent effects on the cell membrane. In the production of alcohols, organisms are selected or engineered for tolerance to the products, which is often the case in higher value diols (Zeng and Sabra, 2011), though an engineered strain is not suitable for all applications due to the extensive investment required in development. Thus a balance must be struck between the productive upper limits of concentration and the technical – and economic – capabilities of a separation and recovery unit operation. Under most circumstances, products at a relatively limited concentration need to be recovered from an aqueous broth that also contains unconverted substrate, the working micro-organism (and other species in a mixed community), salts and nutrients. Specific unit operations are varied and depend on the physical and chemical properties of the target molecule, for example dewatering for involatile products such as succinic acid, distillation for volatile products such as ethanol, solvent extraction for hydrophobic molecules including MCFA, such as hexanoic acid, and electrochemical extraction for charged fermentation products like acetic acid, hexanoic acid and succinic acid in their more neutral broths (Ramaswamy et al. 2013, López-Garzón et al. 2014). The chemical and energy demand of each unit operation will impact the overall sustainability, and the broth concentration, production rate and side products will impact the scale and cost. Separation and recovery unit operations tend to be more efficient at larger concentrations, and less efficient and generally more expensive at trace to low concentrations.

Table 1.2 Upper limit of product concentrations.

Compound	Organism	Carbon source	Conc.	Reference
Ethanol	Yeast	Glucose	130+ g/L	
Acetic acid	Yeast, mixed community	Food waste	25.6 g/L	Li et al. 2015
	Acetobacterium woodii	CO2	44 g/L	Demler et al. 2010
	Acetobacter aceti	Glucose	76 g/L	Awad et al. 2012
		Ethanol	90 g/L	Park et al. 1991
Hexanoic acid	*Megasphaera elsdenii*	Acetic & lactic acid	4.69 g/L	Choi et al. 2013
	Mixed community*	Biorefinery stillage	8.1 g/L	Chapter 4
	Clostridium kluyverii	Acetic acid & ethanol	12.8 g/L	Weimer et al. 2012
	Clostridium group IV spp.	Acetic & lactic acid	23.41 g/L	Zhu et al. 2015
Succinic acid	*Basfia succinogenes*	Glucose, CO2	20 g/L	Becker et al. 2013
	Saccharomyces cerevisiae	unknown	55.2 g/L	López-G. et al. 2008
	Actinobacillus succinogenes	Glucose, CO2	105.8 g/L	Guettler et al. 1996

*Dominated by a *Clostridium* group IV *sp.,* see Chapter 2

Part of the success of bio-ethanol can be attributed to its high titer, and the high volatility / low boiling point that allows distillation. The maximum concentrations for acetic acid, hexanoic acid and succinic acid listed in Table 1.2 varies according to substrate and species, highlighting the connection between conversion and production, and the economy of recovery. Note that for many wastes or complex substrates the maximum concentration is relatively low, while defined substrates with a defined species tends to be higher concentrations and conversions, though with also other costs and challenges. Fermentation of VFA and MCFA have some parallels with bio-ethanol, but stand apart in the Carboxylate Platform.

1.3 The Carboxylate Platform: not just dropping-in

Bio-ethanol has had success as a drop-in fuel, however the chemical industry also requires a broader range of functional chemicals beyond a two carbon chain and a single alcohol group. Microbial production of carboxylic acids for use as bulk chemicals and chemical precursors (*e.g.* for conversion to solvents, fuels, polymers) is known as the Carboxylate Platform (Holtzapple et al. 2009, Agler et al. 2011). The Carboxylate Platform is often associated with second generation biorefinery processes (*i.e.* from substrates such as syngas, agro-industrial residues and sidestreams instead of sugar), but can also be extended to products such as succinic acid (butanedioic acid), a dicarboxylic acid that can spans both 1st generation biorefieneries, produced from sugars, and 2nd generation, with production from wastes such as molasses (Liu et al. 2008, Pateraki et al. 2016). Taking advantage of a variety of substrates, micro-organisms and functional chemical products is central to the Carboxylate Platform, alongside challenges in methanogen suppression, functional limitations in biological conversion and production, and effective, economic recovery. The Carboxylate Platform ranges from simple, bulk chemicals (e.g. acetic acid) through specialty acids (e.g. succinic acid), many of which are already at play in the industrial chemical arena as precursors to plastics, pharmaceuticals, fragrances and fuels (Agler et al. 2011).

Bulk products such as acetic acid can be produced from waste and ethanol by mixed species, often from the *Acetobacter* family, as well as from carbon dioxide and hydrogen gas by *Acetobacterium woodii* (Demler et al. 2010, Awad et al. 2012). More functional chemicals such as succinic acid can be produced from glycerol or sugars by *Actinobacillus succinogenes*, and from sugar by patented species such as *Basfia succiniciproducens* (Pateraki et al. 2016). MCFA fermentation has been demonstrated from synthetic substrates and wastes with pure and mixed microbial communities, often with but not limited to members of the class *Clostridia*. *Clostridium kluyverii* was shown to generate butyric acid, hexanoic acid and hydrogen gas from acetic acid and ethanol by coupling the reduction of crotonyl-CoA to butyrul-CoA with the reduction of ferredoxin and NADH, thus elongating the carbon chain of acetic acid by reverse ß oxidation, as demonstrated in Figure 1.1 (Seerdorf et al. 2008, Spirito et al. 2014). The production of MCFA is covered at length in the reviews of Spirito et al. (2014) and Angenent et al. (2016). MCFA are both valuable and toxic, and the active removal of MCFA is often shown to be critical in sustaining an efficient production (Agler et al. 2012, Choi et al. 2013, Xu et al. 2015).

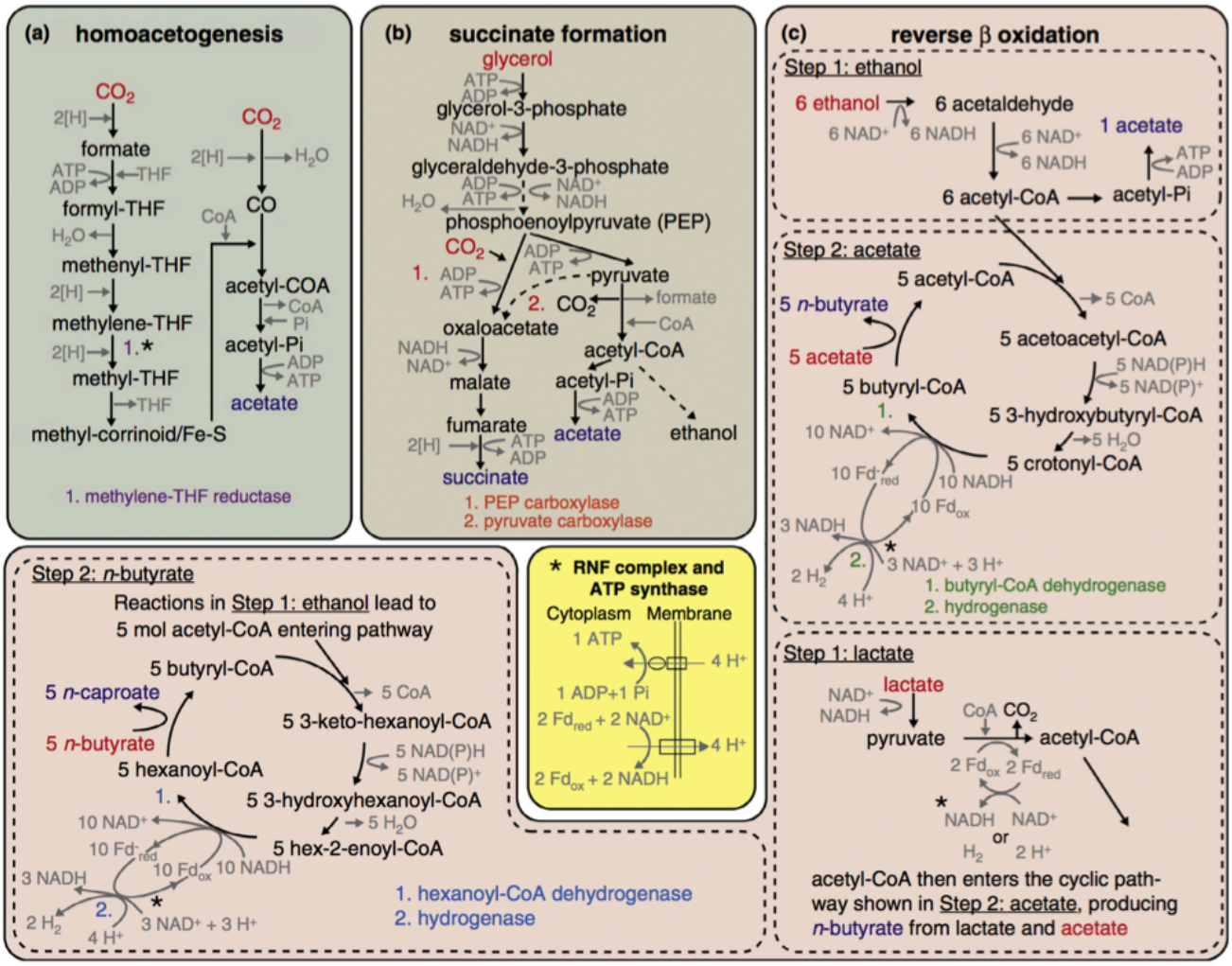

Figure 1.1 Metabolic pathways of **(a)** homoacetogenesis; **(b)** succinate formation and **(c)** reverse β oxidation (from Spirito et al. 2014)

Separation and recovery technologies are recognized as a major challenge within the Carboxylate Platform due to product inhibition both at the production level (fermentation), and in inhibition of conversion (hydrolysis) (Agler et al. 2011, Angenent et al. 2016). Carboxylic acids are an interesting target product because they can be differentiated from other products by volatility, hydrophobicity, and sometimes solubility, however removing trace organic compounds or purifying VFAs with similar physicochemical properties can contribute to the high costs in recovery. The recovery and purification of succinic acid was previously estimated at 60% of the total capital costs, in part due to the removal of trace co-products such as acetic and formic acids, though this has since decreased through process optimisation (Bechtold et al. 2008, Pateraki et al. 2016).

In the carboxylic acid processing pipeline as described by López-Garzón and Straathof (2014) (Figure 1.2), there are a number of different recovery technologies available. Primary Recovery can involve adsorption, precipitation, solvent extraction, and distillation to target the acidic portion, or electro-dialysis and ion exchange to target the dissociated anion. Counter Ion Removal involves adsorption and precipitation to recover salts that were introduced through pH control in Fermentation and Primary Recovery. Concentration & Purification often requires dewatering, solvent extraction and/or distillation, with the extent highly dependent on the end-user requirements and market demands. This stage depends on final concentration and physical properties of the product (Table 1.3), as a concentrating steps targets the product through function group affinity, hydrophobicity, charge, etc. and utilizes it to isolate the product up a concentration gradient (López-Garzón and Straathof 2014).

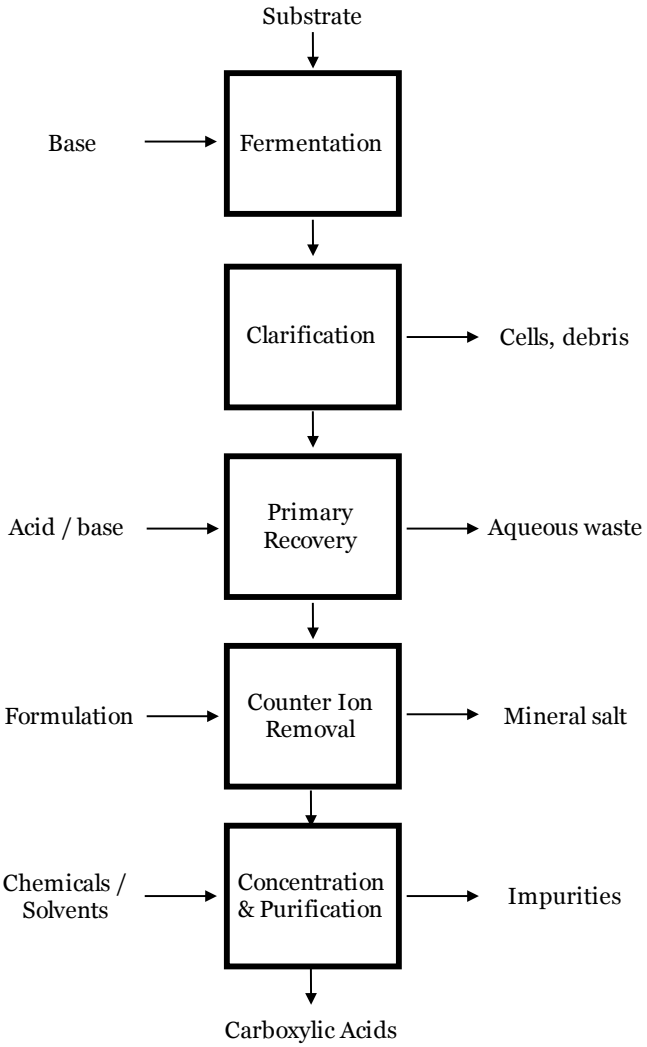

Figure 1.2. A general processing scheme for production and recovery of carboxylic acids (adapted from López-Garzón and Straathof 2014)

The extraction and concentration of a singular, bulk carboxylic acid is challenging due to overlapping properties, the tendency to be formed alongside other carboxylic acid side products, and high solubility in water. Acetic acid from waste may be produced alongside propionic acid, or with formic acid in a CO_2 fermentation, and many short chain VFA including acetic acid and butyric acid are likely to be present in a MCFA fermentation, (Agler et al. 2011, Angenent et al. 2016), while lactic acid and formic acid are common side products in the production of succinic acid (Pateraki et al. 2016). Table 1.3 demonstrates that these products have sufficiently different boiling points that they can be separated through distillation, but with titers less than 1 % w/w (Table 1.1) and a boiling point above that of water, this is a very heat intensive option, particularly for relatively low value, bulk products such as acetic acid. In the protonated form, adsorption is suitable for succinic acid as a dicarboxylic acid in comparison to the singular functional group of lactic and acetic acid co-products. For hexanoic and succinic acid, if the maximum solubility concentration is reached the products will begin to separate under normal conditions. Under more neutral conditions all the acids contain at least one charge and will therefore undergo electro-migration under an applied current or potential gradient.

Table 1.3 Physical properties of some carboxylic acids and common co-products (*italicized*), (Weaste 1972, Windholz 1976, López-Garzón and Straathof 2014), charge number at pH 7

Acid	pKa	Solubility	Boiling point	Charge Number
Acetic acid	4.75	Miscible	118 °C	-1
Propionic acid	4.87	Miscible	141 °C	-1
Hexanoic acid	4.88	10.8 g/L	205.8 °C	-1
Butyric acid	4.81	Miscible	163 °C	-1
Succinic acid	4.16, 5.61	58 g/L	235 °C	-2
Formic acid	3.77	Miscible	100.8 °C	-1
Lactic acid	3.86, 5.11	High	Decomposes	-1

1.5 Electro-migration: ionic transport independent of concentration

Electro-migration is the transport of a charge through a conductive medium. In the same way that a potential applied across a wire results in the passage of electrons as a an electric current, a potential applied across a salty broth can result in the migration of ions – anions towards an anode, and cations towards a cathode. Carboxylic acid anions are also subject to electro-migration, and is used in practice both in analysis, such as ion chromatography, demonstrated in Figure 1.3 and Figure 1.4, and product extraction through electrodialysis. Electrodialysis has been demonstrated as a means of extraction and concentration for short chain carboxylic acids including formic acid, acetic acid, propionic acid, lactic acid, succinic and itaconic acids. Electrodialysis is generally limited to high value products in practice, due to high capital costs and a large power investment, due to electrical resistance. There is a high caustic demand to maintain the fermentation in the neutral region so that the carboxylic acid products remain charged, followed by acidification with added acids (Gohil et al. 2004, López-Garzón and Straathof 2014).

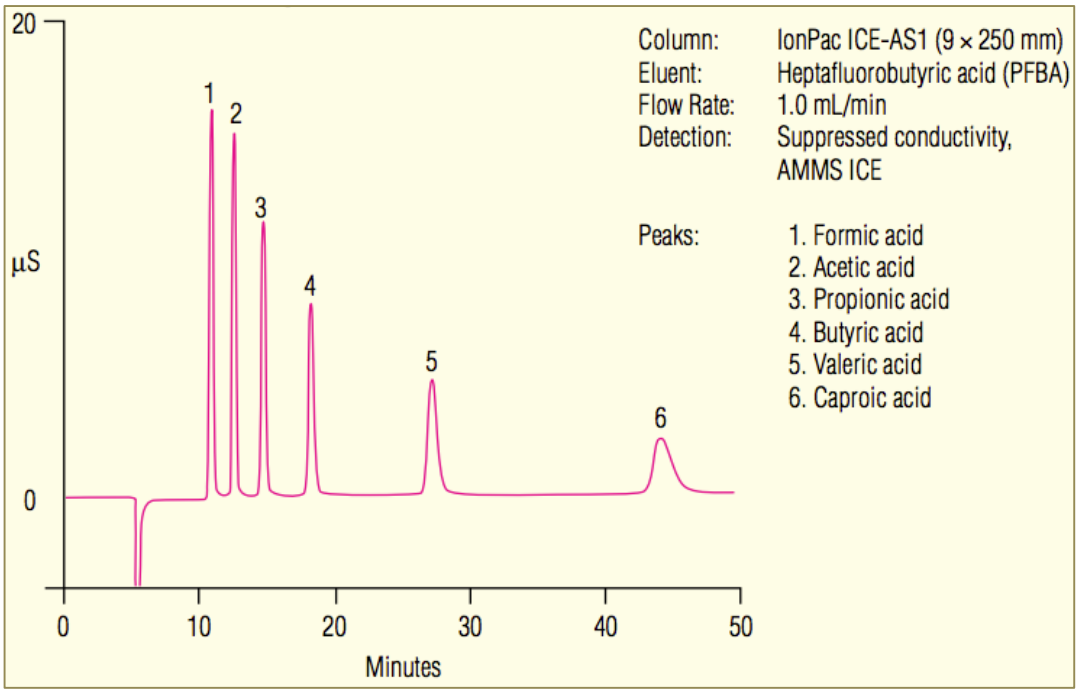

Figure 1.3. Ion chromatography spectrum of IonPac ICE-AS1, Thermo Scientific Dionex, for linear saturated carboxylic acids formic acid (C1), acetic acid (C2), propionic acid (C3), butyric acid (C4), valeric acid (C5) and caproic acid (hexanoic acid, C6).

(Adapted from http://www.dionex.com/en-us/webdocs/4276-DS_IonPac_ICE-AS1_02Apr07_LPN0814_03.pdf)

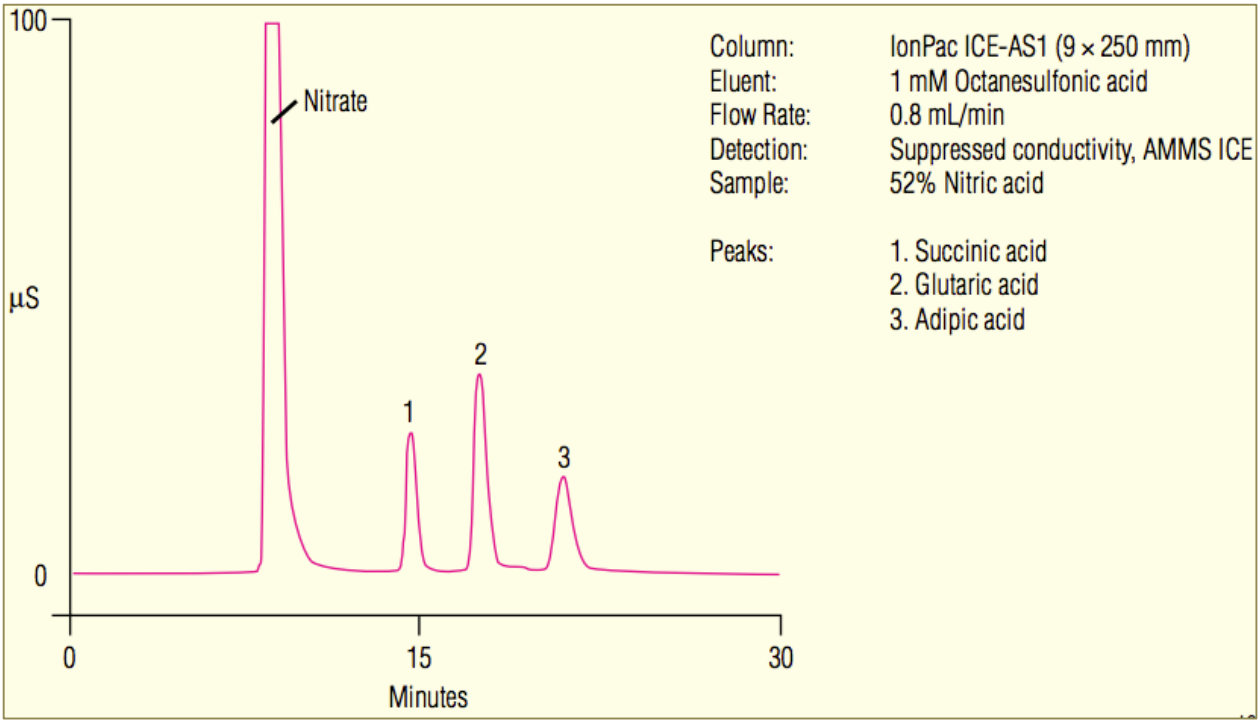

Figure 1.3. Ion chromatography spectrum of IonPac ICE-AS1, Thermo Scientific Dionex, for dicarboxylic acids succinic acid (butanedioic acid, C4), glutaric acid (C5) and adipic acid (hexanedioic acid, C6).

(Adapted from http://www.dionex.com/en-us/webdocs/4276-DS_IonPac_ICE-AS1_02Apr07_LPN0814_03.pdf)

Individual carboxylic acids can be identified with ion chromatography by the separation of peaks that occurs as a result of a characteristic transport of the anion through a polymeric anionic lattice. Electro-migration differs for different species in an ion exchange column due to differences in electro-migration constants, pKa, steric hindrances, and others, but concentration does not play a role in their migration rate, thus allowing discrete, repeatable peaks used to characterize the species independent of the starting concentration. The applied electrical field can motivate charged molecules even at a few parts per million into the ionic lattice. The same concept applies for transport through a cation lattice (*e.g.* an anion exchange membrane, AEM), through which anions migrate at a greater rate under the applied current, such as in electro-dialysis. Considering the tendency towards relatively low concentrations in a VFA fermentation broth, this makes electro-migration an attractive driving force for recovering carboxylic acids from more neutral broths.

1.6 Objectives and outline of this research

There exists an opportunity to tailor an electrochemical extraction system for carboxylic acid products by first understanding the goals of carboxylic acid fermentation, the electrochemical mechanisms of transport and extraction, and ensuring a sound economic argument by utilizing the electrolysis products to valorize and recover added-value products. The objective of this thesis was to develop and apply membrane electrolysis (Figure 1.4), an electrochemical technology to extract and valorize carboxylic acids from a mixed community microbial fermentation. In **Chapter 2**, a semi-continuous mixed-community MCFA fermentation of biorefinery stillage was studied to investigate the product concentration profile and community response associated with toxicity of the product MCFA, with particular attention to the influence of high MCFA on species with different roles in the fermentation. In **Chapter 3**, membrane electrolysis is described in detail. Acetic acid and hexanoic acid streams undergo electrochemical water reduction in a cathodic chamber, resulting in the electro-migration of the carboxylic acid anions across an anion exchange membrane (AEM) into an extract solution in which electrochemical water oxidation results in a low-pH carboxylic acid concentrate. A mathematical description of acetic acid transport and Electrochemical Impedance Spectroscopy (EIS) was used to describe the transport and investigate transport parameters such as membrane resistance, and the membrane specific electro-migration constant of the acetic acid.

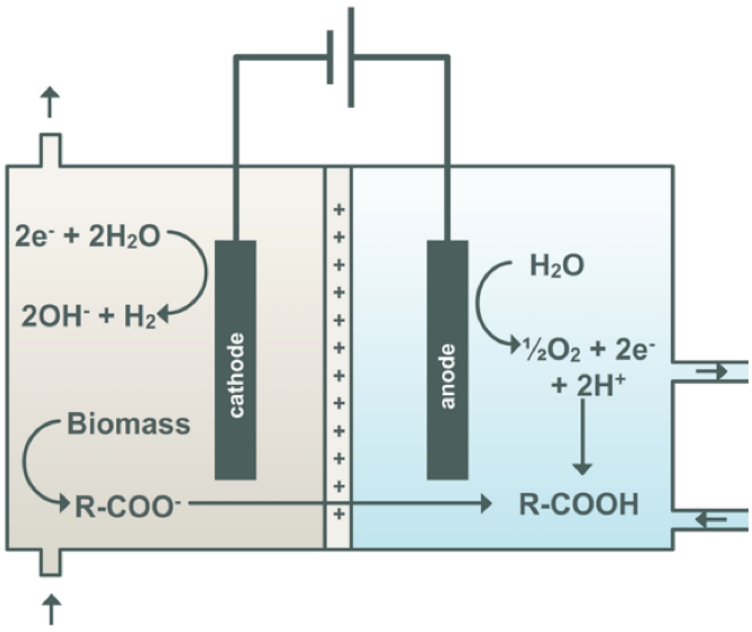

Figure 1.4. Concept diagram of membrane electrolysis. Image by Tim Lacoere.

In **Chapter 4**, membrane electrolysis was applied *in situ* to a fermentation of bio-refinery thin stillage to investigate the effect of current on the microbial community and the product output. The effect of hydrogen on the fermenting community and the extent of chain elongation was investigated on the hypothesis that increased hydrogen gas creates an intracellular excess of NADH that can drive many reductive processes in the so-called Electro-Fermentation (Schievano et al. 2016). The electrolytic generation of hydroxide ions was tested as a counter-measure for the acidification of the fermentation, for chemical-free pH control of the broth. Valorization of the carboxylic acid extract is investigated in **Chapter 5**. Short chain fatty acids are highly miscible and costly to recover from an aqueous broth. An esterification reactive extraction was developed to valorize the VFA, and improve the prospects for recovery increased product volatility in an involatile medium. Ionic liquid (IL) esterification of the aqueous products was demonstrated. ILs have a unique set of properties, and can potentially to be tailored to a range of applications to upgrade carboxylic acids.

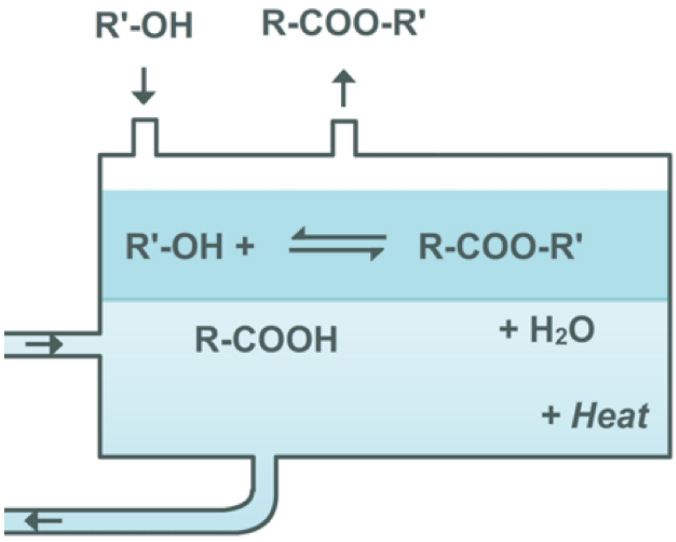

Figure 1.5. Concept diagram of biphasic esterification. Image by Tim Lacoere.

Chapter 6 discusses the potential impact of membrane electrolysis and some interesting target products and co-products were critically analyzed, with an emphasis on sustainability.

CHAPTER 2

Mid-chain fatty acid fermentation and toxicity

This chapter is redrafted from:

Stephen J Andersen, Vicky De Groof, Way Cern Khor, Hugo Roume, Ruben Props, Marta Coma and Korneel Rabaey, *Clostridium* Group IV species dominates and suppresses a mixed culture fermentation by mid-chain fatty acids production and tolerance, *Submitted*, **2016**

2.0 Abstract

A microbial community engages in a complex economy of co-operation and competition. In engineered systems such as anaerobic digestion and fermentation these relationships are exploited for conversion of a broad range of substrates into a defined product, and therefore one must pay attention to inhibitory or toxic compounds that can interfere with the members of the community. An example of this is the bioproduction of carboxylic acids, such as mid-chain fatty acids (MCFA), which have a microbial toxicity at low concentrations. Here we performed continuous mixed-community MCFA fermentations on biorefinery thin stillage at MCFA concentrations that are typically toxic to investigate the impact on the community, substrate conversion and product profile. In this study an uncultured species related to *Clostridium sp.* BS-1 from *Clostridium* group IV became enriched in two independent reactors that produced hexanoic acid (up to 8.1 g L^{-1}), octanoic acid (up to 3.2 g L^{-1}), and trace concentrations of decanoic acid. Decanoic acid is reported here for the first time as a possible product of *Clostridium* group IV species. A strong correlation was present between the community composition and both the hexanoic acid concentration ($p = 0.026$) and total VFA concentration ($p = 0.003$). MCFA suppressed species related to *Clostridium sp.* CPB-6, an uncultured *Clostridium* group IV species, and *Lactobacillus spp.* With respect to relative abundance, the proportion of the species related to *Clostridium sp.* BS-1 relative to *Clostridium sp.* CPB-6 had a strong correlation to the concentration of octanoic acid ($p = 0.003$). The dominance of this species and increase in MCFA resulted in an overall toxic effect on the mixed community, most significantly on the *Lactobacillus spp.*, resulting in a decrease of total hexanoic acid concentration to 32 ± 2 % below the steady state average. *Lactobacillus spp.* and *Acetobacterium sp.* generate lactic acid and acetic acid, intermediates in MCFA production, and their collapse in relative abundance resulted in an overall production decrease.

2.1 Introduction

The conversion of a complex substrate in anaerobic digestion and fermentation relies on the competition for carbon and energy within a mixed microbial community to drive towards the targeted end products, such as methane, acetic acid and other VFA. The environmental conditions in such systems can be engineered (pH, temperature, organic loading, wash out rate, etc) in an attempt to optimize performance throughout this collaborative biological economy. Conditions cannot be ideal for each player, and some applied or inherent conditions can result in favorable – or unfavorable – conditions for others in the community and the role they play in this process. Managing this principle is at the center of engineering a mixed microbial biotechnology (Angenent et al. 2016, Lindemann et al. 2016).

MCFA have a pH dependent microbial toxicity that can disrupt membrane integrity at around 40 mM (4.6 gL^{-1}) for hexanoic acid (pK_a 4.88) and 20 mM (2.9 gL^{-1}) for octanoic acid (pK_a 4.89), as characterized in *E. coli* at pH 4.3, with no toxicity demonstrated at pH 7 (Yang et al. 2010, Royce et al. 2013). Stable, continuous operation of a reactor in the presence of MCFA requires this toxicity to be managed by attentive organic loading and hydraulic residence time, or extraction by an active, robust recovery technology that can work effectively below the toxicity limit. Extraction efficiency and unit operation cost are inherently linked with the concentration of the target compound, and thus extraction and recovery unit operation technologies are recognized as one of the major economic hurdles in bringing sustainable MCFA production to an industrial reality (Agler et al. 2011, Lopez Garon et al. 2014, Xu et al. 2015; Angenent et al 2016).

The microbial communities that do not explicitly produce MCFA are core to the carbon economy of the digestion and fermentation of a complex substrate. A single-stage production from waste requires microorganisms to perform hydrolysis, acidogenesis, acetogenesis, and as necessary, other fermentations (*e.g.* towards ethanol, lactic acid, butryic acid) (Agler et al. 2011, Agler et al. 2012, Angenent et al. 2016), while also contributing some critical co-production of gases (*e.g.* hydrogen gas and carbon dioxide gas). The supporting community in digestion includes the *Bacteroidetes* and *Firmicutes* phyla, which enrich when switching from biogas to VFA production (De Vrieze et al. 2015). *Bacteroidetes* have been related to parallel reactions when a *Clostridium sp.* were enriched for MCFA production (Coma et al. 2016). In mixed microbial chain elongation to MCFA through a lactic acid intermediate, *Lactobacillus spp.* have been found in communities

Clostridium Group IV (Zhu et al. 2016), a species known to consume lactic acid. Ethanol is often added in studies for mixed culture chain elongation of acetic acid and ethanol, but can also be generated by the supporting community from sugars, or acetic acid and carbon dioxide (Spirito et al. 2014). It is somewhat reductive to refer to producers of critical intermediates as a "supporting" community, particularly when the complete conversion of the substrate is critical to the economics of production. Within the carbon and energy economy of the reactor microbiome the non-elongating, supporting community is process critical, and therefore important to study, understand and engineer.

This work investigated a MCFA fermentation of a real, complex substrate, and how the toxic products impact the community and therefore the process. We describe the operation of two identical reactors fed with biorefinery stillage, an organics rich stream from the bottoms of a bio-ethanol distillation column, and track changes in the substrate consumption, VFA concentration and bacterial community composition.

2.2 Materials and Methods

2.2.1 Bioreactor operation. Fermentation of stillage and beer from a wheat bioethanol process (supplied by Tereos Starch & Sweeteners, Aalst, Belgium) was performed in two identical DOLLY twin Bioreactors (Belach Bioteknik AB, Sweden). The working volume was fixed at 5 L and fed at daily intervals from a source stored at 4 °C, and pH 3.5 ± 0.1. The reactors were maintained at a hydraulic residence time of 7 days and pH 5.5, controlled by dosing 5 M NaOH. At start-up, reactors were filled with 4.5 L adapted DMSZ medium 52 (https://www.dsmz.de/microorganisms/medium/pdf/DSMZ_Medium52.pdf) fed with a 5:2 beer to stillage ratio, to target 10 g L^{-1} ethanol in the total reactor volume, followed by regular feeding at approximately 14 % beer to target an ethanol concentration of 6 g L^{-1}.

The feed consisted of 57 ± 9 g sCOD L^{-1} and 101 ± 18 g tCOD L^{-1}, and the greatest concentration of soluble substrates that were measured included sugars at 9.0 ± 0.4 g L^{-1} of xylose, 4.9 ± 0.2 g L^{-1} arabinose and 2.2 ± 0.1 g L^{-1} glucose (n = 4), 6.0 ± 2.4 g L^{-1} ethanol, 3.8 ± 1.2 g L^{-1} glycerol, 1.6 ± 1.3 gL^{-1} lactate and 0.4 ± 0.2 gL^{-1} acetic acid, with a consistent conductivity of 6.0 ± 0.9 ms/cm (n = 18).

2.2.2 Chemical analysis. Reactors were sampled three times and screened for C2 to C10 carboxylic acids (including isoforms C4 to C6), measured by gas chromatography (GC-2014, Shimadzu®, The Netherlands) with a DB-FFAP 123-3232 column (30 m × 0.32 mm × 0.25

μm; Agilent, Belgium) and a flame ionization detector (FID). Liquid samples were conditioned with 2 mL sulfuric acid, 200 mg sodium chloride and 2-methyl hexanoic acid as internal standard for quantification before further extraction with diethyl ether (1:1 volume sample : ether). The sample (1 μL) was injected at 250°C with a split ratio of 50 and a purge flow of 3 mL min^{-1}. The oven temperature increased by 10 °C min^{-1} from 110 °C to 250 °C where it was kept for 5 min. The FID had a temperature of 300 °C. Nitrogen carrier gas was maintained at a flow rate of 2.49 mL min^{-1}. 'Total VFA' is the quantitative sum of all detected linear, unsaturated carboxylic acids, C1 to C8. Decanoic acid (C10) was detected at up to 232 ppm, but interference was observed from unidentified lipids already present in the feed. For a comparative analysis of C10, detection peaks were normalized between 0 to 1 scale with the average integration of the C10 peak in the feed set at 0 ($\sigma = 7 \times 10^{-4}$, n = 4), and the maximum detected peak set at 1. Normalized C10 integrated peaks were clustered into two discrete groupings, the average separated by two standard deviations ($\sigma = 0.27$). Those clustered close to zero are considered a negative detection of the C10 MCFA, with an average of -0.03 ± 0.2 (n = 6), with those outside with an average of 0.60 ± 0.23 (n = 6) considered a positive detection. The separate clusters were compared for distinctness by kmeans clustering, and compared against C8 concentration, *Clostridium sp.* BS-1_{sec} relative abundance, and the ratio of the relative abundance of *Clostridium sp.* BS-1_{sec} to *Clostridium sp.* CPB-6.

To determine lactic acid, formic acid, glycerol, 1,3-propanediol, 1,2-propanediol, methanol, ethanol, propanol and butanol concentrations a Dionex DX 500 ion chromatography system using an IonPac ICE-AS1 column with 0.4 mM HCl as eluent and an ED50 conductivity detector was used. The gas phase composition was analyzed with a Compact GC (Global Analyser Solutions, Breda, The Netherlands), equipped with a Molsieve 5A pre-column and Porabond column (CH_4, O_2, H_2 and N_2) and a Rt-Q-bond pre-column and column (CO_2, N_2O and H_2S). Concentrations of gases in the headspace were determined by means of a thermal conductivity detector. All samples were tested for TSS and VSS according to Standard Methods 2540D and E (APHA 2005). Sugars were determined by the NREL procedure according to Sluiter et al. (2016), measured with high performance liquid chromatography (Agilent Varian ProStar 220 SDM, USA; 5 mM H_2SO_4 mobile phase, 0.6 mL min^{-1} and 60 °C column temperature with a refractive index detector and Rezex H+ column (Aminex).

2.2.3 Community analysis. DNA samples for community analysis of the reactor broth and feed, were centrifuged in 2 mL in sterile Micrewtubes® (Simport, Canada). The supernatant was removed, and the samples were stored at -21°C. DNA extraction was performed using a PowerSoil DNA extraction kit (MO BIO Laboratories, USA) according to Roume et al. (2013). Biomass was concentrated by centrifugation in sterile 2 mL bead beating Micrewtubes (Simport, Canada) for 1 min at 20 238 g in a Fast Prep-96 instrument (2 times 40 s at 1600 rpm) followed by removal of precipitation of diverse polymerase chain reaction (PCR) inhibitors according to the manufacturer's instructions. Total DNA was captured on a silica membrane incorporated into a chromatographic spin column, washed and eluted in the dedicated buffer. Concentration of double-stranded DNA was quantified using the QuantiFluor dsDNA system and measured with a GloMax 96 Microplate Luminometer (Promega GmbH, Germany). For quality control, the isolated DNA was amplified by PCR using Illumina sequencing primers and separated by electrophoresis.

The V3–V4 region of the bacterial 16S rRNA gene was sequenced with Illumina sequencing Miseq v3 Reagent kit (http://www.illumina.com/products/miseq-reagent-kit-v3.ilmn, by LGC Genomics GmbH, Berlin, Germany) using 2 x 300 bp paired-end reads and primers 341F-785R described by Stewardson et al. (2015). The PCRs included 5 ng of DNA extract, 15 pmol of each forward primer 341F 5'-NNNNNNNNTCCTACGGGNGGCWGCAG and reverse primer 785R 5'- NNNNNNNNTGACTACHVGGGTATCTAAKCC in 20 µL volume of MyTaq buffer containing 1.5 units MyTaq DNA polymerase (Bioline) and 2 µL of BioStabII PCR Enhancer (Sigma). For each sample, the forward and reverse primers had the same 8-nt barcode sequence. PCRs were carried out for 30 cycles using the following parameters: 2 min 96 °C pre-denaturation; 96 °C for 15 s, 50 °C for 30 s, 72 °C for 60 s. DNA concentration of amplicons of interest was determined by gel electrophoresis. About 20 ng amplicon DNA of each sample were pooled for up to 48 samples carrying different barcodes. PCRs showing low yields were further amplified for 5 cycles. The amplicon pools were purified with one volume AMPure XP beads (Agencourt) to remove primer dimer and other small mispriming products, followed by an additional purification on MinElute columns (Qiagen). About 100 ng of each purified amplicon pool DNA was used to construct Illumina libraries using the Ovation Rapid DR Multiplex System 1-96 (NuGEN). Illumina libraries were pooled and size selected by preparative gel electrophoresis. Sequencing was done on an Illumina MiSeq using v3 Chemistry (Illumina).

Bioinformatics was executed with the mothur community analysis pipeline (Schloss et al. 2009). The analysis started from the primers clipped 16Sr RNA sequences, containing sequences where primers were detected and removed (allowing 2 mismatches) and turned into forward and reverse primer orientation and combined with the make.contigs command. The use of this open-source software package involved the preparation and de-noising of sequences, and extraction of the V3–V4 region. Low-quality sequences were removed and the frequency of sequencing and PCR errors reduced. The sequences were trimmed using the screen.seqs command (allowing no base name ambiguity and a maximum length of 427 bases). Sequences showing a weak alignment (allowing a maximum of four bases in homopolymere) with a V3-V4 customized SILVA database (v119) were removed as well as overhangs at both end of each sequence. The sequences were pre-clustered (allowing a maximum of 4 mismatches per sequence) and chimeric sequences were removed using UCHIME software (Edgar et al. 2011) and sequences were classified with the RDP v10 database (allowing at least a bootstrap value of 65%) and sequences not identified as bacteria were removed. The second step of the pipeline consisted of clustering sequences into operational taxonomic units (OTUs). OTU binning was completed using a hierarchical clustering algorithm implemented within mothur and considering a cut-off of 0.03. The third step involved assignment of the taxonomic information to sequences and OTUs. The analysis was carried out on randomly subsampled OTUs such that each file contained the same number of sequences (5401). The ade4, stat and psych packages of the R software (R version 2.13.2, http://www.r-project.org/) were used respectively for a principal component analysis (PCA; dudi.pca function), representation of the heatmap (heatmap function) and Pearson coefficient calculation (corr.test function).

Sanger sequencing by LGC genomics (Berlin, Germany) was used to identify cultures on the 16S level, with the samples with relative abundance of around 80 % from days 34 and 41 from Reactor 1, and day 62 from Reactor 2. Only day 34 from Reactor 1 returned a valid sequence. The alignment considered 974 bp of the phylogenetic gene maker16S rRNA. The alignment file was submitted to a phylogenetic analysis using the Phylogeny.fr customized workflow service1 including alignment curation with Gblocks2 (using default parameters), tree construction with PhyML3 (using default parameters), and visualization by TreeDyn4 (Dereeper et al. 2008, Castresana et al. 2000, Guindon et al. 2010, Chevenet et al. 2006).

2.2.4 Statistics. For multivariate abundance analysis, all analyses were conducted in R (v3.2.5) with seed 777 and the mvabund package (Wang et al. 2012). Samples were rarefied until the minimum sample depth (9848 reads) and pruned from OTUs which had a maximum relative abundance lower than 10 % or were absent in at least 50 % of the samples to specifically focus on the abundant bacteria with clear temporal dynamics. A forward-selection based modelling approach was then used to test the relationship between VFA constituents and species abundances. The mean-variance relationship was modelled by a negative binomial distribution. Before hypothesis testing all models were verified for accordance with the model assumptions as described by Wang et al. (2012). Hypothesis testing was performed using likelihood ratio tests with pit resampling (5000 runs). The final model consisted of Hexanoic Acid and Total VFA as continuous predictors and the reactor replicate as categorical predictor. Inference on the model parameters of individual species was assessed using the adjusted P-values, calculated after 5000 resampling runs to account for correlations between variables. Ordination plots were made using the decorana and RDA functions available in the vegan package (Oksanen et al. 2015). Detrended correspondence analysis (decorana) was applied on the rarefied community data to avoid horseshoe artefacts which are frequently associated with time series community data. Principal component analysis (PCA) was used on the VFA dataset to investigate correlations between OTUs of interest and the VFA concentration.

2.3 Results

2.3.1 Production of medium chain fatty acids by a community dominated by *Clostridia spp.* and *Lactobacillus spp.* Hexanoic acid was consistently produced in both bioreactors at pH 5.5, resulting in a steady state concentration of 2.0 ± 1.1 gC L^{-1} (3.2 ± 1.8 g L^{-1}) in Reactor 1 and 3.2 ± 0.9 gC L^{-1} (5.2 ± 1.5 g L^{-1}) in Reactor 2 (Figure 2.1), including a maximum concentration of 5.0 gC L^{-1} (8.0 g L^{-1}) hexanoic acid on day 22 in Reactor 2 (concentrations expressed in gC L^{-1} to enable comparison of carbon utility). As a proportion of the total VFA on a carbon basis, 54 ± 10 % of the VFA present was hexanoic, heptanoic or octanoic acid in Reactor 1, and 45 ± 10 % in Reactor 2 (all averages are based on the steady state period from day 15 to 68, n = 13). The VFA profile of the identical reactors began to diverge at day 20, with Reactor 1 progressively increasing to a maximum of 2.1 gC L^{-1} of octanoic acid from by day 39. The total VFA concentration decreased from 7.35 gC L^{-1} on day 20 to a low of 3.46 gC L^{-1} by day 46, 36 % lower than the average steady

state concentration. This decrease coincided with a shift from almost complete consumption of glycerol in Reactor 1 to no significant consumption of glycerol. Reactor 2, operated identically and fed in parallel from the same source, did not show this trend at this time, but rather maintained a total concentration of 7.7 ± 0.6 gC L^{-1} from day 15 through day 57 with a hexanoic acid concentration of 3.5 ± 0.8 gC L^{-1}, a heptanoic and octanoic concentration between 0 and 0.2 gC L^{-1} and complete conversion of glycerol. The octanoic acid concentration began to rise in Reactor 2 after day 60, which coincided with a decline in the total VFA concentration from 7.4 gC L^{-1} on day 60 to a low of 5.0 gC L^{-1} by day 68, 32 % less than the total average steady state VFA concentration. Decanoic acid was detected above the baseline for days 22 and 41 through 64 with a normalized, relative detection peak average of 0.50 ± 0.01 (n = 6), significantly higher than the baseline of the feed at 0 ± 7 × 10^{-4} (n = 4). Decanoic acid was not detected significantly above the baseline in Reactor 2 with a normalized, relative detection peak average of 0.05 ± 2 × 10^{-3} (n = 6), with the exception of day 67. Across all samples, decanoic acid detection only occurs when octanoic acid is detected (Figure 2.1A and B). The normalized decanoic acid detection peak was compared against the concentration of octanoic acid by kmeans clustering. Decanoic acid tended to be detected when a octanoic acid threshold was exceeded, with the average of the kmeans cluster at 2874 ± 408 ppm and a 0.50 ± 0.18 (n = 5) decanoic detection peak (Figure 2.2 A), further evidence that decanoic is only detected alongside octanoic acid.

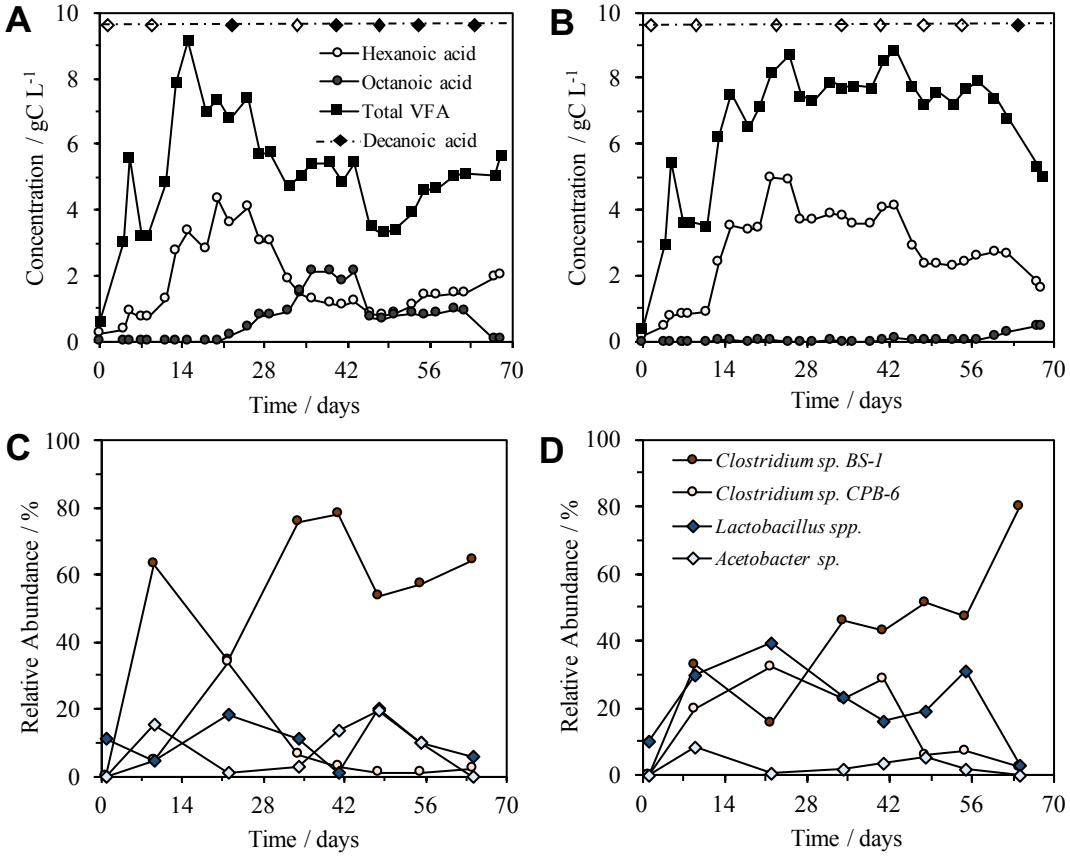

Figure 2.1. A and B. Concentration over time of total VFA (C1 to C8), hexanoic acid (C6) and octanoic acid (C8), including the detection (dashed line) of decanoic acid (C10), in Reactor 1 (A) and Reactor 2 (B). A filled diamond represents decanoic acid detection, the blank diamond represents no significant detection. **C and D.** The top four most relatively abundant micro-organisms over time in the two identical reactors, Reactor 1 (C) and Reactor 2 (D). In both reactors, the HRT and SRT is 7 days.

In both reactors the community was dominated by *Clostridium* and *Lactobacillus* species (Figure 2.1, C and D). Multivariate abundance testing shows that the community composition had a statistically significant correlation with the hexanoic acid concentration ($p = 0.026$) and total VFA concentration ($p = 0.003$), with a significantly different community composition between the two identical reactors ($p = 0.05$). These differences can be significantly attributed to the *Lactobacillus spp.* (Otu 0001) ($p = 0.002$), which generates lactic acid that the *Clostridia* species are likely to metabolize (Jeon et al. 2010, Kim et al. 2015, Kucek et al. 2016). The two reactors had a high functional similarity in terms of VFA output (Figure 2.3 A) despite a large dissimilarity in community profile throughout the 70 days of operation (Figure 2.3 B). The peak of dissimilarity in functionality corresponds to the increase of octanoic acid in the broth.

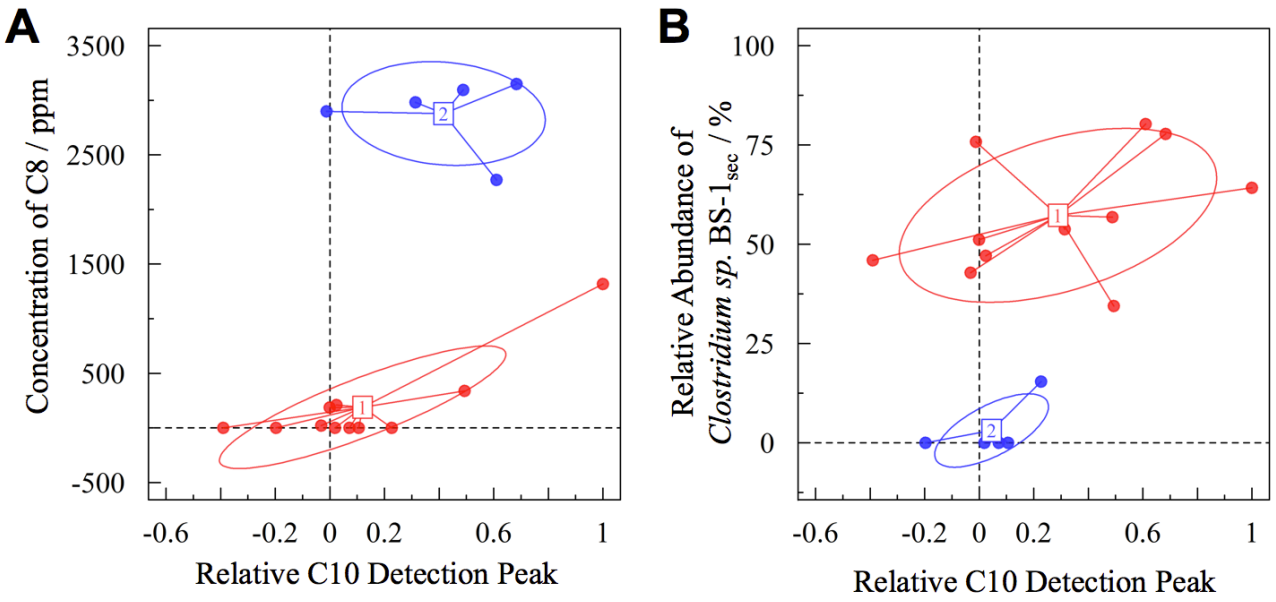

Figure 2.2. A. Relative decanoic acid (C10) detection peak plotted against the corresponding measured octanoic acid concentration, kmeans clustering with 2 centers for visualization purposes. (1) represents the negative detection cluster, while (2) represents the positive detection cluster. **B.** Relative decanoic acid (C10) detection peak plotted against the corresponding relative abundance of Clostridium sp. $BS1_{sec}$, kmeans clustering with 2 centers for visualization purposes. (1) represents the negative detection cluster, while (2) represents the positive detection cluster.

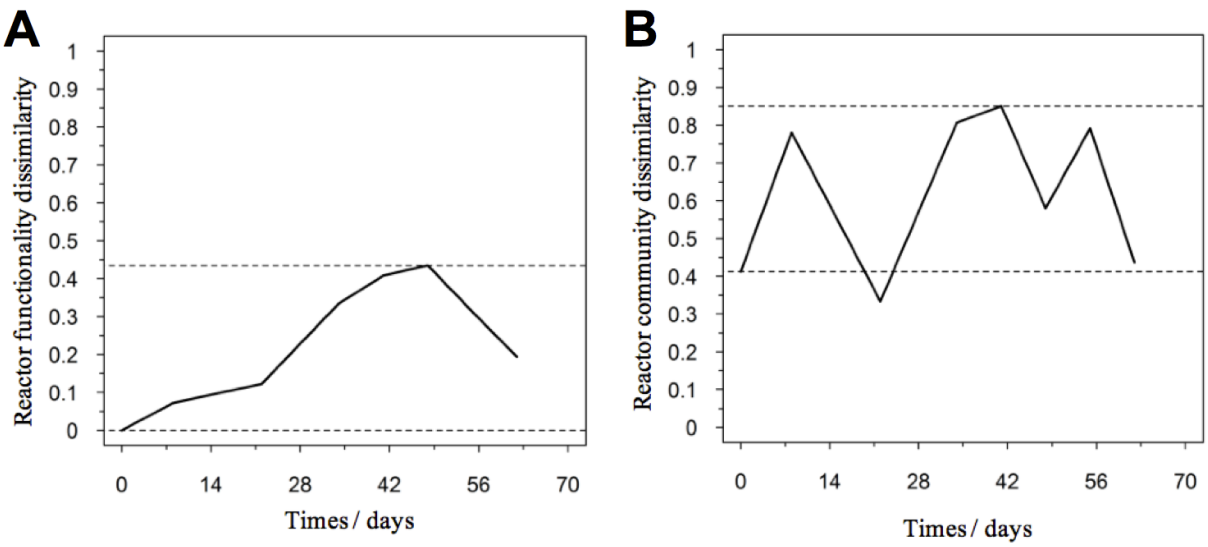

Figure 2.3 The level of dissimilarity between the reactors as measured in time (1 = dissimilar, 0 = identical). Dissimilarities between VFA concentration (**A**) and community profile (**B**) were calculated using the Bray-Curtis distance metric ($1 - 2 \sum \min (S_{R1,i}, S_{R2,i}) / (\sum S_{R1,i} + S_{R2,i})$ where S is the number of individuals in the *i*th OTU (**A**) or VFA species (**B**) of Reactor 1 (R1) and Reactor 2 (R2), based on all quantifiable VFA (C1 to C8) and top four most abundant OTU, as per http://www.mothur.org/wiki/Braycurtis.

The two reactors were dominated by an uncultured *Clostridium* species (Otu004) with 95 % similarity to *Clostridium sp.* BS-1 over 427 bp. This operational taxonomic unit (OTU) correlates with the concentration of hexanoic acid and total VFA (Figure 2.4), and the relative abundance of this species coincides with periods of high octanoic acid and the detection of decanoic acid in both reactors (Figure 2.2). This species will be referred to here as *Clostridium sp.* BS-1_{sec} (*ie.* secundum) for brevity, as although it is a relation to *Clostridium sp.* BS-1, the results do not conclusively identify this strain as such. *Clostridium sp.* BS-1 was recently identified as a D-galactitol consuming, fermentive micro-organism capable of producing acetic acid, butyric acid and hexanoic acid. Another highly abundant OTU was identified as *Clostridium sp.* CPB-6 (Otu008) with 100% similarity over 427 bp, and this OTU showed a correlation with heptanoic and octanoic acid, and high total chain elongation (*i.e.* the cumulative total concentration of VFA greater than C5 chain length) (Figure 2.4), though its relative abundance fell as octanoic acid concentration rose (Figure 2.1 C and D). No further information exists on the *Clostridium sp.* CPB-6 strain though it is closely related to *Clostridium sp.* BS-1, and likely a member of the *Clostridium* group IV, with a 96 % similarity identified in Otu022. *Clostridium sp* BS-1_{sec} had the greatest relative abundance in both reactors with the exception of day 20 in Reactor 2. In the most stable period of consistent hexanoic production, Reactor 2 had an average *Clostridium sp* BS-1_{sec} relative abundance of between 15 and 46 %, *Clostridium sp.* CPB-6 between 22 to 32 %, and *Lactobacillus spp.* between 16 and 40%. *Lactobacillus spp.* are fermentive micro-organisms that can convert a wide variety of substrates into lactic acid, including glycerol (Cantoni and Molnar, 1967). Lactic acid can be used by some micro-organisms, including some species in the *Clostridium* Group IV (Zhu et al. 2015) to elongate the VFA chain from acetic acid (C2) through butyric acid (C4) to hexanoic acid (C6), and our results indicate this may continue through octanoic acid (C8) and decanoic acid (C10). *Acetobacter sp.*, present in both reactors, is an obligate aerobe that is able to convert ethanol into acetic acid in the presence of oxygen (Cleenwerck et al. 2002). There was no significant identification of methanogenic archea, nor detection of methane in the headspace. The reactors were fed from an identical source, an undiluted mixture of biorefinery beer and stillage that was not stored anaerobically, which could account for the abundance and survival of this bacteria. The feed had an average (n = 6) relative abundance of 72 ± 19% for *Lactobacillus spp.,* 22 ± 19% for *Acetobacter sp.,* 3 ± 5 % for *Gluconobacter sp.,* and 3 ± 1 % of other species.

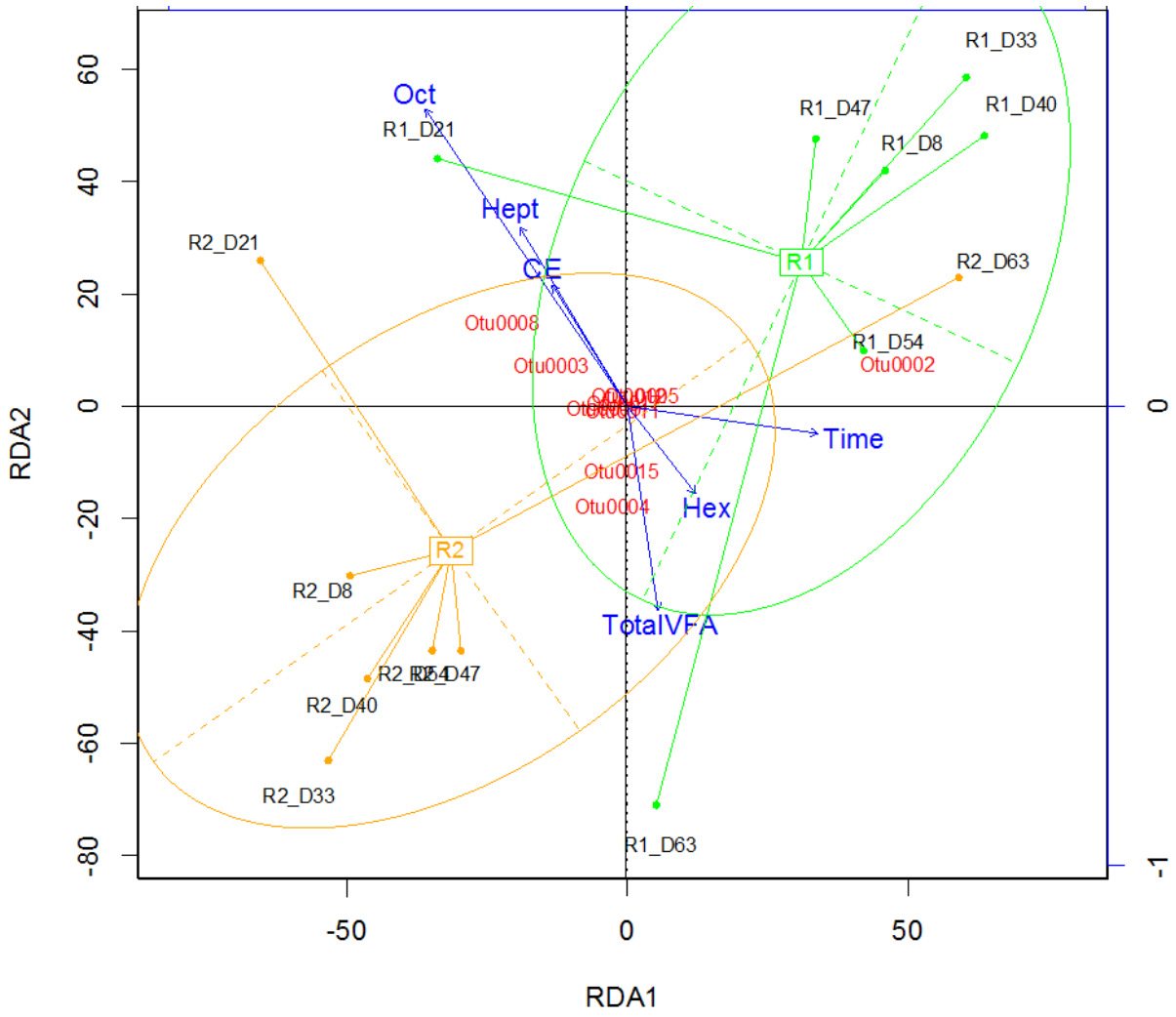

Figure 2.4. Redundancy analysis demonstrating the alignment of octanoic acid (Oct), heptanoic acid (Hep) and CE (chain elongation, *ie.* concentration of volatile fatty acids greater than C5 chain length) in the opposite direction to the Total VFA and hexanoic acid (Hex) concentration.

2.3.2 MCFA toxicity decreases hexanoic acid production by suppressing the supporting community. One must take care when implying function from relative abundance, however some inferences can be made by correlating the VFA products with relative abundance, combined with functional knowledge from previous studies. *Clostridium sp* BS-1_{sec} is the only species identified with a high relative abundance recognized to produce hexanoic acid, likely through the reverse β oxidation pathway, which in principal could also produce octanoic acid and decanoic acid, though decanoic acid has

not been previously reported as a product of the reverse β oxidation pathway, though it has been described in the β oxidation pathway. As a close relative, *Clostridium sp*. CPB-6 is likely to also produce hexanoic acid, but there appears to be an antagonistic relationship between the two species. There is a significant linear correlation between the concentration of octanoic acid and the ratio of *Clostridium sp* BS-1_{sec} to *Clostridium sp*. CPB-6 (R^2 = 0.63, p = 0.003, n = 12), and a weaker but still significant correlation for the detection peaks of decanoic acid (R^2 = 0.25, p = 0.006). When both species have similar proportions, the concentration of octanoic is low, however the further *Clostridium sp* BS-1_{sec} exceeds *Clostridium sp*. CPB-6 in abundance, the greater the concentration of octanoic acid. This may be a result of MCFA toxicity decreasing the relative abundance of *Clostridium sp*. CPB-6, or the capacity of *Clostridium sp*. BS-1_{sec} to thrive by generating MCFA through the reverse β oxidation pathway. Octanoic acid has been reported as product of *Clostridium kluyveri* in mixed cultures (Steinbusch et al. 2011, Spirito et al. 2014), however not explicitly confirmed for any species in pure culture studies. The kmeans clustering of points (Figures 2.2) distinctly separates the negative detection case from the positive case, with the positive C10 detection peak clusters co-occurring with high concentrations of C8 and a high relative abundance of *Clostridium sp*. BS-1_{sec}. This supports the hypothesis that the domination of *Clostridium sp*. BS-1_{sec} leads to C8 and C10 MCFA, but here we cannot conclusively state that C10 is a result of reverse β oxidation production, as opposed to the presence of lipid fragments from dead cells, for example fragments of lactobacillic acid.

Clostridium sp. BS-1_{sec} is tolerant to MCFA under these conditions, it is the only species in the community that increases in relative abundance during high octanoic acid concentration, reaching a maximum relative abundance of 78 % in Reactor 1 and 80 % in Reactor 2. Some species within the *Clostridium* group IV have been observed to remain productive up to a hexanoic acid concentration of 25 g L^{-1} (Zhu et al. 2015). In Reactor 1, *Clostridium sp*. CPB-6 reached a relative abundance of 34 % by day 20, and then fell to between 1 and 7% when the octanoic acid concentration rose in the broth. During this period, the relative abundance of *Lactobacillus spp*. shifted between 1 and 20%. In Reactor 2, as *Clostridium sp*. CPB-6 decreased, *Acetobacter sp*. increased in relative abundance to between 3 and 20% from day 20 to 55, before decreasing to less than 1% by the end of the experiment when octanoic acid was at its greatest concentration. The relative abundance of *Clostridium sp*. BS-1_{sec} rose to a maximum of 80 % in Reactor 2 at this octanoic maximum, with the relative abundance of *Clostridium sp*. CPB-6 at 2%, and *Lactobacillus spp*. at 3%.

As mentioned, in Reactor 1 there was a near-total consumption of glycerol until day 25, followed by a shift to almost zero as the octanoic acid concentration rises. This is an indication that the species responsible for glycerol consumption, likely to be *Lactobacillus spp.*, were surpressed by octanoic acid. The *Lactobacillus spp*. OTU 0001 was identified as having a statistically significant effect on total VFA concentration ($p = 0.0016$), an indication that it plays a significant role in carbon conversion.

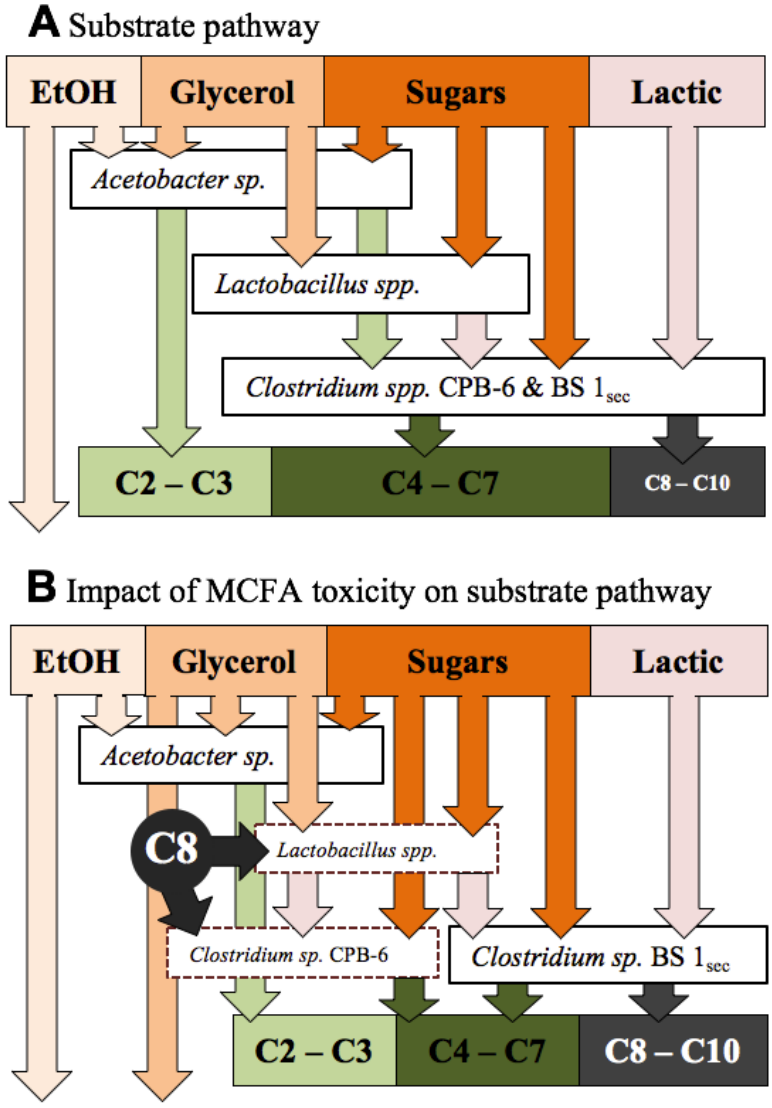

Figure 2.5 A. The proposed substrate pathway for the fermentation prior to the onset of MCFA toxicity, as observed day 14 to 21 in Reactor 1, and day 14 to 52 in Reactor 2. **B** The hypothetical impact of MCFA toxicity on the proposed substrate pathway, as observed from day 21 to 68 in Reactor 1. The red-dashed borders represent stressed, low relative abundance species.

2.3.3 An uncultured species related to the *Clostridium* group IV. A phylogenetic tree analysis (Figure 2.6) of the *Clostridium* species referred to here as *Clostridium sp.* BS-1_{sec} was generated through long 16S rRNA sequencing based on a sample from Reactor 1 on Day 34 in which its relative abundance was 76 % (Figure 2.1C). *Clostridium sp.* BS-1_{sec} has a 95% maximum similarity with *Clostridium sp.* BS-1 according to the BLAST database, with a close relationship to *Clostridium sp.* CPB-6. Both of these *Clostridia* appears to be of the *Clostridium* group IV, recognized as butyrate producers in the gut microbiome (Lopetuso et al. 2013), and capable of elongation of VFA through lactic acid to hexanoic acid (Zhu et al. 2015).

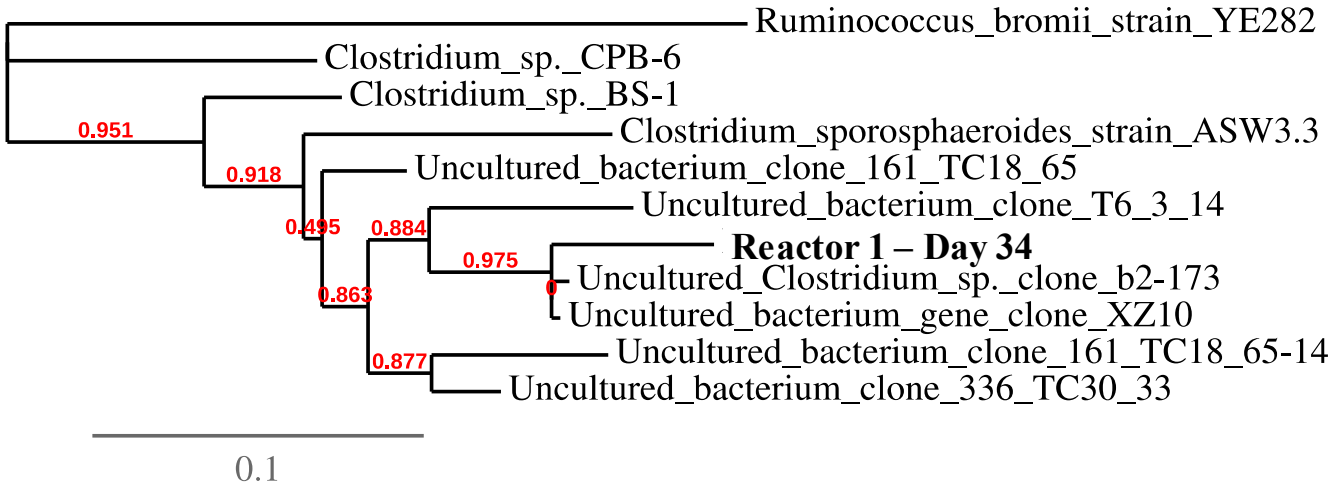

Figure 2.6. Phylogenetic tree at species-level resolution showing some genetic heterogeneity among close relatives of the dominant sequence of Reactor 1 on day 34. The scale bar indicates 0.1 estimated changes per nucleotide. The alignment considers 974 bp of the phylogenetic gene maker16S rRNA.

2.4 Discussion

Octanoic acid has been detected in mixed community MCFA fermentations (Eerten-Jansen et al. 2013, Steinbusch et al. 2011, Spirito et al. 2014), but has not been conclusively identified as a product of reverse β oxidation. This is partly due to the fact that it is not commonly accepted as a likely product, and therefore not commonly tested in analysis. Hexanoic acid production has been observed through reverse β oxidation at up to 23.4 $g.L^{-1}$ (Zhu et al. 2015), which entertains the possibility that some of these micro-organisms attempt to exact more energy by sending hexanoic acid though the reverse β oxidation pathway again. This fermentation by Zhu et al. (2015) is dominated by *Clostridium* Group

IV species engaged in lactic acid elongation, and it is not reported if the broth was tested for MCFA longer than C6. Reports of octanoic acid production are rare and exclusive to mixed culture fermentations, and reports of decanoic acid as a microbial product are non-existent. In this study, the co-occurrence of the detection peaks with a high relative abundance of *Clostridium sp* BS-1_{sec} and high concentrations of octanoic acid adds weight to the hypothesis that decanoic acid may be an unreported reverse β oxidation product that occurs once a threshold of octanoic acid has been passed, and the elongating species, in this case *Clostridium sp*. BS-1_{sec}, has out-competed the flanking community to the point at which the available carbon and energy becomes limited. One counter argument is the decanoic acid is associated with the cellular fatty acids from the collapsing flanking community, such as *Lactobacillus spp*., that coincides with the on-set of the detection of octatonic acid or with sustained exposure to hexanoic acid. Cellular fatty acid fragments from the cells may fit some of the correlations used here to support the hypothesis of decanoic acid through reverse β oxidation. The increase in relative abundance of *Clostridium sp*. BS-1_{sec} can be viewed as the collapse in relative abundance of all other species, and the cellular fatty acid profile of *Lactobacillus spp*. consists of large portions of 2-hexyl-cyclopropanedecanoic acid (lactobacillic acid, $C_{19}H_{36}O_2$), which contains a decanoic acid chain. To negate this possibility, *Lactobacillus spp*. should be isolated, killed with MCFA and its fatty acid profile analyzed, and *Clostridium sp* BS-1_{sec} should be isolated and coaxed to MCFA production to conclusively distinguish the source of the decanoic acid peaks.

Environmental factors such as temperature, pH, organic loading and residence time, and to a certain extent, the mixed community inoculum, are under our control in an engineered system. In this study all these factors were controlled in two identical reactors, chosen to be most conducive to the production of hexanoic acid, as is common practice in a mixed microbial community anaerobic MCFA fermentation. Though both reactors had similar VFA profile (high functional similarity), a high community dissimilarity that arose alongside *Clostridium sp*. BS-1_{sec} domination suggests that octanoic acid and decanoic acid suppressed the activities of the rest of the community to the detriment of overall production. *Lactobacillus spp*. in particular decreased in relative abundance, which is likely to have resulted in a negative impact on conversion of the stillage into VFA. At the highest concentration of octanoic acid (day 39) in Reactor 1, the total VFA concentration was 59 % of the total maximum VFA concentration (day 15). This phenomenon of a co-occurrence in an octanoic peak and a total VFA trough arose independently in each reactor, with the effect separated temporally by around 35 days. The highest concentration of hexanoic acid

occurred in Reactor 2, and coincided with a minimum relative abundance of one of the likely producers of hexanoic acid, *Clostridium sp.* BS-1_{sec}, during a period where *Clostridium sp.* BS-1_{sec}, *Clostridium sp.* CPB-6, and *Lactobacillus spp.* each had a similar relative abundance in the vicinity of 15 to 40 %. The greatest relative abundances of *Clostridium sp* BS-1_{sec} coincided with a relatively low hexanoic acid concentration, and a low total VFA concentration.

It is complicated to parse the origin of octanoic and decanoic acid, the rise in the relative abundance of *Clostridium sp.* BS-1_{sec} and the equal and opposite decrease in relative abundance of the other species, but the co-occurrence of *Clostridium sp.* BS-1_{sec} with the toxic octanoic acid product highlights the process risk of a winner-takes-all approach, and encourages research into the interplay of the complex and competitive microbial community to engineer a stable, productive process that generate sustainable, valuable bio-chemicals. A monopoly of a species such as *Clostridium sp.* BS-1_{sec} that can both produce and tolerate high concentrations of MCFA may be suitable in unified feed (e.g. an acetic and lactic acid rich stream), but in the case of a complex, diverse substrate the interplay and performance of the community must be engineered, and in the case of MCFA, protected from toxicity. Rather than optimizing reactor conditions to the benefit of *Clostridium sp* BS-1_{sec}, perhaps a better approach is ensuring a diverse biological economy to optimize anaerobic digestion and fermentation, through the extraction of the problem compounds. An *in situ* extraction of the toxic MCFA products may protect both the productive species and the full fermenting community, and enable greater conversion and continued production (Xu et al. 2015).

CHAPTER 3

Membrane Electrolysis

This chapter is redrafted from:

Stephen J Andersen, Tom Hennebel, Sylvia Gildemyn, Marta Coma, Joachim Desloover, Jan Berton, Junko Tsukamoto, Christian Stevens and Korneel Rabaey, Electrolytic Membrane Extraction Enables Production of Fine Chemicals from Biorefinery Sidestreams; *Environmental Science & Technology,* **2014**; 48 (12), pp 7135–7142; DOI: 10.1021/es500483w

Stephen J Andersen, Korneel Rabaey and Xochitl Dominguez-Benetton, An Electrochemical Impedance Spectroscopy Characterization of the Membrane Electrolysis of Acetic Acid, (*Manuscript in preparation*).

3.0 Abstract

The anions of carboxylic acids at low concentrations can migrate across an anion exchange membrane (AEM) by applying an electrical current. In the process of membrane electrolysis, carboxylic acid solutions undergo water reduction in a cathodic chamber, and a clean, saline solution undergoes water oxidation in an anodic chamber, separated by an AEM. Carboxylic anions flux across the AEM to close the circuit, resulting in a carboxylic acid concentrate, while also excluding solids are biomass. As the anodic chamber acidifies, the carboxylic acid becomes uncharged, allowing the product to accumulate with ongoing flux. This process can be applied to any carboxylic acid, such as acetic acid or hexanoic acid, provided that the anion has sufficient electrical mobility within the AEM. Electrochemical Impedance Spectroscopy (EIS) can be used to characterize the transport properties of the carboxylic acid anions and the exclusion of protons by their apparent (pseudo-)capacitance as they encounter the membrane. In this chapter, acetic acid and hexanoic acid flux are demonstrated in a selected AEM, followed by a characterization of acetic acid transport through an anion exchange membrane using EIS. Acetic acid had a coulombic efficiency (flux of anion / total applied current) of greater than 90 % at 170 mM (10 g L^{-1}) at an applied current density of less than 30 A m^{-1}. Acetic acid fluxes more efficiently through the AEM than hexanoic acid at concentrations below 170 mM, which indicates that there are some electrical and physical interactions at the membrane surface that differs between acetic acid and hexanoic acid anion flux under the conditions tested here. From the EIS analysis, the polarization resistance of the membrane was extracted from the impedance response and related to the electrical mobility of acetic acid through the membrane, determined to be $(1.40 \pm 0.30) \times 10^{-8}$ m^2 V^{-1} s^{-1}. Understanding and characterizing the transport phenomena of carboxylic acid products through an AEM, and the equally important exclusion of protons, is the first step towards improving the efficiency and efficacy of membrane electrolysis.

3.1 Introduction

VFA fermentations are generally optimal above the pKa of their products, and this the products exist in the free broth as negatively charged acid salts. These products can be driven by electro-migration through an AEM under an applied current. Membrane electrolysis not only extracts charged products, but performs water electrolysis directly in the fermentation broth and extract. The predominant products of water electrolysis are OH^- and H_2 at the cathode, and O_2 and H^+ at the anode, and therefore increases the pH of the cathodic chamber and decreases the pH of the anodic chamber. Ion exchange membranes are also capable of excluding solids, microorganisms, and uncharged molecules larger than the effective pore size of the membrane, and thus membrane electrolysis can also act as a clarification of the broth (Strathman 2005).

The objective of this research was to demonstrate the electrolytic membrane extraction of short (C2) and mid-chain (C6) carboxylic acids, followed by a deeper mathematical description and analysis by Electrochemical Impedance Spectroscopy (EIS). EIS is used to reveal the transport properties of membrane electrolysis, focusing on the transport of the dissociated acetic acid anion across an anion exchange membrane into an acidic medium, and the exclusion of protons in the opposite direction. Acetic acid was used as the model carboxylic acid since acetic acid is a low cost and ubiquitous VFA fermentation product.

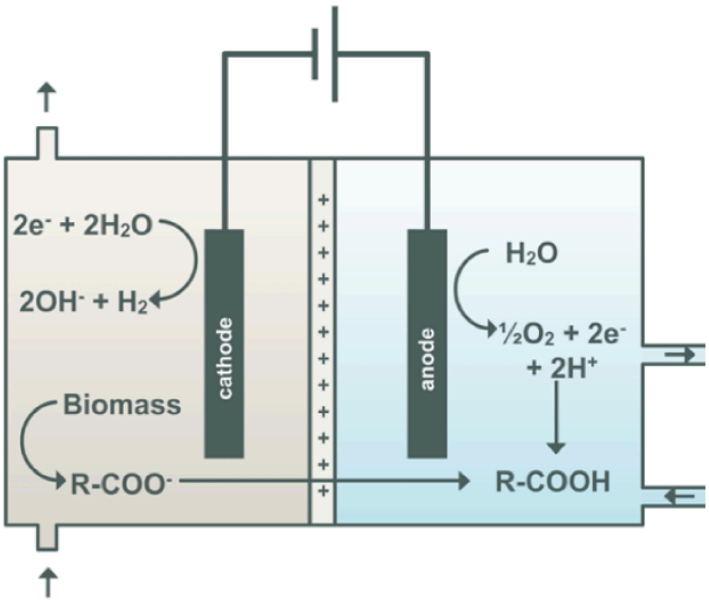

Figure 3.1. Schematic of membrane electrolysis integrated into VFA fermentation. Image by Tim Lacoere.

Impedance is the non-ideal opposition to the passage of an alternating current (AC) when an alternating voltage (AV) is applied to an electrochemical system. It is quantified by the complex ratio of AV to AC, distinguishing the pseudo-resistive components (in the real domain) and the phase shift components (in the imaginary domain) (Heaviside 1888, Kennelly 1893, Macdonald 2006). EIS is a powerful technique for the characterization of non-ideal resistances and has been used previously to reveal transport parameters of water permeable membranes and ion-exchange membrane systems (Sistat et al. 2008, Moya 2014). In engineered systems, it is most common to characterize the transport of inorganic salt and water, such as in reverse osmosis, nanofiltration, and others. Some examples of parameters extracted through with EIS include estimations of the diffusion coefficient or Schmidt number of fluids (Tribollet and Newman 1988); interfacial, boundary layer and internal resistances (Długołecki et al. 2010, Moya 2015); dielectric properties (Efligenir et al. 2015) and operational assessments, such as real-time monitoring of fouling (Cen et al. 2015). Many studies explore ion transport from the electrolyte bulk to the membrane surface, for example the diffusion region and electric double layer (Długołecki et al. 2008, Dominguez-Benetton et al. 2012, Moya 2015). EIS analysis reveals (pseudo-)capacitive and (pseudo-)resistive elements in an electrochemical system, and is therefore well-equipped for investigating the carboxylic acid flux (pseudo-) capacitances and (pseudeo-)resistances across an AEM in membrane electrolysis. With greater knowledge of the core electrokinetic transport properties we hope to enable development of highly effective ion exchange membranes in terms of increased flux of the target ion and exclusion of counter-ions. With this work we aim to link core properties of the AEM with relevant parameters extracted from EIS.

3.2 Materials & Methods

3.2.1 Electrochemical cells for flux characterization. The Sands Plot experiment was executed in the same electrochemical cell described in Długołecki et al. (2010a) purchased from Wetsus (The Netherlands) to test the linearity of electrochemical transport into the AEM at high currents and low concentrations. For the flux characterization in the larger cell, perspex electrochemical cells with two chambers separated by a membrane, each with internal dimensions: 80 mm (l) × 80 mm (w) × 20 mm (d), were used with spacer material (ElectroCell A/S, Denmark) between the surface of the electrode and the AEM. The

membranes (AM-7001 Anion Exchange Membranes, Membranes International Inc, USA, and fumasep FAB, FumaTech GmbH, Germany) were pre-treated in accordance with manufacturer specifications. The anode was an Ir MMO coated titanium electrode (IrO_2/TaO_2: 0.65/0.35), 80 mm × 80 mm, with a centrally attached, perpendicular current collector (Magneto Special Anodes BV, The Netherlands). The cathode was a stainless steel 316L mesh. For high current, high concentration experiments, a low volume two chamber electrochemical cell was used (internal dimensions 70 mm (l) × 10 mm (w) × 20 mm (d) with 50 mm × 10 mm effective membrane area) with a single pass of electrolytes at 1.54 L d^{-1} per chamber for a comparative experiment with minimal use of the expensive sodium hexanoate substrate. The anolyte consisted of sodium sulfate, corrected to pH 2 with sulfuric acid. Synthetic catholyte consisted of a sodium acetate or sodium hexanoate solution (Sigma Aldrich, Belgium), corrected to pH 5.5 with sulfuric acid. The anode and cathode batch experiments were performed with equal volumes of electrolyte at 2 L. Both compartments were continuously stirred at a recirculation rate of 6 L h^{-1}.

All electrochemical experiments were controlled with a VSP multipotentiostat (Princeton Applied Research, France) and an Ag/AgCl reference electrode (+0.197 V vs. SHE, Princeton Applied Research, France) in the cathode compartment. The applied current is reported as current density, defined as the set current divided by the exposed geometric surface area of the AEM, the limiting component of the electrochemical system. The predominant anodic reaction was the oxidation of water ($2\ H_2O \rightarrow 4\ H^+ + O_2 + 4e^-$). The cathodic reaction was the reduction of water ($2\ H_2O + 2e^- \rightarrow H_2 + 2\ OH^-$). All experiments were performed at room temperature.

3.2.2 Membrane electrolysis and flux analysis. Sodium acetate or sodium hexanoate in synthetic broths were tested for flux through an AEM at various current densities (AM-7001 Anion Exchange Membranes, Membranes International Inc., Ringwood, NJ; and fumasep FAB Anion Exchange Membrane, FumaTech BWT GmbJ, Baden-Württemberg, Germany). Next, the anolyte was altered for two synthetic experiments with acetate (i) the concentration of sodium sulfate was increased in the anode to observe the trend of the flux of acetate relative to anode salinity, and (ii) the concentration of sodium acetate at pH 2 was increased in the anode to observe the trend of the negative (anode to cathode) acetic acid diffusion relative to positive acetic acid electromigration (cathode to anode). For these experiments the fluxes were tested at 20 A m^{-2} only. In all cases current density was set at 1.6 mA m^{-2} (a galvanostatic setting of -0.1 mA controlled at the cathode) for at least 4 h

prior to the run to allow for electrode and membrane polarization, then was changed to the set current density of interest. Hydroxide ions generated by water reduction were mitigated by 1 M sulfuric acid by a pH controller (Consort, Belgium). The Sands Plot experiments were executed in the method described in Długołecki et al. (2010a), in which current densities of up to 600 A m^{-2} were applied to a circular AEM with a diameter of 10 mm to record the transition time under galvanostatic control. Carboxylic acid concentrations were measured by gas chromatography (GC), as described in Chapter 2 All ME experiments were performed in triplicate, and error bars represent the standard deviation of the measured samples.

3.2.3 Experimental cells for EIS characterization. An experimental cell was designed to focus the EIS response upon the membrane and minimize external interferences. All experiments were performed in a two chamber, perspex electrochemical cell with internal dimensions of 50 mm (l) × 10 mm (w) × 20 mm (d) per chamber (*i.e.* 20 mm from electrode to membrane), with a hemispheric bevel in the inlets and outlets. This geometry allowed for a stable, single pass flow that was experimentally observed to allow good stability of the electrochemical response (±1 mV variation in whole cell potential with a fixed current). Two reference electrodes (Ag/AgCl, +0.197 V vs SHE, Princeton Applied Research, France) with outbound capillaries filled with 3 M KCl achieved close proximity to both sides of the membrane. The reference electrodes were placed in each chamber at identical and opposite positions on either side of the membrane. The anode was a flat Ir MMO-coated titanium plate electrode (IrO_2/TaO_2; 0.65/0.35, Magneto Special Anodes BV, The Netherlands) while the cathode was a 316 stainless steel plate, which was again observed to generate a more stable response compared to the wire mesh. 50 mm × 10 mm of flat plate electrode and membrane projected surface was exposed in each chamber. Membranes (AM-7001 Anion Exchange Membranes, Membranes International Inc., Ringwood, NJ) were pretreated in accordance with manufacturer specifications (http://www.membranesinternational.com/tech-ami.htm). The cell was oriented vertically, with the electrolyte entering from the bottom of the cell for a single pass. All electrolytes were prepared in distilled water. Cathodic electrolyte was sodium acetate brought to pH 5.5 with sulfuric acid, while the anode consisted of 10 mM sodium sulfate brought to pH 2 with sulfuric acid (all chemicals: Sigma Aldrich, Belgium). As above, the anodic reaction was the

oxidation of water ($2\ H_2O \rightarrow 4\ H^+ + O_2 + 4e^-$) and the cathodic reaction was the reduction of water to molecular hydrogen ($2\ H_2O + 2e^- \rightarrow H_2 + 2\ OH^-$).

All electrochemical experiments were controlled with a VSP multipotentiostat and frequency response analyzer (Princeton Applied Research, France). The cell was controlled galvanostatically for each defined direct current and then switched to direct potentiostatic control at the previously measured potential prior to the single-sine EIS run. The frequency range was from 10 kHz to 1 mHz, with six points recorded per logarithmic decade at an amplitude of 5 mV. This was observed to be the lowest amplitude for consistently acceptable data, while maintaining response linearity. The electrochemical system was confirmed for linearity, causality, finiteness and stability as described in Dominguez-Benetton et al. (2012). If the majority of the EIS spectra data did not correlate well with a Kramers-Kronig transform, the run was discarded and the source of the disturbance was isolated and removed (deviation from Kramer-Kronig is plotted in Figure 3.7). Stability was defined as less than 1 mV of variation in whole cell potential (E_{we} - E_{ce}) for at least 1 h immediately prior to the EIS run. Each EIS run was performed in triplicate with independent media, with the average of each signal used in the figures and data processing. This was also applied to the control cases (Figure 3.6).

3.2.4 Model definition. The impedance response can be described by deterministic models of the physicochemical processes occurring at the interfaces of interest of an electrochemical system. Contrary to fitting with equivalent circuits, approximation of the EIS response with deterministic models can provide insight on fundamental processes, kinetic rates, mass transfer limitations, mechanistic steps, as well as material properties (Dominguez-Benetton et al. 2012). The road taken here is that of deterministic models as the purpose is to expand our knowledge on the underlying phenomena of ME. Figure 3.2 shows the regions represented in the mathematical description.

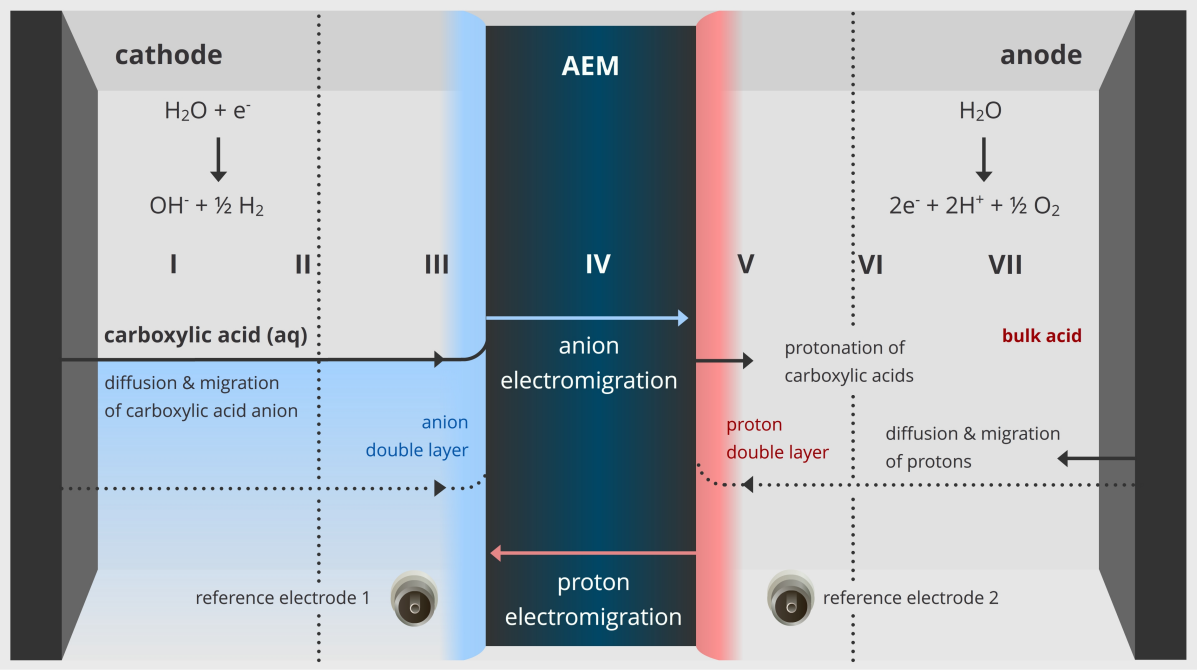

Figure 3.2. Regions of interest described in the mathematical model. Image by Tim Lacoere.

A membrane electrolysis cell is comprised of two solutions separated by an ion exchange membrane. One solution contains a defined concentration of ions (C_i) to be extracted into the second solution. Acetic acid (pH 5.5) is extracted into an acidic (pH 2) solution. The region of interest and the region of measurement are defined in Figure 3.2. Regions I and VII are two bulk solutions assumed to be perfectly mixed and constantly replenished for an unchanging bulk H_i (protons) and C_i concentrations. Regions II and VI are diffusion layers on either side of the membrane associated with transport in the bulk towards the surface of the membrane. Regions III and V are the interfacial Donnan layers that give rise to the electrical double layer in equilibrium, with Region III the double layer of carboxylic acid anions and Region V the proton double layer. Region IV is the AEM. Positive flux is considered when C_i moves from the cathode to the anode (*i.e.* from left to right in Figure 3.2). The concentration of the bulk carboxylic acid in Region I and II is variable, set at the beginning of each experiment. The concentration of the carboxylic acid increases towards the surface of the membrane in Region III, the carboxylic acid double layer. At steady state, the concentration of carboxylic acids in the AEM at Region IV is considered to be constant for each concentration considering the fixed charge density of the AEM and the requirement of electro-neutrality. The flux of carboxylic acids out of the membrane at Region V is therefore dependent on the charge density of the membrane and

the applied current. The AEM is not completely permselective, and will therefore also contain some flux of protons in the negative direction (anode to cathode). The proton double layer at Region V will also be the site of protonation or acidification of the carboxylic acids which transport through the membrane, ultimately negating their charge. In this study, the pH and therefore proton concentration remains set due to the constantly replenished bulk solution, which results in a constant proton concentration through Regions VI and VII. Diffusion and migration from the applied current will draw the protons towards and through the AEM, according to the membrane permselectivity and concentration of acetic acid in Regions I, II and III.

For all EIS measurements, the system is considered to be under a non-equilibrium steady state with a partial exclusion of protons. We reiterate that the experimental set-up was designed to focus the frequency response analysis upon the membrane sector with the two reference electrodes placed directly opposite one another, and as close to the membrane surface as possible. All of the regions we describe here will impact the EIS response, but given the deliberate positioning of the reference electrodes the major contribution to the total impedance narrows down to Regions III, IV and V.

The membrane is considered to be homogeneous and the membrane structure is not taken into account. The Nernst-Planck equation describes the transport of ions through the membrane (Nikonenko et al. 2002, Sistat et al. 2008, Moya 2014). The molar flux of species i (N_i, mol m^{-2}) due to diffusion, migration and convection across the AEM is represented by the following one dimensional model:

$$N_i = -\mathrm{D_i}\nabla C_i - z_i \mu_{\mathrm{mobi,i}} \mathrm{F} C_i \nabla \phi_l + C_i \mathbf{u} \qquad (1)$$

Where D is the diffusion coefficient (m^2 s^{-1}), C is the concentration (mol m^{-3}) z is the charge number, μ_{mobi} is the ionic mobility (s m^2 kg^{-1}), ϕ_l is the electrolyte potential (V), $\mathbf{u}$ is the fluid velocity vector (m s^{-1}) and F is Faraday's constant, 96 485.3399 s A mol^{-1} (Moya 2014).

The convective flux across the membrane can be neglected in the absence of a spacer that creates turbidity, the low cross sectional velocity in the experimental cell, and electroneutrality conditions. Equation 1 can be thus reduced to Equation 2:

$$N_i = -D_i \nabla C_i - z_i \mu_{\mathrm{mobi,i}} \mathrm{F} C_i \nabla \phi_l \quad (2)$$

In the electrolyte domains where C_i and H_i are present the gradients of electrolyte concentration are not negligible, but if the assumption that the bulk diffusion is excluded due to placement of the reference electrodes holds, the concentration of permeable ions can be assumed to be constant, and therefore Equation 2 can be reduced to Equation 3 in the membrane domain due to electroneutrality. Diffusion across the membrane was measured and observed to be negligible relative to migration for the concentration range tested and are thus disregarded.

$$N_i = - z_i \mu_{\mathrm{mobi,i}} \mathrm{F} C_i \nabla \phi_l \quad (3)$$

The resulting current density (j, A m^{-2}) will be the sum of all ionic currents (N_i, mol m^{-2} s^{-1}). In the ME system there are also Faradaic currents under steady state conditions, which do contribute to the total impedance of the system (*i.e.* hydrogen and oxygen evolution), but the positioning of the reference electrodes should also mitigate the impact on the overall response. Where there exists a conservation of current, the one-dimensional system can be defined as (Newman and Thomas-Alyea 2004):

$$j = \mathrm{F} \sum z_i N_i \quad (4)$$

Flux through the membrane can also be expressed as a function of the electrolyte conductivity (σ_l, S m^{-1}) as in Equation 5. This is the governing equation to describe the transport of ions within the membrane (Newman and Thomas-Alyea 2004):

$$\mathrm{F}\, N_i = - \sigma_l \nabla \phi_l \quad (5)$$

The charge density within the membrane (*i.e.* the fixed charges of the membrane) is constant and the corresponding variation of ionic concentration is assumed to be negligible. Therefore, the flux of ions *i* through the membrane can be expressed by Equation 6, where t_i is the effective transport number.

$$N_i = t_i \frac{j}{z_i \mathrm{F}} \quad (6)$$

The concentration gradient is considered to be constant throughout the membrane and through the double layer (Sistat et al. 2008). The current density (*j*) can be expressed as the limiting current density (j_{lim}) when the concentration gradients towards the electrical double layers reach their maximum (*i.e.* C_s and H_s at the surface of the membrane, therefore dC_s and dH_s within the membrane is equal to zero).

$$j_{lim} = \frac{\mathrm{F}\, D_i C^b}{\Delta t_i \delta} \quad (7)$$

J mol-1 K-1dedicated to ion mobility, which is not strictly the case in an experimental cell (*e.g.* Ohmic losses, non-Faradaic current) but is assumed to be true for this model.

The total potential (U_{Tot}, V) between the two reference electrodes (left and right, located at both sides in close proximity membrane) is defined as follows (Sistat et al. 2008):

$$U_{Tot} = -\frac{\mathrm{R}T}{\mathrm{F}} \int_{left\ tip}^{right\ tip} E(x)\, dx \quad (8)$$

Where R is the gas constant (8.3145 J mol^{-1} K^{-1}), *T* is the temperature (K), and F is the Faraday's constant.

The following considers the theoretical description of transport in membrane systems as described by Coster et al. (1996) and Długołecki et al. (2010b). The total impedance (Z_{Tot}) of the system at steady state can be regarded as the sum of three contributions between the reference electrodes:

$$Z_{Tot} = -\frac{\partial U_{Tot}}{\partial i} = Z_{dif} + Z_{ohm} + Z_{mig} \quad (9)$$

The ohmic impedance (Z_{ohm}) accounts for the resistance of the electrolyte between the two reference electrodes, the resistance due to diffusion (Z_{dif}) accounts for diffusion near the membrane (within the diffusion regions), and the migration resistance (Z_{mig}) consists of the concentration polarization resistances that arise due to the transport of ions throughout the membrane. These elements can be obtained by measuring the EIS response of the experimental system in operation. Z_{ohm} can be approximated from the intercept of the EIS curve with the real impedance axis, or Equation 10 (demonstrated in Results, Figure 3.8). The concentration polarization resistance can be considered as the sum of the diffusion resistance and the migration resistance, and can be extracted from the semi-circle of the impedance response, or Equation 11. In this way, the contributions to the polarization resistance/impedance (Z_p) or the total impedance (Z_{Tot}) can be evaluated by EIS (Sistat et al. 2008, Dominguez-Benetton et al. 2012).

$$\lim_{\omega \to \infty} Z_{Tot} = Z_{ohm} \quad (10)$$

$$\lim_{\omega \to 0} Z_{Tot} - \lim_{\omega \to \infty} Z_{Tot} = Z_{dif} + Z_{mig} = Z_p \quad (11)$$

Considering Ohm's Law:

$$U_{Tot} = jZ \quad (12a)$$

$$Z = \frac{U_{Tot}}{j} \quad (12b)$$

Substituting Equations 3, 4 and 7 into Equation 12, given the premise of Equation 11, the polarization resistance (Z_p) can be expressed as:

$$Z_p = Z_{dif} + Z_{mig} = \frac{U_{Tot}}{j_{lim}} + \frac{U_{Tot}}{j} \quad (13a)$$

$$Z_p = \frac{U_{Tot} T_i \delta}{\mathrm{FD_i} C_i^b} + \frac{1}{\mu_{\mathrm{mob,i}}} \frac{U_{Tot}}{\mathrm{F} z_i^2 C_i^b \nabla \phi_l} \quad (13b)$$

The diffusion term is negated partly due to placement of the reference electrodes at the surface of the electrode, and partly due the negligibly small diffusional term on the right hand side of Equation 13b. The relatively small concentration (10^{-3} mol m^{-3}), diffusion coefficient (D_i) (12.1×10^{-6} cm s^{-1} for acetic acid, 20×10^{-6} cm s^{-1} for chloride) and diffusion boundary layer thickness of around 10^{-4} to 10^{-6} m (Sistat et al. 2008) (δ) results in a term of 10^{-1} to 10^{-3} ohm, while the second term that pertains to electro-migration, specifically to the migration within the membrane, is in the vicinity of 10^2. The electro-migration term will therefore overwhelm the diffusion term. Dismissing the diffusion term gives Equation 14 (Equations 14a and 14b are interchangeable considering Equation 5), an approximation of the (concentration) polarization resistance (Z_p) in the membrane:

$$Z_p = \frac{1}{\mu_{\mathrm{mob,i}}} \frac{U_{Tot} \sigma_l}{\mathrm{F}^2 z_i^2 C_i^b N_i} \quad (14a)$$

$$Z_p = \frac{1}{\mu_{\mathrm{mob,i}}} \frac{U_{Tot}}{\mathrm{F} z_i^2 C_i^b \nabla \phi_l} \quad (14b)$$

Carboxylic acid concentrations are experimentally set, fluxes were determined analytically and the remainder of the components can be determined from the EIS response. A range of EIS spectra were generated for independent solutions at different concentrations of sodium acetate (pH 5.5), operated at steady state at different current densities. The Z_p values generated from the EIS spectra were compared against a calculated Z_p from the measured potential across the membrane, measured flux of acetate across the membrane an assumed ionic mobility within the membrane of 1.53×10^{-8} m^3 V^{-1} s^{-1}, and the ionic mobility for chloride in dilute solutions (Disabb-Miller et al. 2013), a value assumed to be in reasonable agreement with that of acetic acid as a stand-in value.

The pseudo-resistive part of the impedance response can be explained as described above for the polarization resistance (Z_p), and the total impedance also has pseudo-capacitive contributions. An artefact that is frequently used to model such pseudo-capacitive response is the constant phase element (CPE) (Hirshcorn et al. 2010). The impedance response of this CPE is based on a mathematical representation similar to the

electrical reactance of a pure capacitor, but it considers some deviation in the complex plane, given by an angle of rotation α. The impedance response of a CPE (Z_{CPE}) is represented by Equation 16:

$$Z_{CPE} = 1/(\boldsymbol{i}\,\omega)^{\alpha}\ Q \qquad (15)$$

The CPE parameters Q and α are frequency-independent constants. $\boldsymbol{i}$ is the imaginary unit ($\boldsymbol{i}^{2} = -1$) and ω is the angular frequency ($\omega = 2\pi f$, f being the ordinary frequency in Hz) (Jorcin et al. 2006). Q represents the differential capacitance of the interface, and α is a parameter that is descriptive of the pseudo-capacitive behavior. When $\alpha = 1$, Q represents the differential capacitance of the interface and then Equation 15 becomes equal to that of a capacitor. Thus, the CPE represents a pseudo-circuit element with limiting behavior as a capacitor for $\alpha = 1$, and behavior as a resistor when $\alpha = 0$. However, many electrochemical systems behave somewhere between these two extremes, *i.e.* $0 < \alpha < 1$, and under these circumstances Q cannot represent either a capacitance or a resistance (Hirschorn et al. 2010). In this way, the CPE is used as a flexible parameter for fitting impedance data, but must be related to the electrical and physical processes of the the electrochemical interface rather than forcing strict definitions of capacitance and resistance. The parameter α can be estimated from the graphical representation of impedance relative to the minus imaginary component ($-Z_{Im}$) against the frequency (ω), with both parameters in logarithmic scale (Devos et al. 2006). The first derivative $d(-Z_{Im})/d\omega$ is obtained to determine the relative maxima of the function at $d(-Z_{Im})/d\omega = 0$. The logarithmic slope of the curves on either side of the relaxation frequency directly correspond to the magnitude of α on either side of the relaxation frequency. Each α corresponds to "fast" and "slow" electrochemical processes, with the lower frequency corresponding to slow processes to the left of the relaxation frequency on the x-axis (α_{left}), *i.e.* towards lower frequencies while the higher frequency corresponds to faster processes to the right of the relaxation frequency (α_{right}) *i.e.* towards greater frequencies (demonstrated in Figure 3.6, section 3.3.2).

The existence of a CPE in the model of the EIS response of a AEM interface can be justified from the magnitude of α (Devos et al. 2006), though the physical interpretation cannot be clarified from the CPE mathematical description alone (Hirschorn 2010a and 2010b). CPE parameters may arise from a distribution of time-constants with either normal

or surface distributions. The distribution of these time-constants results from dispersed physical properties, *e.g*. structure, reactivity, dielectric constants, and resistivity. A normal distribution of time constants can be anticipated in systems that involve dielectric- or conductive-dispersion, such as oxide films, organic coatings, skin, and systems with distributed porosity or surface-roughness (Hirschorn 2010a and 2010b). For other systems, the local surface-distributed ohmic resistance ($Z_{ohm,i}$) significantly contributes to the impedance response. An example of this type of geometry-dependent distribution has been suggested for the ideally polarized blocking electrode (Hirschorn 2010b). In the case of the present work, distribution of ion exchange groups at the surface and within an AEM are likely to also lead to such behavior, particularly a distributed transport of different types of competing ions. A normal-distribution of the physical properties of the electrochemical interface is anticipated due to the polymeric AEM, in which the charged functional groups are distributed through the membrane.

Quantitative and qualitative comparisons of the CPE parameters Q and α, together with information provided by the distinct characterization methods can provide insight into the phenomena and mechanisms taking place at the AEM:

$$Q = -\sin(\alpha\boldsymbol{\pi}/2)/|-Im(Z)|\,\omega^{\alpha} \qquad (16)$$

The ω and *-Im (Z)* magnitudes correspond to those evaluated at the relative maximum of the time constant (R_iC_i) in question. The pseudo capacitance can be considered to be proportional to the ion exchange capacity of an AEM. The ion exchange distribution across the membrane is not expected to vary as a function of the experimental parameters, but will be tested with the method described in Długołecki et al. (2010a). A constant α is expected when varying current or concentration of C_i, though the apparent capacitance would indeed change, as this will intrinsically depend on the ratios transported of competing ions which will confer characteristic electrical properties to the AEM at a given condition.

3.3 Results

3.3.1 Membrane electrolysis extraction. In the first phase, we demonstrated membrane electrolysis on synthetic solutions of low concentrations of acetic acid (up to 10 g L^{-1}) as a model compound (Figure 3.3A) in a reactor designed to isolate migration into the membrane (Figure 3.4A). The linearity of the transition time relative to the inverse of the square of the applied current in the Sands' Plot (Figure 3.3A) indicates that the acetic acid anion migration is independent of the applied current density for set catholyte concentrations (Długołecki et al. 2010a). The relationship of flux to increasing current density (Figure 3.3B) in the larger cell (Figure 3.4B) is non-linear, demonstrating that "real" conditions (acid anolyte, larger reactor geometry, etc.) results in a a lower coulombic efficiency, likely due to the competitive transport of ions other than acetic acid.

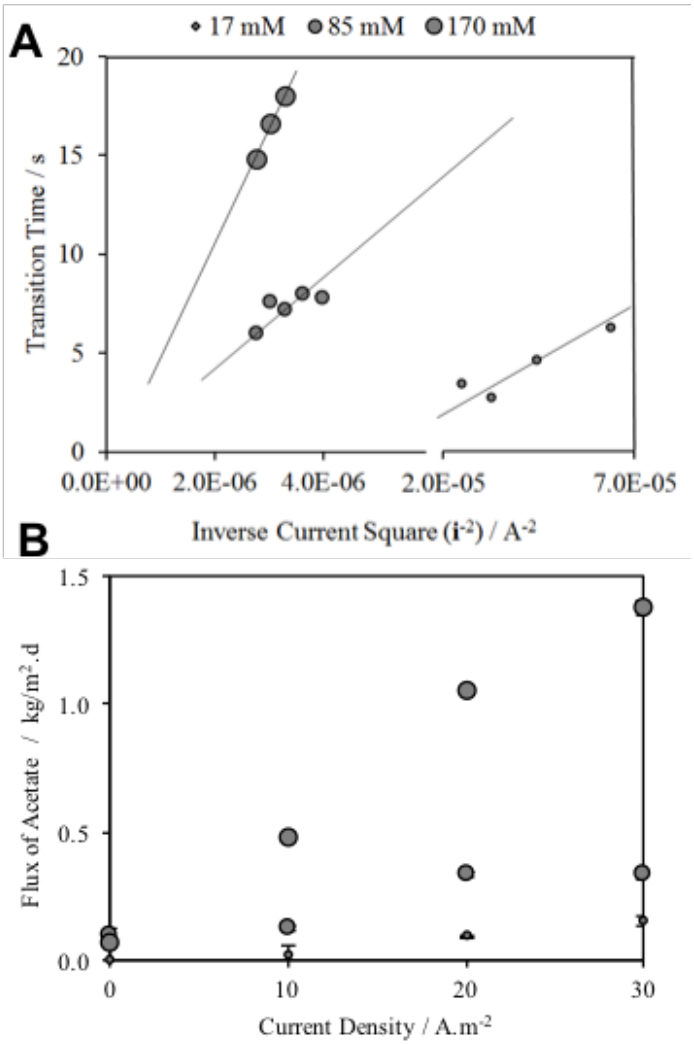

Figure 3.3. Acetic acid anion flux characterization for Membrane International AMI. **A** Sand's plot demonstrating linearity of transition time relative to the inverse of the applied current **B** Membrane electrolysis acetic acid flux measured at 0, 10, 20 and 30 A m^{-2} cell.

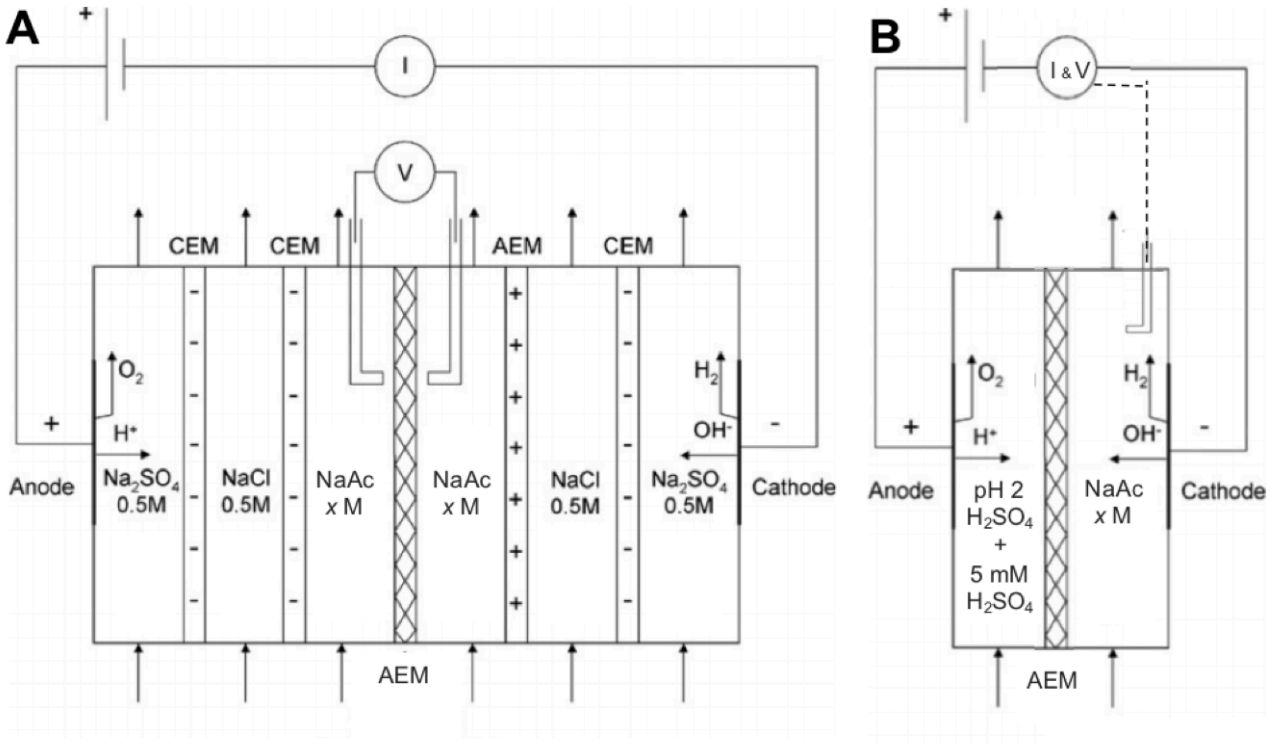

Figure 3.4. Schematic of cell used in Figure 3.3A, as described in Długołecki et al. (2010a), with an effective AEM area of 2.835 cm². **B** Schematic of cell used in Figure 3.3B with an effective AEM area of 100 cm². Adapted after a figure in Długołecki et al. (2010a).

The architecture of an electrochemical cell impacts the transport of ions through the ion exchange membrane, particularly at low concentrations. The study of Długołecki et al. (2010b) showed that transport limitations manifest in the membrane resistance and the ion transport number with low concentration salt solutions (17, 50 and 100 mM NaCl). The electrochemical cell (schematic in Fig 3.4A) was designed to isolate a small area of membrane and measure the transition time, which relates to the time required to exhaust the supply of ions at the surface, and compare this against the inverse of the applied current. This relationship should be linear within an ion exchange membrane if we assume that the transport numbers in both directions do not change at different starting concentrations, and there is no convective transport within the membrane (Sand's equation does not hold for convection). Equation 17 describes this in a modified version of the Sand's equation, where A is the area of the membrane, D_i is the diffusion coefficient, C_o is the starting concentration, t_m is the transport number in the positive direction, and t_s is the transport number in the negative direction (Długołecki et al. 2010b).

$$\tau = A \frac{D_i}{i^2} \left(\frac{C_0 \, \mathrm{F} \, z_i}{t_m - t_s}\right)^2 \qquad (17)$$

In the larger electrochemical cell (schematically described in Figure 3.4B), the transition times couldn't be measured accurately as current densities up to 600 A m-2 are required, but flux compared against applied current gives an indication of the performance when the membrane is not isolated. For an initial catholyte concentration of 170 mM (10 g L^{-1}) the flux of acetate was 1.05 kg m^{-2} d^{-1} at 20 A m^{-2} (coulombic efficiency of 99.4 ± 0.1%). At 30 A m^{-2}, the maximum flux of acetate was 1.38 ± 0.03 kg m^{-2} d^{-1} (coulombic efficiency of 87.0 ± 1.8 %). The extraction efficiency was lower for 1 g L^{-1} and 5 g L^{-1} acetic acid broth, corresponding to less availability of the target anion in the bulk, likely resulting in an increased flux of protons in the negative direction to close the charge balance (Figure 3.3). A target molecule at high concentration (170 mM in this case) will transport efficiently at low current densities (*i.e.* below 30 A m^{-2}), as seen with acetic acid in Figure 3.3, though this will also be dependent on other factors such as applied pressure, temperature, cross sectional velocity, etc. (Strathman 2005). This will impact the real performance in a fermentation that will be described in Chapter 4 and discussed in Chapter 6.

The inherent properties of the membrane and the concentration of other ions in the anolyte also impact transport, demonstrated in Figure 3.5 with two different membranes, the AMI-7001 (Membrane International, United States), and the proton-blocking fumasep FAB (FumaTech, Germany). Increasing the anolyte concentration of salts results in diffusion of negative charge from anode to cathode that must be balanced under the electroneutrality condition. The net flux of acetic acid through the AMI-7001 does not increase, but does for fumasep FAB. To maintain electroneutrality, any passage of ions must be met by an equal and opposite flux, thus sulfate diffusion must be countered by either increasing acetic acid anion positive flux or proton negative flux. The fumasep FAB is marketed as a "proton blocker," and assuming this is true electroneutrality must be met by a net increase in acetic acid flux if proton flux is not an option, as was observed. For the Membrane International AMI-7001, no increase in the net acetic acid positive flux was observed, likely due to negative proton negative flux. Future work should include a greater experimental set to investigate proton/counterion exclusion and transport.

Acetic and hexanoic acids were tested separately at equal molar concentrations (170 mM, corresponding to 10 g.L^{-1} acetic acid and 19.6 g.L^{-1} hexanoic acid, respectively) and display some deviation from linearity for current densities up to 100 A m^{-2} (Figure 3.6). Hexanoic acid and acetic acid display strikingly different efficiency profiles. A sufficiently high molar concentration is critical for effective transport through the membrane, but the deviation of behavior in transport between acetic acid and hexanoic acid indicates that there

is likely to be other physical and chemical interactions at the membrane level that impact flux, either at the surface or within the AEM bulk.

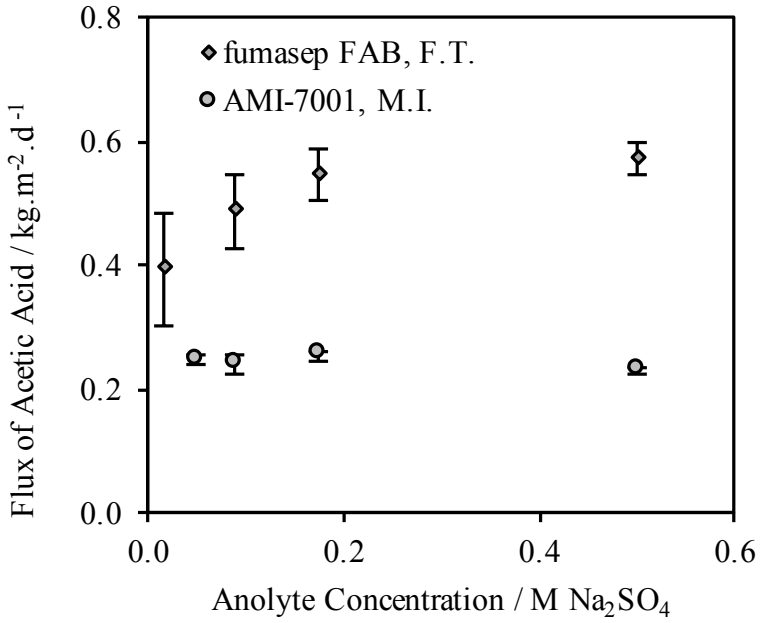

Figure 3.5. Flux characterization for acetic acid anion flux from 5 g L^{-1} catholyte at 20 A m^{-2} through Membrane International AMI 7001 anion exchange membrane and the FumaTech fumasep FAB anion exchange membrane, at different anolyte concentrations of sodium sulfate in the anolyte.

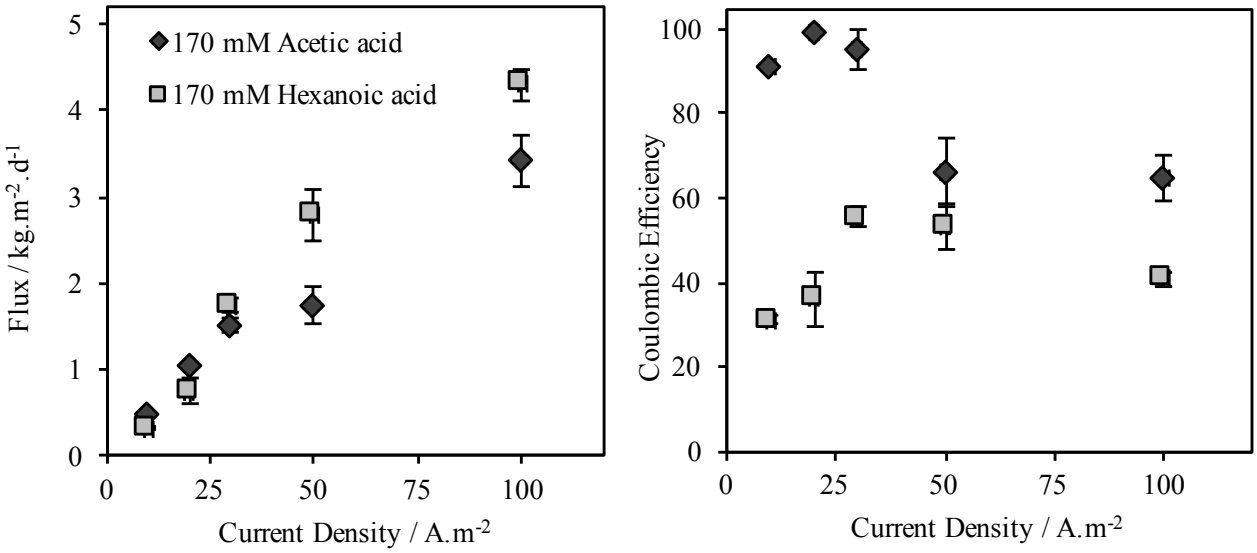

Figure 3.6. Flux characterization for acetic acid anions compared against hexanoic acid anions through Membrane International AMI 7001 anion exchange membrane. **Left.** Flux measured at 0, 10, 20, 30, 50 and 100 A.m^{-2}. **Right.** Coulombic efficiency (%) of the flux experiments.

3.3.2 EIS interpretation: two sides of the same spectra. An ion exchange membrane has two inherent roles, (i) the transport of target ions, and (ii) the exclusion of oppositely charged ions. This functionality in two directions is at the core of membrane electrolysis. Classically, an ion exchange membrane is used for transport and exclusion in the same direction (*i.e.* selective diffusion down a concentration gradient to generate current), while this is not the case in membrane electrolysis, which is more related to electrodialysis where current is applied for ion transport. Here, anions in the positive direction are in competition with protons in the negative direction, and the AEM therefore needs to balance transport of the target acid against transport of protons. An AEM has a high preference for anion transport (*i.e.* positive in the x-axis, direction of flux) over negative proton transport, however unless the AEM has perfect selectivity the negative transport of a positive charge will always occur, and protons are highly mobile.

The transport properties of the positive flux of acetic acid through the AEM in competition with the negative flux of protons can be revealed by an EIS response. The acetic acid anions and the protons will each display unique pseudo-capacitance as they encounter and interact with the AEM, either by transport for the anion, or exclusion (and some transport) in the case of the proton. For anion transport through an AEM, the membrane resistance will be lower and the transition from the double layer to the bulk membrane will require less electrical work. The opposite is true for the proton in the negative direction, which will encounter a greater resistance at the membrane and work is required to negate the electromotive force that drives the proton into the cation excluding AEM. If the concentration of the anion in the bulk is not limiting and we assume the transport efficiency of the applied current is 1 (the applied current = flux of anions) and thus no protons migrate across the membrane, there will still be work done on the protons in migration to and formation of the double layer. The pseudo-capacitance that arises from both anion and proton transport will in result in unique capacitive parameters in an EIS response, demonstrated in Figure 3.4 with the α parameter on the left and right of the phase transition angle. The α parameter is often associated with, but not limited to, an electric double layer (EDL), and can arise when a process displays some effective capacitance when work is required to drive a charge through a resistive impeding element) (Hirschorn et al. 2010b). In the EIS spectra there exists two defining α parameters corresponding to the fast processes (α_{right}) and the slow processes (α_{left}), demonstrated in Figure 3.7.

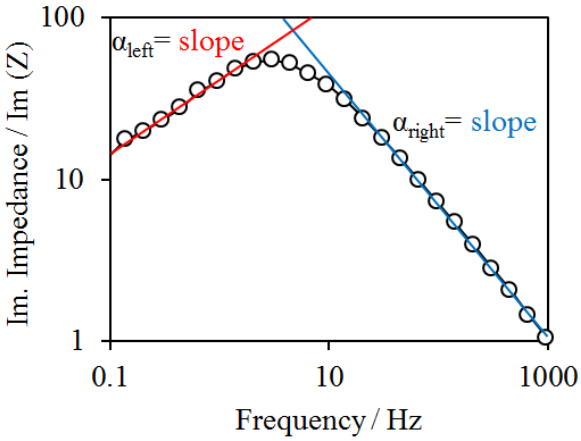

Figure 3.7. Example of the CPE α parameters for acetic acid flux through AMI-7001 as measured from 0.5 mA applied across a cell with 170 mM acetic acid in the catholyte.

The so-called fast processes are those in the frequency range above the maximum phase shift (where $d(-Im\ (Z))/d\omega = 0$) were consistent across all experiments regardless of applied current or bulk carboxylic acid concentration. The α_{right} parameter is around 0.81 with a variation of ± 1 % when compared across all currents and concentrations (Figure 3.8), and holds in the low frequency range for the control case without an AEM (Figure 3.9A). The EIS spectra indicates pseudo-capacitive aspects inherent to a process that is consistent across all applied currents and concentrations of acetic acid, presumably related to the diffusion of acetic acid. The control case with no membrane has a similar α_{right} until the frequency range between 1 Hz and 10 Hz, above which point a deflection begins, indicating a unique pseudo-capacitive effect. The frequency range of this deflection suggests a process associated with mass or momentum transfer, most likely electro-migration within the membrane, while the frequency range above about 10 Hz is generally associated with the physico-chemical processes related to the electrode. The deflections in the low frequency range for the control cases without acid in the anolyte (Figure 3.9B and C) demonstrate that the α_{left} is related to proton processes and transport, while Figures 3.9B and 3.9D demonstrate that the width of the semi-circle created by the EIS response, the polarization resistance in the membrane (Z_p), is a function of both positive anion transport and negative proton exclusion / transport, as the low frequency, right hand tail of the EIS response does not project towards the x axis when no acid is present in the anolyte (Figure 3.9B).

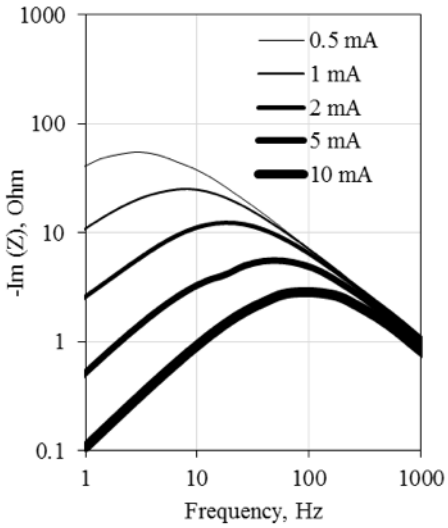

Figure 3.8. Frequency and imaginary impedance relationship for 170 mM acetic acid flux through AMI-7001 Trends in the 5 and 10 mA range at less than 10 Hz are projected data points.

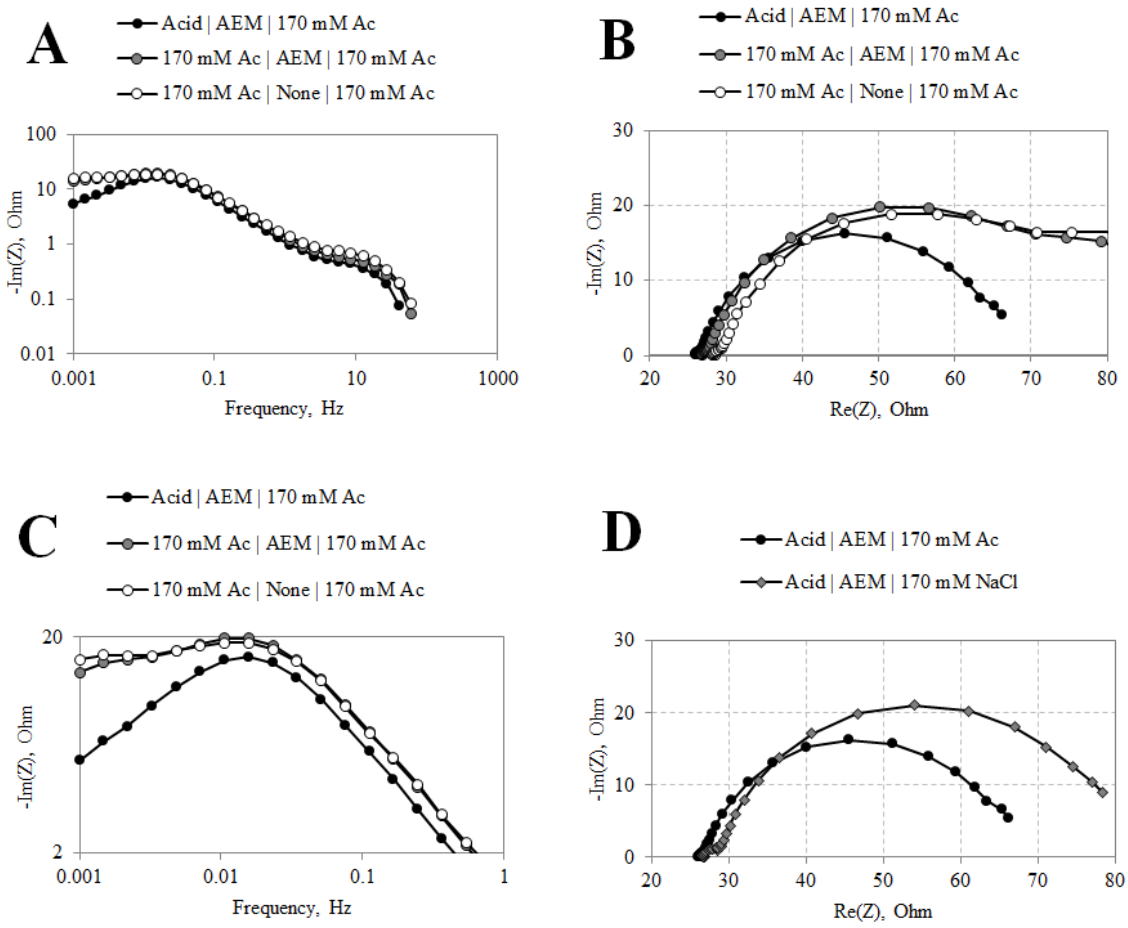

Figure 3.9. Electrochemical Impedance Spectra for comparative control cases. (Catholyte | AEM | Anolyte)

The so-called slow processes (*i.e.* related to α_{left}) include diffusion and counter-ion migration as the defining parameters for transport into the membrane, and may all contribute to the pseudo-capacitive element revealed by the EIS spectra in the frequency range below the phase angle. The measured α_{left} in this slow region behaves differently to the fast processes with increasing current, tending towards a value of 0.85 in a logarithmic relationship between α and the applied current. At a low applied current this parameter denotes a more heterogeneous distribution of electrical properties tending to more homogenous as the applied current is increased. The processes in question are observed at a higher frequency, with the frequency of the phase angle shifting from 3 Hz at 0.5 mA applied current to 86 Hz at 10 mA. This is due to the pseudo-capacitive behavior of the cationic counter-ions transitioning from a predominantly diffusive effect into the balance of EDL capacitance and transport through the membrane. In comparison, the control case without acid in the anolyte (Figure 3.9C) the pseudo-capacitive component is not evident. The low frequency domain is therefore the most critical to parameters inherent to proton exclusion/competition and by extension acetate transport, however this range is dependent on the applied current (Figure 3.8).

3.3.3 Extracting parameters and fitting the response. Higher current and lower concentrations of acetic acid tend towards a higher relative error distribution below approximately 0.01 Hz and above 100 Hz (Figure 3.8), but the projected trend through the distribution data points hold well and it is through parameters extracted and extrapolated from this region that the Z_p can established, as described in Section 3.2.3, as the intersection of the spectra with the *Re (**Z**)* axis, albeit with some interference (Figure 3.10). As the current increases, the semi-circle tends to decrease and shifts slightly to the left, denoting a slight shift in the membrane resistance likely due to water co-transport. The real impedance does not increase proportionally with increased current, which can be interpreted as the membrane resistance to the excluded proton species. The phase angle decreases in both the real and imaginary impedance domains linearly with respect to increasing current. On the higher frequency side of the phase angle, the impedance response tends to be very similar in both the imaginary and real impedance domains.

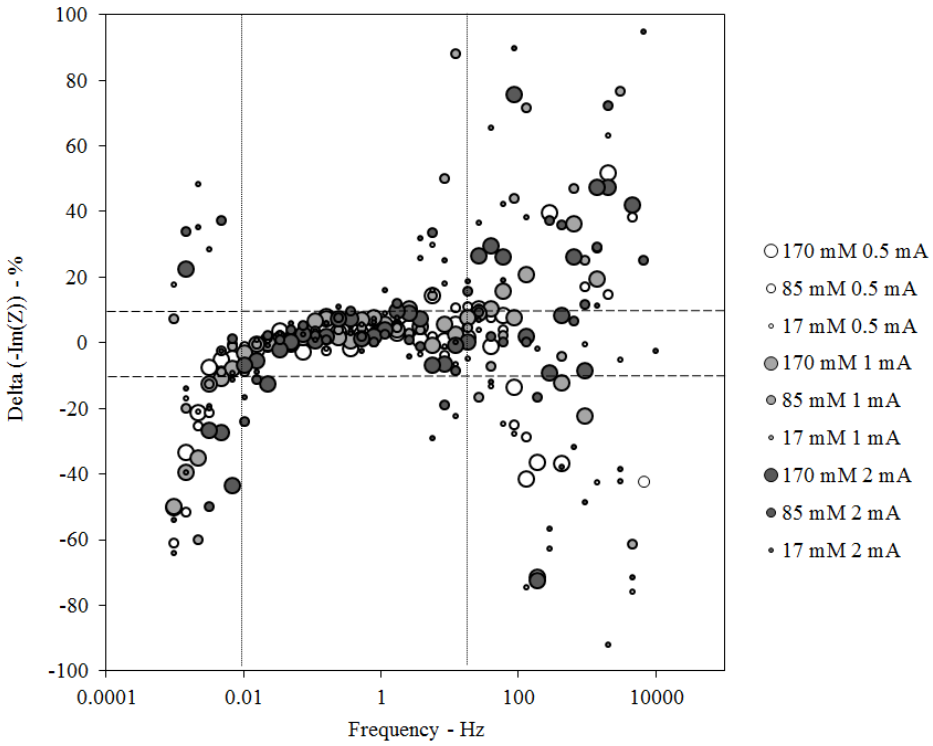

Figure 3.10. Relative error distribution of some selected data points for–*Im(Z)*, representative of the overall distribution of error. The dotted line represents a 10 % divergence from the Kramers Kronig transform. The relative error distribution for *Re(Z)* and other impedance parameters such as the phase angle, hold consistent with this trend.

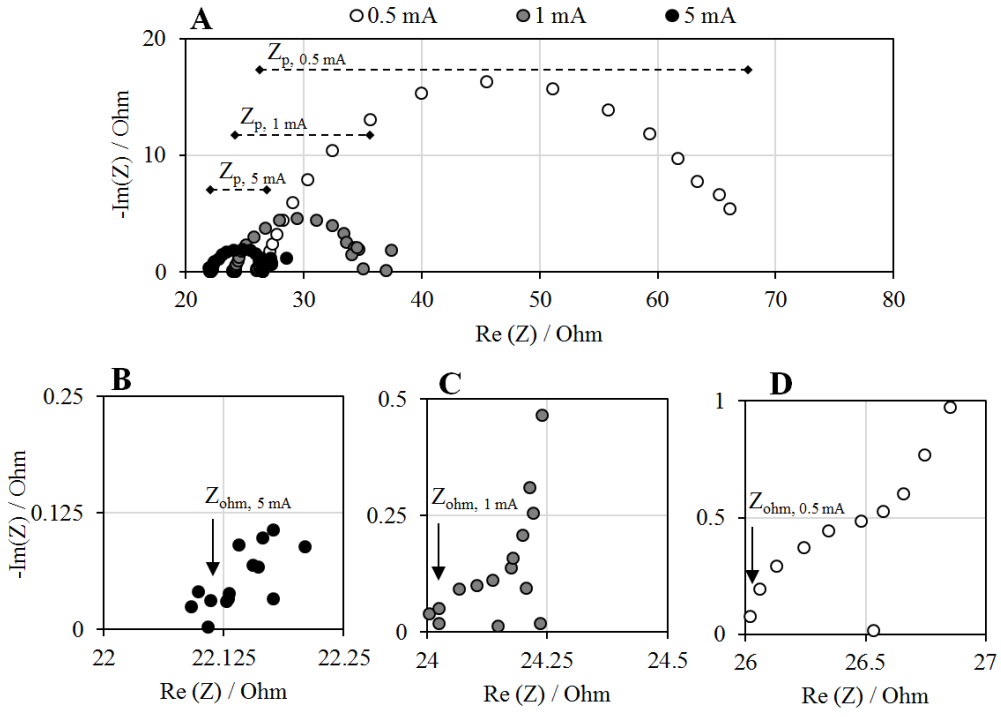

Figure 3.11. Extraction of parameters Z_p and Z_{ohm} from the average of three independent EIS spectra for extraction from 170 mM acetic acid catholyte, presented as Nyquist diagrams.

The polarization resistance (Z_p) can be interpreted in this context as the transition resistance between the electrolytes and the anion exchange membrane. We have demonstrated that this value is a function of the transported acetic acid anions, observable with EIS in the high frequency domain, and excluded cations (protons), in the low frequency domain. The relationship between the measured Z_p and the Z_p calculated with the ionic mobility of chloride (Disabb-Miller 2013) holds well for measured values of 170 mM of acetate (Figure 3.12), but not for lower bulk concentrations of acetic acid. The EIS response collectively measures the contributions of both the transport of the acetic acid anions and the transport and exclusion of protons. The measured Z_p represents the net sum of transport through the membrane, and therefore as the bulk concentration of the acetic acid decreases, the transport of protons increases and the transport number of the AEM decreases. The measured Z_p as a fraction of the Z_p calculated at lower transport numbers from the mathematical model described in 3.2.3 correlates with the transport number (Figure 3.13). Equation 14b requires a counter ion component to account for the negative contribution of competitive ions for the measured Z_p to be representative of the whole system, and here we demonstrate that the measured Z_p indeed holds for cases at which the transport number approaches 1 (*i.e.* proton transport number approaches 0), such as when the concentration in the catholyte is sufficiently high.

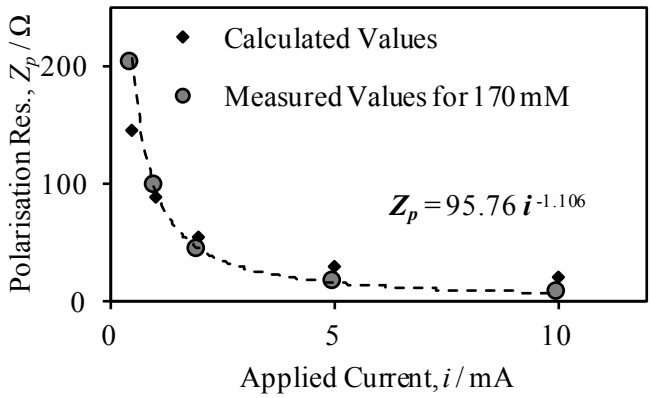

Figure 3.12. Calculated values for Equation 14b hold well for 170 mM only.

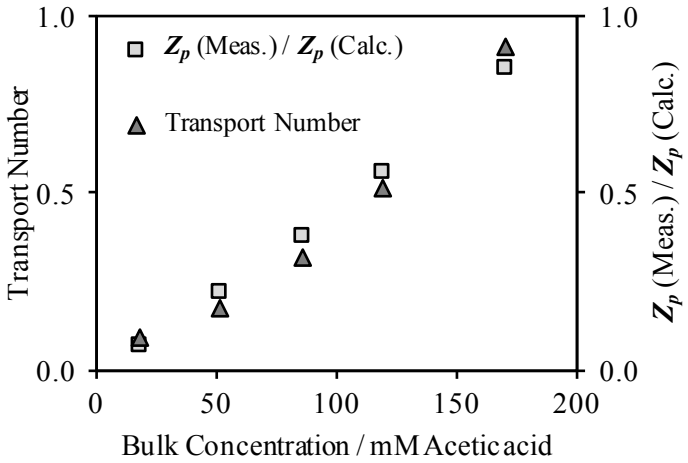

Figure 3.13. Relationship of the ratio of Z_p (Measured) / Z_p (Calculated) to the membrane transport number, demonstrating the influence of the transport number on Z_p at limiting concentrations, inferring that

Considering the relationship found in Figure 3.10 and Equation 14b:

$$Z_p = \frac{1}{\mu_{mob,i}} \frac{U_{Tot}}{Fz_i^2 C_i^b \nabla\phi_l} \qquad (14b)$$

An inference can be made for establishing some the critical parameters that relate to membrane transport, specifically the electrical mobility in the membrane ($\mu_{mob,i}$) for the compounds of interest (i), in terms of the measured polarization resistance (Z_p(Measured)) and the transport number (t) as a function of the bulk concentration ($C_i{}^b$):

$$\mu_{mob,i} = \frac{t\,(C_i^b)}{Z_p(Measured)} \frac{U_{Tot}}{Fz_i^2 C_i^b \nabla\phi_l} \qquad (18)$$

Measuring the transport number at various bulk concentrations alongside measuring the Z_p with EIS can be used to retrieve the electrical mobility of the ion of interest in the membrane. The electrical mobility of acetic acid through the AEM tested here is (1.40 ± 0.30) × 10^{-8} m^2 V^{-1} s^{-1}. Note that this mobility is specific for the solution at pH 5.5, in competition with the proton extract solution at pH 2, at standard temperature and pressure.

3.4 Discussion

Membrane electrolysis can efficiently extract charged carboxylic acid anions species from a sufficiently high bulk concentration, though competition with protons from the extract is an issue at high currents and low bulk concentration of the target anion. The ionic mobility of the species and protons, along with transport resistances are core parameters in the electro-migration through the membrane, and can be revealed through EIS. Impedance is powerful, but sensitive, and is prone to difficulties in reproducibility due to cell design, temperature changes, electrical interference, and as such future experiments should be carefully designed with interpretation and application of the outcomes clearly in mind. Other characterization methods have identified important factors for testing and optimizing ion transport system parameters. For example, a study by Kwak et al. (2013) used vortex visualization to reveal the impact of the current scheme on fluid dynamics and ion transport. Such a technique points towards surface interactions and current scheme for optimization opportunities, both of which were neglected in our study. As mentioned, here we largely neglect some critically important aspects in fluid dynamics and ion transfer at the surface, and other avenues for optimizing the ion/membrane interface should be explored in future research.

This study is intended as a first step towards analyzing carboxylic acid transport within an AEM with the intention of optimizing flux, tailoring selectivity to specific carboxylic acids, and allowing an acidic extract to accumulate without acting parasitically on flux efficiency nor power. The polymer backbone, charge density, functional groups and more can be adapted and examined for transport of C1 through C10 carboxylic acids, including dicarboxylic acids, such as succinic acid. It is clear that the membrane structure and morphology influences transport, but it is not clear to what extent the properties of an IEM can be tailored. For example, by manipulating the ion concentration in the co-polymer block, Disabb-Miller et al. (2013) demonstrated a link between the ion concentration of the membrane with electrolyte conductivity as a function of the hydration of the membrane. However, if the charge density is decreased, and assuming the membrane bulk becomes more hydrophobic, will the ionic mobility of more hydrophobic ion, such as MCFA, increase? Or, perhaps the MCFA will be more prone to diffusion back through the

hydrophobic membrane once in the protonated acid form. In principle the EIS spectra can rapidly reveal some of the core transport parameters to help answer such questions.

CHAPTER 4

Electro-fermentation of thin stillage

This chapter is redrafted from:

Stephen J Andersen, Pieter Candry, Thais Basadre, Way Cern Khor, Hugo Roume, Emma Hernandez Sanabria, Marta Coma and Korneel Rabaey, Electrolytic extraction drives volatile fatty acid chain elongation through lactic acid and replaces chemical pH control in thin stillage fermentation; *Biotechnology for Biofuels* **2015**, 8:221 DOI: 10.1186/s13068-015-0396-7

4.0 Abstract

Thin stillage is an organics-rich biorefinery side stream that can be fermented in order to produce short to mid chain fatty acids, products that can be recovered by membrane electrolysis. A current applied across an anion exchange membrane reduces the fermentation broth (catholyte, water reduction: $H_2O + e^- \rightarrow ½\ H_2 + OH^-$), and for an *in situ* extraction it is critical to understand how this affects the stream, the community and the product output. In this study, we fermented thin stillage to generate a mixed carboxylic acid extract without chemical pH control. Membrane electrolysis at 10 A m^{-2} (0.1 A, 3.22 ± 0.60 V) extracted 28 ± 6 % of the carboxylic acid generated per day (on a carbon basis) and completely replaced caustic control of pH, with no impact on the total carboxylic acid production amount or rate. Hydrogen generated from the applied current shifted the fermentation outcome from predominantly C2 and C3 carboxylic acid (64 ± 3 % of the total carboxylic acid present in the control) to majority of C4 to C6 (70 ± 12 % in the experiment), with identical proportions in the acid extract. A strain of *Megasphaera elsdenii* (maximum abundance of 57 %), a bacteria capable of producing mid-chain fatty acids, was enriched by the applied current, alongside a stable community of *Lactobacillus spp*. (10 %), enabling chain elongation of VFA through lactic acid. A conversion of 30 ± 5 % carboxylic acid produced per sCOD fed (60 ± 10 % of the reactive fraction) was achieved, with a 50 ± 6 % reduction in suspended solids likely by electro-coagulation. The electrolytic water reduction products were utilized in the fermentation: OH^- for pH control without added chemicals, and H_2 metabolized by species such as *Megasphaera elsdenii* to produce greater value, longer chain fatty acids. Electro-fermentation displays promise for generating added value chemical co-products from biorefinery sidestreams and wastes.

4.1 Introduction

During membrane electrolysis, hydrogen gas is produced at the cathode where it can interact with the fermenting community, thus potentially creating a surplus of biological reducing equivalents that may drive reverse β-oxidation and VFA chain elongation via replenishing intracellular NADH (Steinbusch et al. 2008; Angenent et al. 2013). This is known as electro-fermentation, where the metabolism of a pure or mixed community is driven by the direct integration of an electrochemical cell (Schievano et al. 2016). The other electrolysis products; hydroxide ions at the cathode, protons at the anode; can be utilized as base and acid without the addition of their conjugate salt ions. Hydroxide can counter acidogenic fermentation, while protons acidify the extracted carboxylic acid, allowing acid accumulation that can enable reactive extraction or phase separation, which will be discussed at greater length in Chapter 5. Xu et al. (2015) used membrane electrolysis to extract, acidify and phase separate hexanoic acid from a chain elongation reactor, however the membrane electrolysis was separated from the broth by two units (solids separation, liquid-liquid membrane extraction) and did not interact directly with the fermentation (Xu et al. 2015).

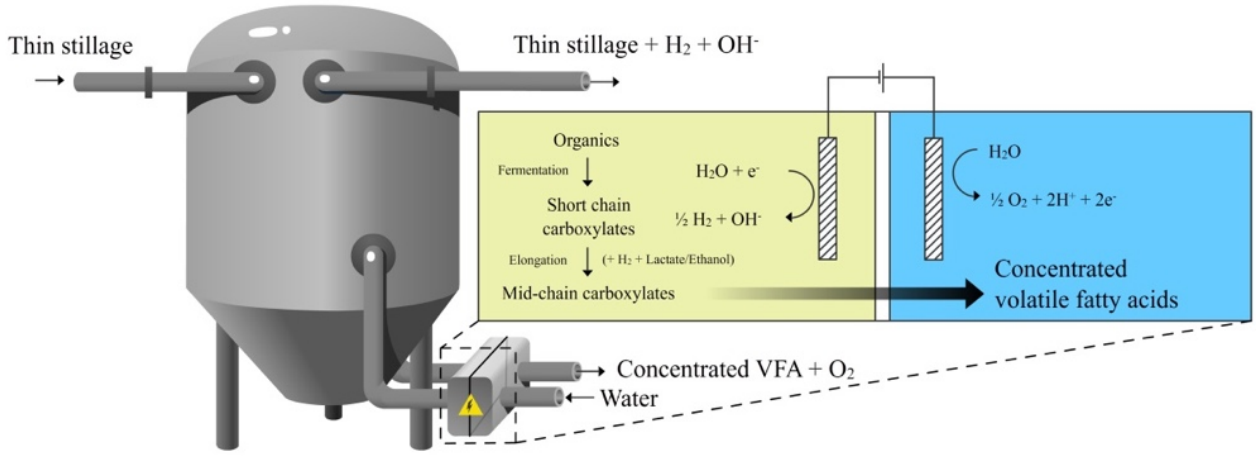

Figure 4.1. Schematic of electro-fermentation and membrane electrolysis. Image by Tim Lacoere.

Petrochemical era extractions typically sit downstream of the production process, while membrane electrolysis can interact directly with the fermentation for maximum utility of hydrogen and hydroxide. It is therefore critical that the process implications of membrane electrolysis on the fermentation are understood in detail. In this chapter, the impact of *in situ* membrane electrolysis is explored on a VFA fermentation of a real, biorefinery stream, thin stillage, focusing on changes in the native bacterial community and product output. Thin stillage is an unconverted organic fraction of bioethanol production, and is a rich, untapped source of complex organic compounds (Kim et al. 2004; Kim et al. 2008). This unconverted fraction most commonly is valorized as distiller's grains (also known as 'dried distiller's grains with solubles,' DDGS), a low value agricultural feed product that is an integral co-product in modern bioethanol refineries (Liu and Rosentrater 2012, Lupitsky et al. 2015). Thin stillage varies depending on the size and operation of the plant, but in general is generated in the vicinity of 10^5 tons per year per plant and retains a high portion of solids, between 0.1 to 1%, that are directed back to the production of DDGS after dewatering. Targeting the fermentation of thin stillage allows for a VFA bio-production strategy on a low cost, organics-rich, low impact stream.

4. 2 Materials & Methods

4.2.1 Fermenter and electrochemical cell. In all experiments, semi-continuous fermentation was coupled with a membrane electrolysis cell. Multi-ported vessels of 1 L were used as fermenters (Glasgerätebau Ochs Laborfachhandel e.K., Germany) connected to a perpex electrochemical cell, internal dimensions 200 mm (l) × 50 mm (w) × 20 mm (d) (Gildemyn et al. 2015). The total working liquid volume was 1.2 L, accounting for both the fermenter, the electrochemical cell and tubing. The anolyte was circulated from a 1 L Schott bottle to the electrochemical cell, with an identical working volume of 1.2 L. Both the anolyte and the catholyte was recirculated at 6 L h^{-1} by a peristaltic pump. The chambers were separated by an AEM (fumasep FAB, FumaTech GmbH, Germany). The cathode was an AISI Type 316L stainless steel wire mesh of 200 mm × 50 mm exposed working area with 564 μm mesh size, 140 μm wire thickness (Solana nv, Belgium), and the anode was an iridium mixed metal oxide coated titanium electrode (IrO_2/TaO_2: 0.65/0.35), 200 mm × 50 mm, with a centrally attached, perpendicular current collector (Magneto Special Anodes BV, The Netherlands). The electrolysis reactions consumes water (catholyte, water

reduction: $H_2O + e^- \rightarrow ½ H_2 + OH^-$; anolyte, water oxidation: $H_2O \rightarrow 2e^- + 2 H^+ + O_2$), however assuming complete efficiency at the maximum current used here of 100 mA this would account for only 1.6 g of water per day from the catholyte and 0.8 g per day from the anolyte. In the control case, the pH was controlled between pH 5.4 (2 M NaOH dosing) and 5.7 (2 M H_2SO_4 dosing), whereas in the experimental case (with applied current), the pH was controlled between 5.4 and 5.7 by electrochemical water reduction and dosing with the acidified extract in case of pH overshoot. The current was applied by a potentiostat (VSP, Biologic, France) in chrono-potentiometry mode. The current was manually adjusted according to pH of the fermentation broth. Following feeding, an applied current of 100 mA (*i.e.* 10 A m^{-2}) was applied for the first 20 to 24 h, or until pH 5.7 was reached. The pH controller would automatically dose acidic extract from the previous period to return the pH below the set point. A maintenance period followed at which 20 mA was applied until the next feeding event as to minimize dosing the acid extract. All experiments were performed in a 35 °C temperature controlled room.

In the first experiment, 400 mL of the reactor volume was replaced with thin stillage at two-day intervals for an equal HRT and SRT of six days. The six day HRT was chosen to allow good conversion of substrate and sufficient time for adaption of the community to the conditions. The fermentation broth and the extract solution were replenished at the same rate and the reactors were sampled every 2 days before feeding. After a steady state was reached the experimental cell was operated for four HRTs. The applied current was removed after 24 days to confirm the negation of the effect.

In the second experiment, the current was applied and the residence time of the fermentation broth was decreased to three days by replacing 400 mL of reactor volume daily, and sampling daily. The volume of the extract was decreased to 600 mL from 1200 mL and operated in batch mode during this experiment, to mimic more realistic operation of extract solution concentration and accumulation.

Supplementary batch tests explored a range of applied currents in which the reactor and extraction cell were filled with thin stillage and run for six days for each run. The reactors were emptied and refilled between each test. The applied current was set at 0.1 mA for the no current case, 50 mA (5 A m^{-1}), 100 mA (10 A m^{-1}) and 200 mA (200 A m^{-1}) and the pH was controlled between pH 5.4 and 5.7 with 2 M NaOH and 2 M H_2SO_4. The AEM

was replaced between each test and reactor components were scrubbed with a brush and tap water only to limit cross-contamination.

4.2.2 Stream characterization, community and chemical analysis. Thin stillage of Alco Bio Fuel NV (Ghent, Belgium) (stored at 4 °C) was used in the fermentation without inoculum, and as such the fermentation proceeded according to the bacterial community already present in the broth. New batches of stillage were periodically retrieved, with one batch requiring dilution to the appropriate COD range to maintain consistent organic loading. Stream characterization confirmed that after dilution the stream remained sufficiently consistent for these experiments, with some variation in solids content. Reported feed concentrations are averages of all feed streams including the diluted stream.

Stream characterization, community and chemical analysis were performed according to Chapter 2, with some minor modifications. Management of pH was tracked by mass of acid or base dosed, and gas production was quantified with an external gas trap and assessed with a Compact Gas Chromatograph (Global Analyser Solutions, Breda, The Netherlands), equipped with a Molsieve 5A pre-column and Porabond column (CH_4, O_2, H_2 and N_2) and a Rt-Q-bond pre-column and column (CO_2, N_2O and H_2S). Concentration of gases were determined by means of a thermal conductivity detector. Eight samples were selected at random from the thin stillage feed samples for further characterization, alongside four samples from the control effluent, four from the experimental effluent, plus an additional four from the extract solution during the steady state period with the average reported of the following analyses: total and soluble COD by Nanocolor® kits (Macherey-Nagel GmbH, Germany); lactate, glycerol, 1,3-propanediol, ethanol, propanol and butanol by ion chromatography (Dionex DX 500); hemicellulosic and cellulosic fragments in the soluble phase (reported in this text as “soluble cellulosic fragments,” as to differentiate from (hemi)cellulosic material in the solids) by the NREL procedure according to Sluiter et al. (2016), soluble and insoluble proteins by Kjeldahl nitrogen measurements according to Standard methods (4500-Norg B; APHA, 1992), and calculated to protein COD content based an assumed carbon to nitrogen ratio of 5:1. The “Total Other Solids” is based on the difference between the measured tCOD and the sCOD, and its difference from the calculated insoluble protein COD. Non-organic anions chloride, nitrite, nitrate, sulfate and phosphate were determined on a 761 Compact Ion Chromatograph (Metrohm, Switzerland) equipped with a conductivity detector. The total phenolic content was assessed with the Folin Ciocalteu Assay method (Swain and Goldstein 1964).

4.2.3 Electrochemical analysis. The resistance of the whole cell was assessed by Current Interrupt (Bard and Faulkner 2001). 10 mA of current was applied at a period of 100 ms over 10 cycles successively, and the resulting voltage recorded at 0.2 ms intervals. The cell voltage change during the first interval of 0.2 ms is the ohmic drop of Current × Resistance, assuming that faradaic and diffusional processes present much slower relaxation times and therefore do not impact the voltage amplitude.

4.3 Results

4.3.1 Stable fermentation with extraction and electrochemical pH control. Thin stillage was semi-continuously fermented under control and experimental (applied current) conditions, with membrane electrolysis extraction in the experimental case. No significant difference was observed between the total amount of VFA produced under control conditions compared to the applied current conditions (Figure 4.2A). The control is defined as the thin stillage fermentation without an applied current, with sodium hydroxide supplied for pH control, while the experimental case had an applied current (100 mA, 3.22 ± 0.6 V, approximately 20 to 24 h) until the upper pH set point of pH 5.7 was reached, and then the current was lowered until the next feeding (20 mA, 2.36 ± 0.25 V, approximately 24 to 28 h) to prevent pH overshoot. Where the pH exceeded the upper set point, VFA rich acid from the anolyte was dosed back into the reactor, which occurred on average at less than 1 mL d^{-1}. The average production rate of short chain linear unsaturated C2 to C7 VFA in the control and the experimental case were similar at 1.9 ± 0.8 g COD L^{-1} d^{-1} (2.5 ± 1.0 gC L^{-1} d^{-1}) and 1.9 ± 0.5 g COD L^{-1} d^{-1} (2.3 ± 0.6 gC L^{-1} d^{-1}) respectively at the 6-day hydraulic retention time (HRT) condition.

In both the control and experimental fermentation, a similar maximum amount of VFA was generated per total initial volume of thin stillage, with a total conversion of 31 ± 2% sCOD for the control and 30 ± 5% sCOD for the experiment (see 'Total Carboxylic Acids', Figure 4.3B). If the sCOD that can be attributed to protein and oils is excluded, the conversion was 44 ± 2% for the control and 43 ± 7% for the applied current fermentation on a sCOD basis. The broth appears to have approached the maximum conversion to VFA under these reactor conditions.

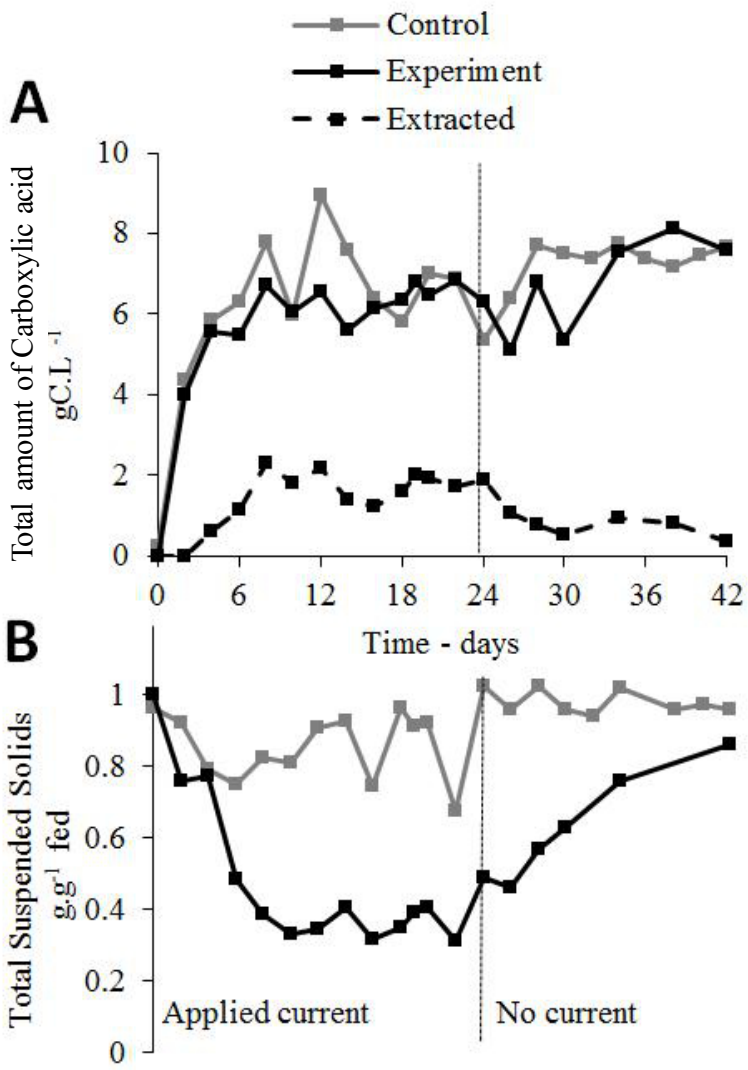

Figure 4.2. Control and experimental fermentation over time; total amount of carboxylic acids and total suspended solids. In the experiment, current was applied prior to the vertical dotted line. **A.** The total amount of measured carboxylic acids. Note the experimental case includes the amount extracted. **B**. Total suspended solids measured represented by the proportion of total suspended solids in the fermenter relative to that of the feed.

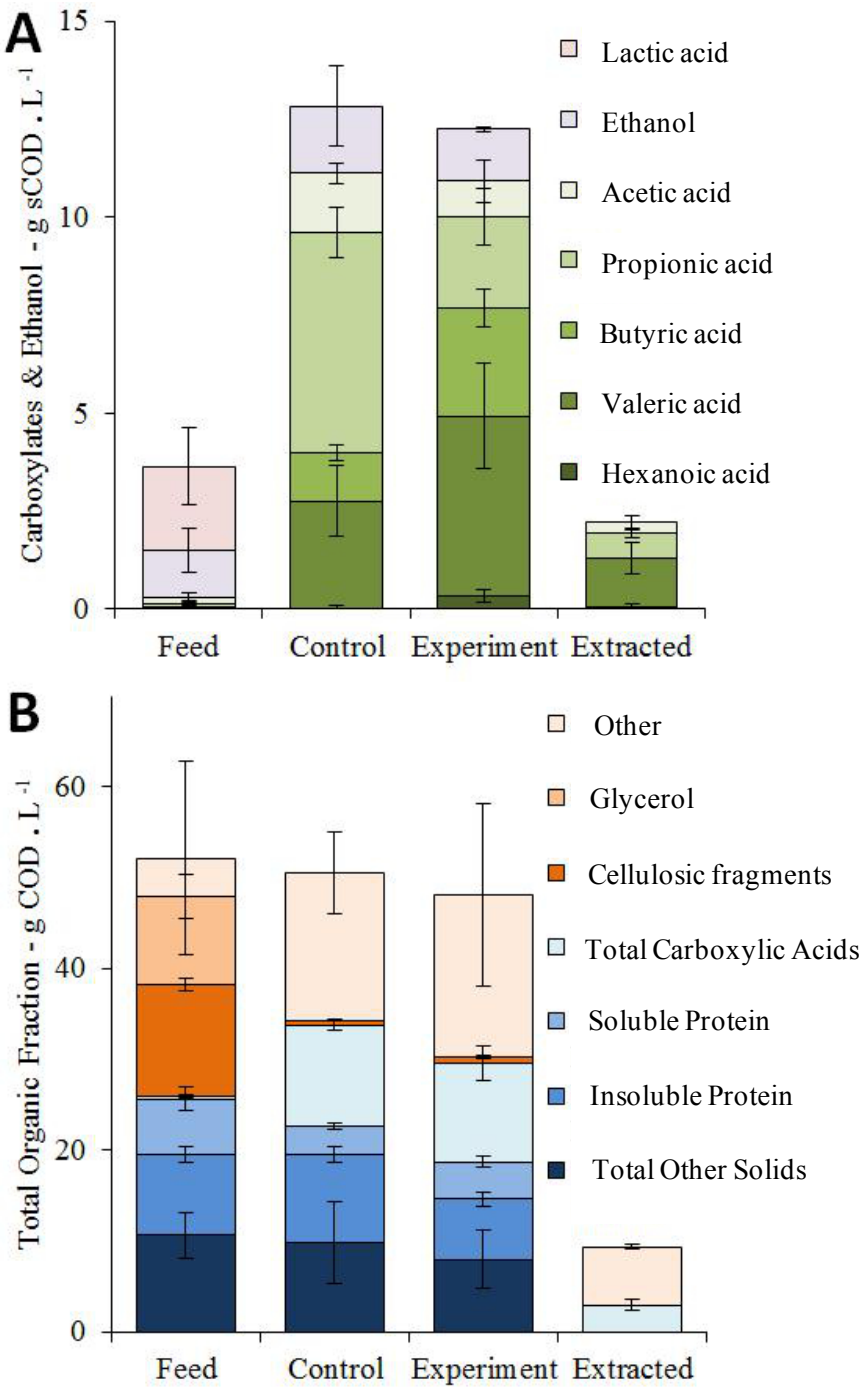

Figure 4.3. Carbon oxygen demand (COD) comparison in the feed, control fermentation, experiment fermentation (applied current) and in the extract solution, measured during steady state (day 6 to 24). Note the extract solution is also considered in the experiment column. **A.** Total concentration of measured carboxylic acids and ethanol. **B**. Total amount of all identified components. (n = 9 for carboxylic acids, n = 4 for other components, per stream.)

Membrane electrolysis extracted 28 ± 6% of carboxylic acids generated (rate of extraction / rate of production). The extraction rate was not optimized in this study, which pertains more to electrochemical reactor design and operation (e.g. solids separation, membrane crossflow velocity, surface convection, optimized applied current scheme). The membrane flux rate is closely linked with the total molar concentration in the broth, as demonstrated in Chapter 3. In this study we focused on the effect of the electrolysis products on the fermentation rather than exclusively extraction.

The applied current will experience losses due to membrane fouling and solids between the electrode and the membrane, thus requiring increased power input for the same applied current. Current interrupt experiments reveal the change in resistance and the ohmic drop over a five-day period due to solids build-up between the electrode and the membrane. The resistance attributed to the region between the electrode and the membrane was calculated at 3 Ω at the beginning of the experiment with a new membrane, and increased to 10 Ω after one day. The resistance peaked at 19 Ω after four days. Cleaning the space between the membrane and the electrode decreased this resistance to 10 Ω. Solids build up on the electrode and membrane can therefore account for almost 1 V of ohmic drop, representing a third of the applied potential of 3.22 ± 0.6 V and 100 mA applied current. An improved flow design and cleaning regime would translate into a significant power saving, with increased cross flow velocity also likely to improve anion flux.

Acidification of the fermentation broth was countered by the cathodic generation of hydroxide for zero chemical input pH control. Upper limit pH control was managed by dosing the acid extract solution back into the fermentation broth, at less than 1 mL d^{-1} on average, as the applied current scheme was designed to avoid excess electrolysis. In the control case, 24 ± 17 mL d^{-1} of 2 M NaOH was added to maintain the pH, equivalent to approximately 10 kg d^{-1} of caustic soda per cubic meter of thin stillage fed. For each kilogram of COD_{VFA} generated this equates to 0.83 kg of sodium hydroxide required to manage the fermentation. At the anode, the oxidation of water generates oxygen gas and protons in the anolyte (extract solution), resulting in the protonation of the carboxylic acid and other anions (phosphate, chloride, sulfate, etc.) that have crossed the AEM.

The experimental reactor decreased in total suspended solids (TSS) relative to the control case after current is applied (Figure 4.2B), stabilizing at 0.36 ± 0.04 g . g^{-1} TSS fed, relative to the control case of 0.86 ± 0.11 g . g^{-1} TSS fed in the control case during the steady

state (Solids content is reported here as grams per liter of $TSS_{Reactor}$ / gram per liter of TSS_{Feed} fed due to inconsistency of solids in the fed thin stillage, *i.e.* minimum 14 g TSS L^{-1}, maximum 25 g TSS L^{-1}). The total suspended solids in the control stabilized at a rate of 0.7 ± 1.4 g TSS L^{-1} d^{-1} compared to the applied current case which decreased at an average rate of 3.9 ± 1.9 g TSS L^{-1} d^{-1} in the steady state period from day 8 to day 24. This corresponds to a 4.5 times greater decrease in suspended solids, albeit with large variability. The current was stopped at day 24 to confirm the effect. The stoppage coincided with the suspended solids concentration returning to that of the feed. No equivalent decrease in the measured solids COD nor increase in measured soluble cellulosic fragments or VFA production was observed. This phenomenon is likely related to electro-coagulation, in which the applied current is neutralizing suspended particles, resulting in the formation of coagulated particles (Mollah et al. 2004). Some evidence to support this is revealed in nitrogen analysis, where 85 ± 6% of total fed nitrogen remains in the broth in the control case, whereas 71 ± 5% of total fed nitrogen is measured in the broth in the experimental case, with this difference accounted for mainly in the insoluble nitrogen compounds. Protein or lignin polymers can form colloids at high pH, which may adsorb at the high local pH on the cathode surface, or settle within the electrochemical cell. More research is required into the electrocoagulation phenomenon and the implication for the bacteria and their access to the substrate. If membrane electrolysis is applied in a similar broth in which conversion of solids are targeted, it is not clear if the apparent electro-coagulation will have an effect on the ability of the microbial community to metabolize these solids.

4.3.2 Fermentation and carboxylic acid chain elongation. The COD balance of the thin stillage fermentation revealed that membrane electrolysis resulted in a shift in the fermentation of VFA, from a majority C2 and C3 (64 ± 5% C2 and C3, 36 ± 2% C4 to C6, as an average percentage of the total carboxylic acids on a COD basis during steady state, n = 10) to a majority of C4 to C6 (30 ± 5% C2 to C3, 70 ± 12% C3 to C6) without a change in the total amount of VFA on a COD basis (Figure 4.3A). The proportion of acetic acid was lower in the applied current case, but not significantly across all measured time points during the steady state (n = 10) (14 ± 2% control, 8 ± 5% with current). The proportion of propionic acid was lower with applied current, at 51 ± 6% in the control compared to 21 ± 7% with current. The proportion of butyric acid was greater under applied current (11 ± 2% control, 25 ± 7% with current), with a similar trend with valeric acid (25 ± 8% control, 42 ± 11% with current), and hexanoic acid (0 ± 1% control, 3 ± 2% with current). The extent of chain

elongation can be compared as "chain elongation equivalents," the concentration of carbon (gC L^{-1}) at steady state that has been added through a chain elongation pathway on the theoretical assumption that all VFA starts at either acetic acid (C2) or propionic acid (C3). The extent of VFA chain elongation at steady state in the applied current case was 2.6 ± 0.6 gC L^{-1} of chain elongation equivalents, significantly higher than the control case at 1.4 ± 0.4 gC L^{-1} (t-test: $\alpha = 0.05$, $p = 1.9 \times 10^{-4}$, $n = 10$).

Only a fraction of the feed was converted to VFA, consisting of soluble cellulosic fragments, consisting of 4.4 ± 0.6 g L^{-1} glucose, 4.2 ± 0.5 g L^{-1} xylose and 2.9 ± 0.4 g L^{-1} arabinose (in total 12.3 ± 0.7 gCOD L^{-1}); glycerol (9.8 ± 2.4 gCOD L^{-1}), lactic acid (2.1 ± 1.0 gCOD L^{-1}), and C1 to C8 carboxylic acids (0.3 ± 0.2 gCOD L^{-1}). The remainder of the thin stillage consisted of a solid fraction of proteins (8.9 ± 0.9 gCOD L^{-1}) other lignocellulosic solids (10.6 ± 2.5 gCOD L^{-1}), a soluble COD fraction (sCOD) of protein (6.1 ± 1.3 gCOD L^{-1}), and an assumed balance of lipids, oils and other biomass (4.2 gCOD L^{-1}), in good agreement with a previous thin stillage characterization (Kim et al. 2008). Membrane electrolysis did not alter any of the other main components characterized in this study (Figure 4.3B). Zhou et al. (2013) studied glycerol fermentation with applied current, resulting in a mixed outcome with approximately 15 to 30% of the carbon ending as VFA (mostly propionic acid), 20% ending as biomass, 3 to 6% as ethanol and 20 to 50% as 1,3 - propanediol. Insignificant quantities of 1,3 – propanediol were detected in this study, and propanol and butanol were detected at less than 1 gCOD L^{-1} each. Phenolic compounds were identified in the feed and fermentations at 1.2 g L^{-1}. Both the control and applied current case showed no net increase of ethanol in the broth from 1.2 ± 0.6 gCOD L^{-1} fed to 1.7 ± 1.0 gCOD L^{-1} and 1.3 ± 0.1 gCOD L^{-1} respectively. Alcohol and phenolic compounds were detected in the extract solution in trace quantities.

Soluble cellulosic fragments, glycerol and lactic acid were consumed equally in both the control and experimental reactors (Figure 4.3B). In the control, this resulted in predominantly acetic acid and propionic acid. Lactic acid is present in the fed thin stillage and can be used to elongate acetic acid to butyric acid, as can ethanol (Spirito et al. 2014). Approximately 0.14 gC L^{-1} d^{-1} of lactic acid and 0.05 gC L^{-1} d^{-1} of ethanol enters the system by feeding. This fed lactic acid and ethanol can account for the chain elongation of C2 and C3 species to C4 and longer, assuming all carboxylic acids of C4 and longer are a result of chain elongation. The control case needs a total of 0.2 gC L^{-1} d^{-1} to elongate C2 and C3, compared with the applied current case which requires 0.7 gC L^{-1} d^{-1}.

4.3.3 Increased organic loading and current increased VFA production. A brief, secondary experiment tested the system under doubled organic loading rate and a constant applied current of 100 mA, resulting in a 5.5 times increase in the VFA production rate to 10.4 ± 1.1 $gCOD_{VFA}$ L^{-1} d^{-1}. The disproportional increase in production can be partially attributed to removing the substrate limitation, in addition to the constant supply of hydrogen gas to the fermentation. The VFA production rate was 10.4 ± 1.9 g COD L^{-1} d^{-1} (3.3 ± 0.6 gC L^{-1} d^{-1}), at an extraction of 26 ± 5% of produced VFA. The conversion rate of sCOD was also higher at 60 ± 11% of the total sCOD fed, or 86 ± 16% of the reactive fraction, with a higher proportion of C6 and now also C7 VFA. In the previous experiment, heptanoic acid (C7) was not detected (Figure 4.4). The constant current appears to have increased the total conversion of the reactive fraction. The greater supply of hydrogen gas (per litre of reactor volume), 66 mmol L^{-1} d^{-1} compared with 25 mmol L^{-1} d^{-1} in the first experiment, resulted in a lower concentration of butyric acid at 8 ± 0% and valeric acid at 19 ± 1% of the C2 to C7 VFA. The proportion of hexanoic acid was 11 ± 6%, compared to 3 ± 6% in the previous experiment, and heptanoic acid at 1 ± 0% (Figure 4.4). The chain elongation equivalents increased relative to hydrogen generation, though not proportionally (Figure 4.5). This suggests that the high organic loading rate, high current case (Exp II, Figure 4.5) was either under excess hydrogen or the hydrogen was escaping the system before it could be utilized. Short term batch tests at a range of applied current (Figure 4.6) showed a similar trend for total carbon chain elongation equivalents generated in the broth, where even though the applied current is doubled from 100 mA to 200 mA, the total chain elongation equivalents only increased incrementally.

In this high loading, constant current experiment, the volume of the extract solution was halved and operated in batch to demonstrate acid accumulation and mimic a more realistic recovery strategy. A maximum concentration of 11.7 gC L^{-1} was reached in the acid extract solution, compared with the maximum of 2.3 gC L^{-1} in the previous experiment. Phenolic acids were concentrated at up to 2.5 g L^{-1}. Phosphoric acid (H_3PO_4, pH < 1) accumulated at up to a maximum of 4.1 g L^{-1} and hydrochloric acid to 1.6 g L^{-1}.

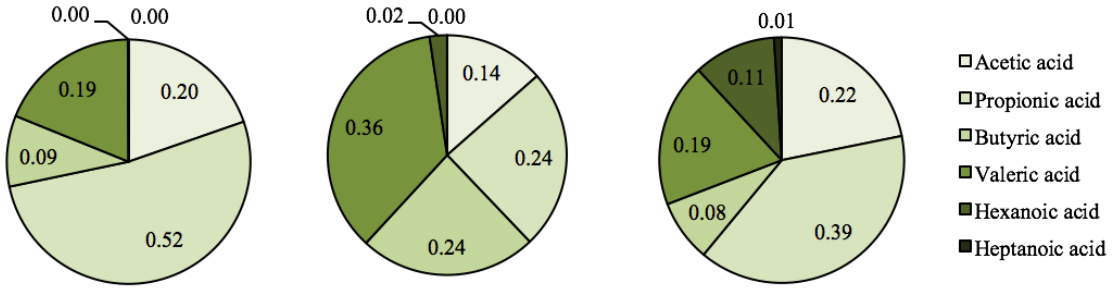

	Control	Experiment	Experiment II: High Loading Rate, High Current
Production Rate	1.9 ± 0.8 $gCOD_{VFA}$ L^{-1} d^{-1}	1.9 ± 0.5 $gCOD_{VFA}$ L^{-1} d^{-1}	10.4 ± 1.1 $gCOD_{VFA}$ L^{-1} d^{-1}
Maximum Anolyte conc.		4.0 $gCOD_{VFA}$ L^{-1} 2.3 gC_{VFA} L^{-1}	18.9 $gCOD_{VFA}$ L^{-1} 11.7 gC_{VFA} L^{-1}

Figure 4.4. Comparison of the average outcome of VFA and production for the control case, experimental case (applied current) and experimental case with increased loading rate and current.

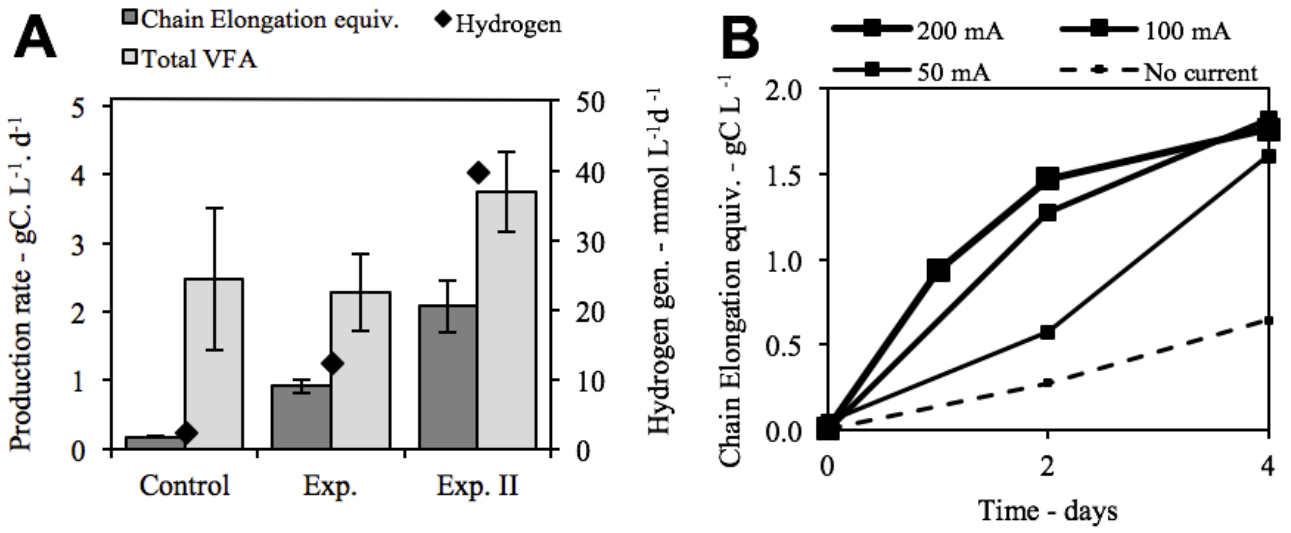

Figure 4.5. Chain elongation equivalents vs. electrolytic hydrogen. **A.** Production rate of total VFA compared against production of ethanol equivalents required for chain elongation to C4 to C7 carboxylic acids. Hydrogen gas reported is the average of that measured from the headspace and gas column. **B.** Chain elongation equivalents as measured in batch tests over time, for 0, 50, 100 and 200 mA.

4.3.4. Membrane electrolysis favors hydrogen metabolizing fermenters. The fermentation was initiated without an inoculum, and thus only organisms native to the thin stillage were cultivated (Figure 4.6). *Lactobacillus spp.* represented a relative abundance between 96 and 99 % of the bacteria at time zero and in the thin stillage fed throughout the experiment, with *Hallella sp.* and others making up the balance. *Lactobacillus spp.* abundance swiftly diminished in the control case to a maximum relative abundance of 1 %, and moved to a dominance of *Hallella sp.,* with a relative abundance of 65 % after two days and a maximum relative abundance of 94 %, and an average of 75 ± 21 % across the whole experiment similar to 42 ± 26 % under applied current. The next most abundant species in the control case were *Dialister sp.* and *Megasphaera sp.,* both of the family Veillonellacae. *Dialister sp.* had a relative abundance between 3 and 26 %, with an average across all measured time points of 13 ± 8 %, while *Megasphaera sp.* had a relative abundance between 1 and 5 %, with an average of 3 ± 2 %. The applied current case contained *Dialister sp.* at a similar relative abundance to the control case at between 0 and 22 %, with an average of 11 ± 7 % across the whole experiment. The greatest difference between the control and experimental case arose from the abundance of *Lactobacillus spp.* and *Megasphaera sp.* The *Megasphaera sp.* was present with a relative abundance between 0 and 57 %, with an average of 15 ± 21 % (n = 9, at steady state). *Lactobacillus spp.* in the applied current case slowly decreased over the first 8 days, and was then present between 6 and 17 % from day 8 to 24, in stark contrast to the control case of between 0 and 1 %. *Pectinatus sp.*, *Bifidobacterium sp.* and *Prevotella sp.* are also present in the applied current case at a relative abundance of up to at least 5 %, which is similar to the control case with the exception of *Pectinatus sp.* which never exceeded 0.7 %. The *Lactobacillus spp.* had a minimum abundance under applied current of 5.9 % and a maximum of 67.0 %, compared to the control case with a minimum of 0.0 % and a maximum of 1.3 % (ignoring t = 0, at which both had greater than 99 % abundance of *Lactobacillus spp.*, identical to the feed). In the control case, the *Lactobacillus spp.* dropped from 99 % to a relative abundance of 1.3 % after two days. The time point of the greatest abundance of the *Megasphaera sp.* (57 %) coincided with a slight increase in *Lactobacillus spp.* and an increase in chain elongation, albeit following a slump possibly related to competition with *Pectinatus sp.* Day 14 of the applied current fermentation coincided with a low point of chain elongation in the steady state fermentation, a high relative abundance of *Pectinatus sp,* and the *Hallella sp* maximum. In a brief period where *Pectinatus* outcompeted *Megasphaera*, minimal C4 to C6 carboxylic acids were produced and a peak of propionate was observed.

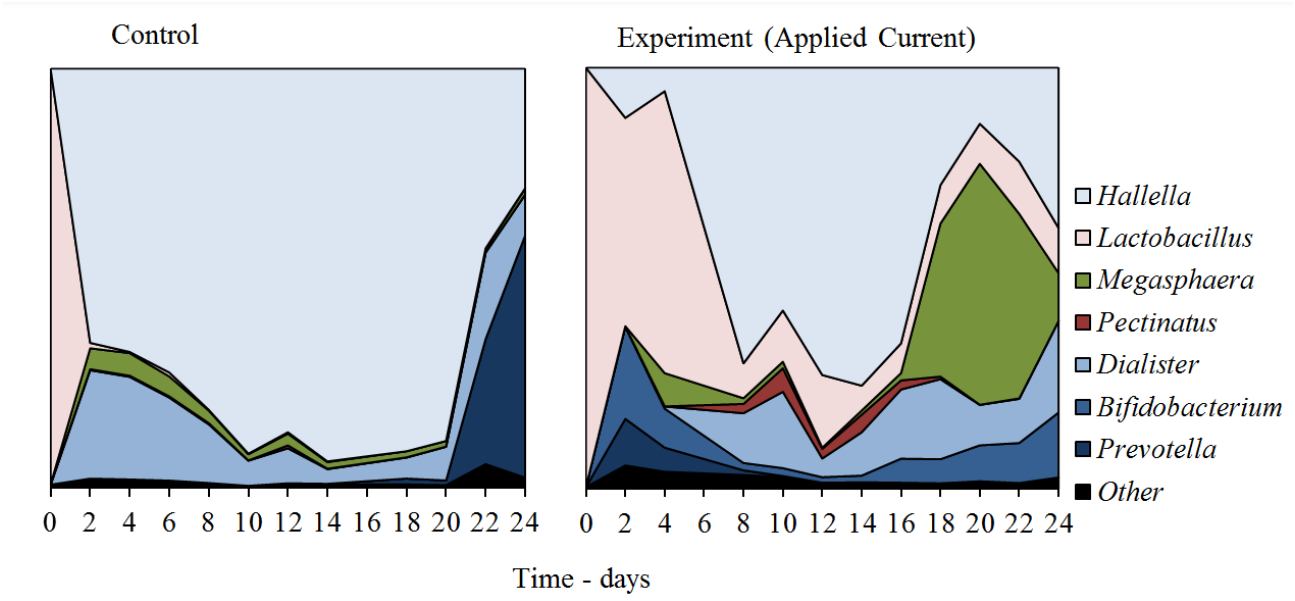

Figure 4.6. Cumulative line plot of species abundance over time. Data points at day 16 for the control and day 6 for the experiment are assumed values due to data collection error. Feed abundance was consistently in excess of 99% *Lactobacillus spp*.

Soluble cellulosic fragments, glycerol and lactic acid were consumed in both the control and experimental reactors (Figure 4.3A). In the control, this resulted in predominantly acetic acid and propionic acid while with an applied current a greater concentration of MCFA was observed (Figure 4.3A and 4.5). *Megasphaera sp*. can ferment glucose, lactic acid and short chain VFA towards short to mid-chain VFA, alongside CO_2 and H_2 (Rogosa 1971), while the majority of the other bacteria of high relative abundance produce short chain VFA and intermediates. *Hallella sp.,* consistently the most abundant species, is known to produce acetate and succinate, that latter of which can be decarboxylated to propionic acid, or lactic acid, while *Dialister* is a nonfermentive bacillus (Moore and Moore 1994). *Dialister*'s consistent abundance alongside *Hallella* suggests that it may have produced propionic acid from succinic aicd. Neither *Hallella* nor *Dialister* have been associated with longer chain carboxylic acids (Moore and Moore 1994, Jumas-Bilak et al. 2005). *Bifidobacterium sp*. produces lactic acid and acetic acid (Sgorbati et al. 1995), *Prevotella sp*. mainly produces acetic acid and succinic acid, with a slight production of iso-butyric and iso-valeric (Shah and Collins 1990) while *Pectinatus sp*. is associated with the production of acetic and propionic acid (Lee et al. 1978; Caldwell et al. 2013). *Pectinatus sp*

has been observed to produce propionic acid from glycerol at a biological cathode (Denis et al. 2013).

Reverse β-oxidation VFA chain elongation with lactic acid has been described in *Megasphaera elsdenii* (Spirito et al. 2014), and *Lactabacillus spp*, can produce lactic acid from a variety of substrates (Beijerink 1901; Gänle and Follador 2012). The butyric, valeric and hexanoic acids present in (Figure 4.3A) were likely generated through a similar pathway in both the control and applied current case by *Megasphaera sp.* (Rogosa 1971; Hino et al. 1994):

$Lactate^- + Acetate^- + H^+ \rightarrow n\text{-}Butyrate^- + CO_2 + H_2O$; $\Delta G^o = -59.43$ kJ mol^{-1} at 37°C

$Lactate^- + Propionate^- + H^+ \rightarrow Valerate^- + CO_2 + H_2O$

$Lactate^- + Butyrate^- + H^+ \rightarrow Hexanoate^- + CO_2 + H_2O$

Megasphaera sp. stands out as one of few bacteria in this consortia with a high relative abundance that is known to generate mid chain VFA, and there is evidence here to suggest that it was able to utilize hydrogen from membrane electrolysis to drive VFA chain elongation. *Megasphaera sp.* was the only species whose relative abundance correlated positively with the concentration of chain elongation equivalents (*i.e.* extent of VFA chain elongation) by the Pearson correlation test ($R = 0.63$, $p = 0.04$) in the applied current case, whereas no correlation can be seen in the control case ($R = 0.05$, $p = 0.89$). When compared in the RAST database, 100% similarity was found with "Megasphaera NP3," a sequenced species closely related to *Megasphaera elsdenii* (RAST, http://rast.nmpdr.org/). Megasphaera NP3 contains genes for fatty acid production, glycolysis/gluconeogenesis and β-oxidation metabolism (for VFA chain elongation), along with genes for four NiFe hydrogenase mettalocenter assembly proteins, which makes it a good candidate for the ability to metabolize hydrogen (Shafaat et al. 2013). Organisms that are both capable of reverse β-oxidation VFA chain elongation and hydrogen oxidation could gain energy by an increase of intreacellular hydrogen which leads to an increase in NADH and NADPH, thus driving VFA reduction (Rabaey and Rozendal 2010, Shafaat et al. 2013, Velt et al. 2008). In these experiments, the majority of hydrogen was generated extracellularly *in situ* by membrane electrolysis and then transported into the cell to drive the so-called electro-fermentation.

A Redundancy Discriminant Analysis (RDA) was performed to examine the impact of applied current (experimental case) on the bacterial community, and their association with chain elongation over time, in comparison with a control (Figure 4.7). The bacterial community in the applied current fermentation (Exp) was significantly different from that in the control case. The length of the chain elongation (CE) vector indicated a high relative association with the bacterial community in the Exp case ($r = 0.561$, RDA1 p-value: 0.004). Within this community, Megasphaera sp (Otu005) and Lactobacillus spp (Otu006) are significantly correlated with chain elongation under the condition of the applied current (Exp), unlike in the control fermentation. In the control case, only time was significantly associated with the variations in the bacterial community ($r = 0.778$, RDA2 p-value: 9.19×10^{-5}). The position of each arrow (time or CE) with respect to the plot axis represents its degree of correlation with particular OTUs. In this way, the differences in the relative abundance of *Lactobacillus spp*. may be associated with CE, while the variations in *Megasphaera sp*. may also be influenced by time. The species-environment correlation values confirmed these observations (RDA1 = 0.649, RDA2 = 0.778). The relationship between *Lactobacillus spp.*'s lactic acid production with the lactic, reverse β-oxidation and hydrogen utilizing capability of *Megasphaera sp*. enables the community to take advantage of the hydrogen generated in membrane electrolysis (Figure 4.8). While *Lactobacillus spp*. are generally not recognized as hydrogen producers – or consumers – *Lactobacillus spp*. are often found in hydrogen producing consortia (Sikora et al. 2013), and in this study a hydrogen consuming consortia. *Lactobacillus spp*. were always present in the applied current case during steady state at a relative abundance greater than 6 % at an average of 10.3 ± 3.4 % in the applied current case compared with an average relative abundance of 0.3 ± 0.4 % in the control.

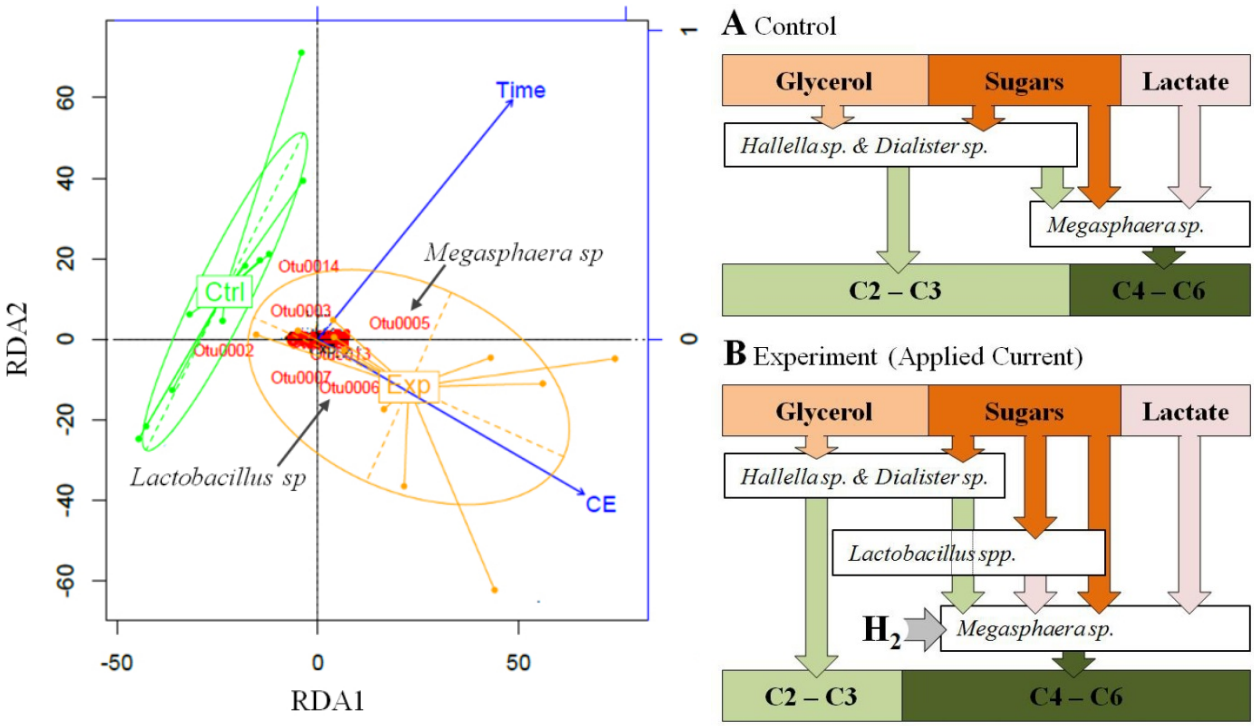

Figure 4.7. (Left) Redundancy analysis highlighting the dissimilarities among the relative abundances of the bacterial communities in the control and experimental (applied current) cases. "Ctrl" represents the community of the control reactor, which was described in RD2, while "Exp" indicates the community of the experimental (applied current) reactor, included in RD1. The blue axis represents time (days) and CE (extent of chain elongation).

Figure 4.8. (Right) Schematic of species with the top four greatest relative abundance and the proposed pathway of substrates, VFA intermediate and VFA product. **A.** In the control case some acetate (C2) and propionate (C3) may be used as an intermediate by *Megasphaera sp*. **B.** In the experimental (applied current) case the *Megasphaera sp*. can metabolize electrolytically generated H_2 to gain additional energy and generate more reduced, longer chain VFA by lactate elongation.

All species present in the fermentations were introduced from the feed, or whatever contamination followed. Enriching a native species from the target stream is attractive if the species fulfills the requirements of the process, though most chain elongation mixed culture studies use inocula with the intention of introducing *Clostridia*. None of the *Clostridia* species identified in Chapter 1 were present in this fermentation, most likely due the different source of stillage (corn thin stillage here, versus wheat stillage in Chapter 1) and the lack of beer (ethanol) in this study. In this study *Clostridium sp*. are only observed in low abundance: less than 1% in both the control and the experimental case.

Understanding the principal actors in the community, be it in chain elongation or production of an intermediate, has implications in operational parameters such as temperature, residence time, pH and the substrate (Vanwonterghem et al. 2015). Both stream and strain selection is critical to ensure a targeted substrate conversion to the final product, be it in the conversion of oligosaccharides by, for example *Lactobacillus spp (*Gänle and Follador 2012), the production of hexanoic acid from sugars and lactic acid with *Megasphaera elsdenii* (Rogosa 1971), and the myriad of supporting community.

4.4 Discussion

In this work, we have demonstrated the impact of membrane electrolysis, a chemical-free extraction technology, on the fermentation of thin stillage to generate reduced VFA. The reactive fraction of thin stillage is attractive as a target substrate as the cellulosic fragments and glycerol are readily convertible and have little value, though it is important not to detract from the contribution of these solids to existing production of DDGS in the current biorefinery market. Avoiding degradation of solids is attractive considering the market demand for low-cost livestock feed, as thin stillage is generally dewatered with the solids and syrup contributing to the production of DDGS, whose value is linked to protein and fibre content. At this stage, it appears that membrane electrolysis allows most solids and proteins to pass without degradation.

Within the fermentation, this study has shown that membrane electrolysis can result in an increased abundance of *Megasphaera sp.* and *Lactobacillus spp.* in thin stillage, resulting in an increase in VFA chain elongation through lactic acid, likely driven by *in situ* hydrogen generation. Membrane electrolysis can provide a driving force to select for hydrogen metabolisers such as *Megasphaera elsdenii* and potentially *Clostridium kluyverii* or others. Further studies should focus on the question of hydrogen metabolism by some of the *Clostridium* Group IV species discussed in Chapter 2, and *Lactobacillus spp.*

VFA fermentation can incur considerable base and acid costs, and the control fermentation in this experiment required 0.83 kg caustic per 1 kg COD_{VFA} produced. This is one point in which membrane electrolysis stands apart from electrodialysis, as the acid and caustic electrolysis products are directly utilized in the fermentation. The mixed VFA as produced in this study is not a marketable product, so as a point of comparison we will instead consider hexanoic acid as a target product at around 1000 EUR t^{-1} unrefined, and

up to 2000 to 3000 EUR t^{-1} refined (price assumptions here are based on discussions with industry partners and may vary). Assuming a conservative price of 300 EUR t^{-1} of caustic, if the 0.83 kg caustic per 1 kg COD_{VFA} ratio holds and all the COD_{VFA} generated in this study could be directed to hexanoic acid (2.21 tCOD per 1 t hexanoic acid), then 1.83 t of caustic soda (550 EUR) would be required for 1 t hexanoic acid. For unrefined hexanoic, this is more than half the market price, and 18.3 to 27.5% for the refined hexanoic acid price range. pH control may indeed be further optimized, but this control fermentation on real thin stillage demonstrates the clear and present issue of a large caustic dosing requirement. Moreover, on top of caustic dosing to maintain the fermentation in the biocompatible range for production, acidification is often required in primary recovery, as discussed in Chapter 1. The production of OH^- and H^+ by membrane electrolysis avoids caustic and acidic dosing, and by extension also avoids salts entering the fermentation and extract solution.

The power input from these experiments was approximately 2 kWh per kg COD_{VFA}. Assuming 0.05 EUR kWh^{-1} electricity cost, this is around 100 EUR t^{-1}_{COD}, though we stress this is specific to these experimental conditions. This includes the caustic correction and, unlike the control case, extraction and acidification. If the issue of solids build-up between the electrode and the membrane can be avoided and the theoretical power saving of 30% holds, the power cost comes to 70 EUR t^{-1}_{COD}. In principle this power input can come from renewables to improve the sustainability argument. This is also true when comparing membrane electrolysis against electrodialysis, however membrane electrolysis has the potential for considerably lower ohmic drop due to the close proximity of electrodes (potentially only a few millimeters in a plate and frame arrangement) and thus lower power input compared against electrodialysis. Note that these calculations disregard downstream processing, which can be capital and energy intensive when separating compounds with similar properties, such as mixed VFA. For industrial, bulk chemicals, high product selectivity is critical to the economics of recovery and purification. A more detailed cost and market analysis is covered in Chapter 6.

A central tenet of thesis is to move from chemical and heat intensive petrochemical processes towards more sustainable processes, as chemicals and heat both imply embedded petrochemical energy. Membrane electrolysis is electricity driven, and can only be a sustainable technology if this electricity can be sourced sustainably, however the integration of clarification, primary recovery and concentration into one technology, alongside on site

acid and base production, favors the potentially sustainable credentials of membrane electrolysis. There are many common features between electrodialysis and membrane dialysis, but membrane electrolysis stands out for a process that requires extensive caustic correction, the fermenting community can metabolize hydrogen to the benefit of the process and the extracted products have increased value in the acidic form.

CHAPTER 5

Concentration, Recovery and Valorization

This chapter is redrafted from:

Stephen J Andersen, Tom Hennebel, Sylvia Gildemyn, Marta Coma, Joachim Desloover, Jan Berton, Junko Tsukamoto, Christian Stevens and Korneel Rabaey, Electrolytic Membrane Extraction Enables Production of Fine Chemicals from Biorefinery Sidestreams; *Environmental Science & Technology,* 2014; 48 (12), pp 7135–7142; DOI: 10.1021/es500483w

Stephen J Andersen, Jan Berton, Pieter Naert, Sylvia Gildemyn, Korneel Rabaey, Christian Stevens, Extraction and Esterification of Low-Titer Short-Chain Volatile Fatty Acids from Anaerobic Fermentation with Ionic Liquids; *ChemSusChem*, 2016; 9 (16), pp 2059 – 2063; DOI: 10.1002/cssc.201600473

5.0 Abstract

Membrane electrolysis can extract carboxylic acids from a fermentation broth into a clean acid concentrate with neither solids nor biomass. Products such as hexanoic acid can be concentrated and separated when it surpasses its solubility to form a hydrophobic liquid phase, while succinic acid can be extracted to the point of precipitation. Short chain carboxylic acids, however, are highly miscible in water. We therefore developed a pipeline to extract and upgrade VFA to esters (R_1-COOH + R_2-OH ⇌ R_1-COO-R_2 + H_2O) via Biphasic Esterification, in which the aqueous VFA concentrate reacts with added alcohol in a water-excluding phase to generate volatile esters. In a batch extraction, 96 ± 1.6% of the total acetate was extracted in 48 h from biorefinery thin stillage (5 g L^{-1} acetic acid) at 379 g m^{-2} d^{-1} (36% Coulombic efficiency). With continuously regenerated thin stillage, the extract solution was concentrated to 14 g L^{-1} acetic acid, and converted at 2.64 g L^{-1} h^{-1} (g of acetic acid per L of xylene) in the first hour to ethyl acetate by the addition of excess ethanol and heating to 70 °C, with a final total conversion of 58 ± 3%. Ionic liquids can both act as an involatile solvent and mediate esterification, and thus are an intriguing reactive extraction site for Biphasic Esterification. Four phosphonium ionic liquids were tested for single stage extraction of acetic acid from a dilute stream and esterification to ethyl acetate with added ethanol and heat. The esterification proceeded with a maximum conversion of 85.9 ± 1.3 % after 30 min at 75 °C, from a 1:1 stoichiometric ratio. Extraction and esterification can be tailored with mixed anion ionic liquids, demonstrated here with a common trihexyl(tetradecyl)- phosphonium cation and a mixed chloride and bis(trifluoromethylsulfonyl)imide anion ionic liquid. The mixed anion IL had a maximum acetic acid extraction rate of 40 g L^{-1} h^{-1} (g of acetic acid per L of IL) and an esterification rate of 38.2 g L^{-1} h^{-1} (g of acetic acid per L of IL). In a further proof-of-concept, ethyl acetate was generated from an ionic liquid driven esterification of an acetic acid extract solution generated with CO_2 as the only carbon source by microbial electrosynthesis.

5.1 Introduction

The electrical driving force of membrane electrolysis can migrate ions across an ion exchange membrane into a lower volume, acidic extract thereby increasing the concentration of the acid product. Once the acid is completely protonated, depending on the properties of the membrane (*ie.* resistance to diffusion of organic compounds, hydrophobicity) the product will not pass back through the anion exchange membrane, but accumulate in a solids separated, salty aqueous mixture. This is particularly useful for carboxylic acids that are immiscible below their pKa, because their physico-chemical properties can be exploited for recovery. Xu et al. (2015) took advantage of the low solubility of MCFA in the acid form and used membrane electrolysis to concentrate and acidify these fermentation products. Figure 5.1 shows how these MCFA can then simply be recovered from the upper, oily phase. In this study, the extraction system generated a product of approximately 90 % hexanoic (*n*-caproic) acid and octanoic (*n*-caprylic) acid in this phase.

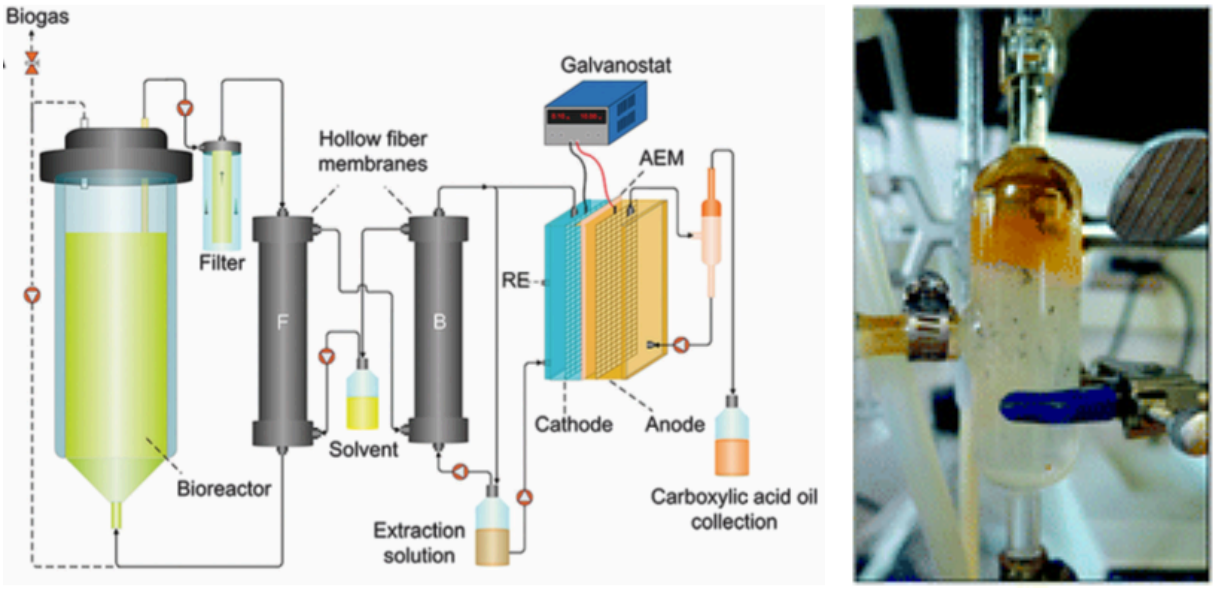

Figure 5.1. Combined liquid-liquid and membrane electrolysis extraction system to enable phase separation of hexanoic (*n*-caproic) acid and octanoic (*n*-caprylic) acid.

From Jiajie Xu, Juan J.L. Guzman, **Stephen J. Andersen**, Korneel Rabaey and Largus T. Angenent, In-line and selective phase separation of medium-chain carboxylic acids using membrane electrolysis, *Chem. Commun.*, 2015, 51, 6847.

This phenomenon can also be applied to drive ions into an acidic extract above their solubility for recovery through precipitation. Pateraki et al. (*Manuscript in preparation*) performed an in situ membrane electrolysis on a succinic acid fermentation by *Basfia succiniciproducens*. Succinic acid has a normal solubility in water of 58 g L^{-1}, and this concentration was exceeded by maintaining the extract solution at 37 °C and applying a current of approximately 600 mA (60 A m^{-2}) to extract from the fermentation broth into an extract solution volume 15 times smaller. A succinic acid product with a purity of 75 % was precipitated by the cooling the extract solution and removing the liquid layer, as pictured in Figure 5.2.

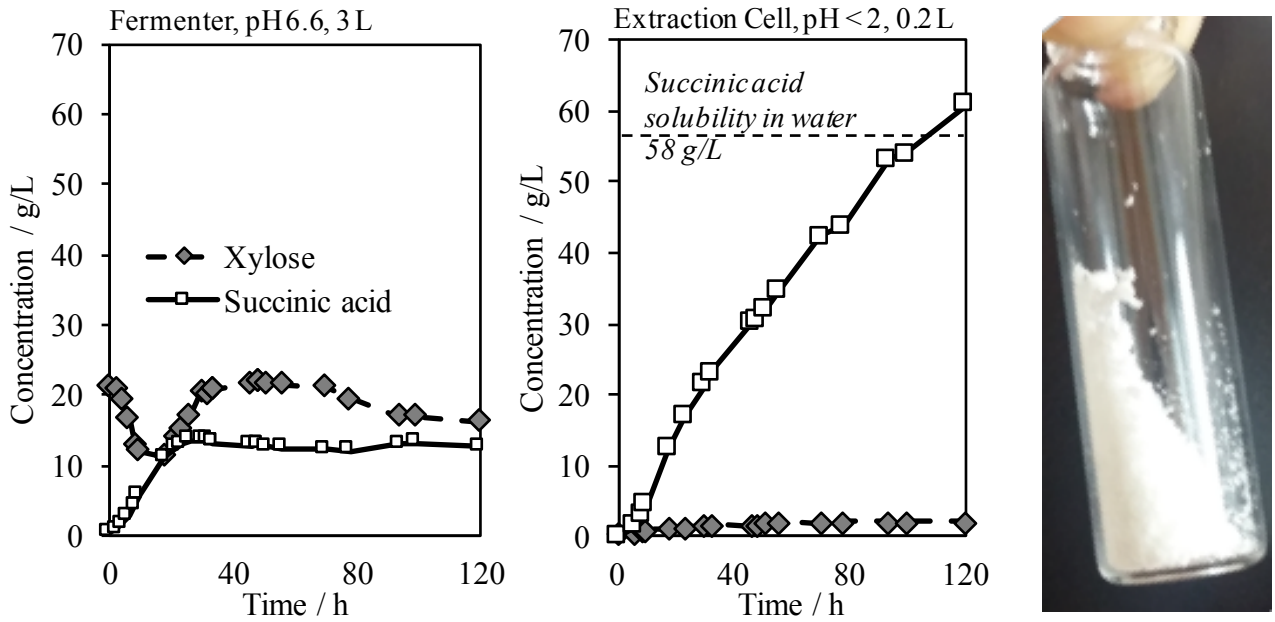

Figure 5.2. In situ membrane electrolysis to enable precipitation of succinic acid. The fermenter is semi-continuous and the extraction cell was operated in batch at 37 °C, resulting in accumulation of succinic acid above the normal solubility of succinic acid. The recovered precipitate (pictured) was 75 % w/w succinic acid.

From Chrysanthi Pateraki, **Stephen J. Andersen**, et al. (*Manuscript in preparation*)

Not all carboxylic acids have the convenient physical properties of MCFA and succinic acid that enable easy recovery, even after concentration. SCFA are more challenging to recover and valorize, both acetic and propionic acid remain miscible in water in the acid form, and only begin phase separation or crystallization at temperatures around -20 °C. Distillation is an expensive, energy intensive option for relatively low-titer, low value products such as acetic acid, with a normal boiling point of 118 °C, and 141 °C for propionic acid. Esterification was investigated as a potential reactive extraction route, as

short chain esters (i) have a relatively low solubility in water (ethyl acetate, 8.3 g per 100 mL water at 20°C), (ii) are less miscible than VFA and ethanol, (iii) have a low standard boiling point (ethyl acetate at 77.1 °C), and (iv) ethyl acetate is an energy dense solvent with a greater value than that of the sum of acetic acid and ethanol. Though esterification is an alcohol consuming process, bio-ethanol is increasingly abundant and mostly limited to use as a drop-in fuel (OECD 2014). Until now, esterification of biologically produced VFA has been largely ignored, as esterification is a reversible, water producing reaction and biological VFA are only generated in relatively low-titre, aqueous broths. Industrial esterification from petrochemical VFA proceeds dry, typically at a 5:1 molar excess of ethanol and catalyzed with sulfuric acid, all of which are not conducive to biological conversions. Reactive extraction has been explored in industrial ethyl acetate production, but exclusively with petrochemically produced, highly concentrated VFA (Liu et al. 2008, Santaella et al. 2015).

In this study we present a biphasic esterification (*ie*. aqueous phase and hydrophobic solvent phase) for reactive extraction of VFA from dilute aqueous streams. Carboxylic acids, such as acetic acid, can be transferred to a hydrophobic phase to react with an alcohol, such as methanol or ethanol, to generate a low solubility, volatile, added-value ester. The biphasic esterification was first executed with a xylene solvent, and then followed up with a series of experiments exploring ionic liquid (IL) mediated esterification, as ILs can be tailored through anion and cation selection, and can thus be hydrophobic yet have a high affinity for the polar VFA. The process was investigated with a view of integration as per the scheme in Figure 5.3.

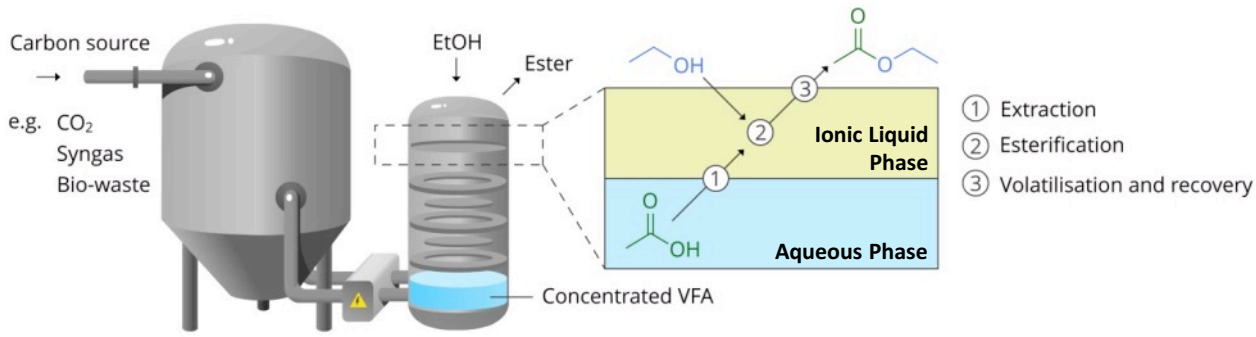

Figure 5.3. Schematic for fermentation, membrane electrolysis extraction and esterification of VFA**.** Image by Tim Lacoere.

For a reactive extraction esterification, we aim for (i) a solvent to extract low-titre VFA; (ii) a water excluding site for esterification; and (iii) a highly non-volatile vector for evaporation. ILs exhibit some unique properties, including a very low volatility and high chemical and physical stability, allowing the ester to be evaporated from the solvent with a substantially decreased energy input compared to distillation, thus avoiding energy loss as latent heat of vaporization of the extract solution (Neves et al. 2011). ILs can be tailored to a wide variety of applications through a combination of ions, and for this reason ILs are often referred to as 'designer solvents' (Huddleston et al. 2001; Plechkova et al. 2008). IL selection and characterization was based on the capacity for solvent extraction and esterification with a specific focus on acetic acid and ethanol as the model VFA and alcohol. ILs are largely uncharacterized for liquid-liquid extraction and reactive extraction parameters, such as the partition ratio and reaction rate constants. This is not unexpected when considering the broad variety of ILs and the limited knowledge linking structure and function. Trihexyl(tetradecyl)phosphonium ($[P_{666,\ 14}]^+$) ILs were selected in this study for their hydrophobicity, melting point below room temperature and potentially high extraction capacity, relative to other common classes of ILs (Martak et al. 2007).

5.2 Materials & Methods

5.2.1 Membrane electrolysis concentration. Perpex electrochemical cells (two chambers separated by a membrane, each with internal dimensions: 80 mm (l) × 80 mm (w) × 20 mm (d)) were used either with a synthetic acetic acid solution or thin stillage of Alco Bio Fuel NV (Ghent, Belgium), as described in Chapter 4. In all these experiments the current remained set at 20 A m^{-2} and both compartments were continuously mixed by a recirculation rate of 6 L h^{-1}.

To demonstrate extraction up a concentration gradient, the cathode concentration was maintained at 10 g L^{-1} acetic acid (pH 5.5) to simulate conditions after carboxylate fermentation, and flux was assessed for a starting anolyte concentration of 5, 10, 20, 30 and 50 g L^{-1} acetic acid (pH 2).

Next, the cathode compartment (fermentation broth, 5 g L^{-1} acetic acid, pH 5.5) and the anode compartment (0.5 M Na_2SO_4) were tested in a batch extraction to observe the extent of extraction from catholyte to anolyte in a real fermentation matrix. The cathode was then continuously fed while the anode compartment was run in batch to better mimic

realistic operating conditions (accumulation in the anode, excess broth relative to extract solution). To prevent clogging this broth was centrifuged at 10 000 rpm for 10 min and solids were removed prior to the experiment. The electrochemical cells were fed at a rate of 0.8 L d^{-1} to achieve a residence time of 5 h, and feed was replaced daily.

5.2.2 Biphasic esterification in xylene. Esterification experiments were executed with a synthetic anolyte and a real anolyte. The synthetic anolyte consisted of 20 g L^{-1} acetic acid (pH 2) and 0.5 M Na_2SO_4. In all cases, 20 mL of anolyte was used with a xylene (Sigma-Aldrich, Belgium) solvent layer of 20 mL in a 100 mL bottle, with approximately 60 mL of headspace. The layered liquids were vacuumed to a slight under-pressure and heated to 70 °C. At t = 0 h, 5 mL of either ethanol, methanol, or distilled water (control) was injected. The bottles were then stirred and maintained at 70 °C for 20 h. The aqueous fraction was sampled at t = 0 and t = 20 h and analyzed for carboxylate concentration by GC, as described in Chapter 3. These experiments were performed in quadruplicate.

5.2.3 Screening of ionic liquids for esterification and evaporation. A common phosphonium cation and different anions were screened for esterification. These anions included dicyanamide (DCA), chloride (Cl), tetrafluoroborate (BF_4), bis(trifluoromethylsulfonyl)imide (Tf_2N) and a 1:1 mixture of Tf_2N and Cl. Hereafter for brevity each IL will be referred to as follows: $P_{666,14}$ DCA, $P_{666,14}$ Tf_2N and $P_{666,14}$ Cl (Sigma-Aldrich, Belgium). Each were used without prior purification. $P_{666,14}$ BF_4 was prepared through metathesis of $P_{666,14}$ Cl and sodium tetrafluoroborate (Blundell et al. 2014). 1 g of the ionic liquid was added to a 15 mL pressure vial, with 10 mL of 0.33 M acetic acid. 49 mg H_2SO_4 was added to the aqueous phase to obtain a concentration of 0.05 M. The vial was sealed and placed in a 75° C temperature controlled oil bath and magnetically stirred. 25 mg of the IL layer was sampled after stopping the stirrer to allow phase separation, and analyzed with quantitative ^1H NMR. To test esterification, 1 g of the ionic liquid, 0.33 M acetic acid and 5 mg H_2SO_4 (0.3 equivalent of protons compared to the acetic acid) were transferred to a 2 mL vial. After addition of a small stirring bar, the vial was sealed, placed in a 75 ° C temperature controlled oil bath and magnetically stirred. 46 mg ethanol (1 mmol) was added to intitiate esterification. Samples were analyzed with quantitative ^1H NMR. For evaporation of the ester, 1 g of ionic liquid was added to a 10 mL flask containing a stirring bar, to which 30 mg ethyl acetate was added. This was connected to a liquid nitrogen cooled cold trap with a vacuum pump and manometer (Vacuubrand PC 2001 Vario). The flask was

maintained at 55 °C in an oil bath and stirred. A vacuum (40 mbar) was applied for 5 minutes, after which the pressure was allowed to rise by gradually decoupling the connecting tube from the flask. The ethyl acetate concentration before and after evaporation was determined through quantitative ^{1}H NMR.

For the microbial electrosynthesis extract solution from Gildemyn et al. (2015), 10 mL of the extractant solution was contacted with 1 mL $P_{666,14}$ Tf_2N, and magnetically stirred at 75 °C for 2 hours. After phase separation, the IL layer was transferred into a 2 mL Eppendorf and centrifuged for 5 minutes at 22 °C and 30 000 rcf. The IL layer was transferred and weighed in the 2 mL vial for esterification after removal of the supernatant. The acetic acid concentration was determined through quantitative ^{1}H NMR analysis. The IL layer was transferred to a 2 mL vial, to which 3 equivalents ethanol and 5 mg H_2SO_4 were added. This was heated to 75 °C in a temperature controlled oil bath and magnetically stirred. Samples were analyzed by quantitative ^{1}H NMR analysis.

5.2.4 Screening of reaction conditions. Esterification was executed with a modified temperature or ethanol concentration. To study the influence of water on the esterification, 455.4 mg of ethanol (3 stoichiometric equivalents) was added to the IL layer after 2 hours of extraction. Mixing was maintained for 2 hours with frequent sampling of the IL layer to monitor the esterification and analyzed through quantitative ^{1}H NMR analysis. For phase separation, the aqueous layer was removed after 2 hours of extraction followed by centrifugation for 5 minutes by an Eppendorf 5430 R centrifuge, at 22 °C and 30 000 rcf. The IL layer was transferred and weighed in the 2 mL vial for esterification after removal of the supernatant. The acetic acid concentration was determined through quantitative ^{1}H NMR analysis. The IL layer was transferred to a 2 mL vial, to which 3 equivalents ethanol and 5 mg H_2SO_4 were added, heated to 75 °C in a temperature controlled oil bath and magnetically stirred. Samples were analyzed by quantitative ^{1}H NMR.

5.2.5 Chemical analysis. ^{1}H NMR and ^{13}C NMR were performed at 400 MHz and 100 MHz respectively on a Bruker Avance III Nanobay 400 MHz spectrometer. 400 µL DMSO-d_6 was added to 25 mg of IL layer sample, stirred and transferred to an NMR tube. Quantification was performed relative to 1,4-dioxane as standard (0.2 M in DMSO-d_6), contained in a NORELL 100 µL capillary insert. ^{1}H NMR experiments were run with 8 scans and 1 second relaxation delay.

5.3 Results

5.3.1 Carboxylic acid concentration by membrane electrolysis. Acetic acid flux from the catholyte (fermentation broth) to the anolyte (extract solution) continues despite acetic acid accumulation in the anode up to 50 g L^{-1} for the membrane tested (Figure 5.4). Accumulation of the organic product is possible by the low pH of the extract solution, as the AEM allows the transport of AEM to the exclusion of other species. This is clearly not absolute, as the net flux of the acetic acid ion is countered by the diffusivity of acetic acid from the extract back to the catholyte. Assuming the projected trend continues forward linearly according to the Nernst-Planck equation (Chapter 3, equation 1), the net flux of acetic acid for this membrane would become zero at approximately 70 g L^{-1} acetic acid in the extract solution, at which point back-diffusion equals flux.

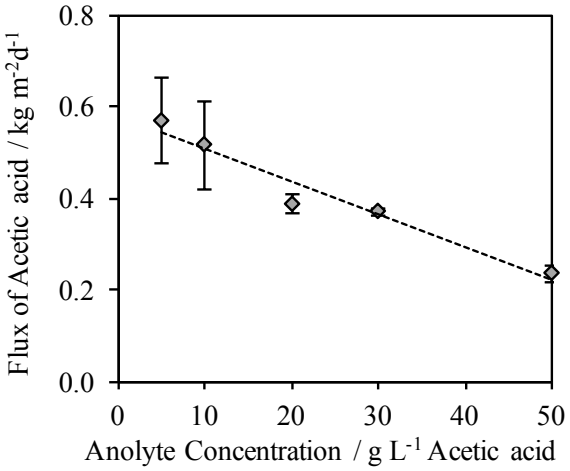

Figure 5.4. Net flux (positive migration – negative diffusion) of acetic acid into a concentrated extract solution at 20 A m^{-2}

From a 5 g L^{-1} acetic acid source in clarified thin stillage, 96 ± 12% of the acetic was transferred to the extract solution after 48 hours, with an average flux of 0.379 kg m^{-2} d^{-1} corresponding to a coulombic efficiency of 35.9 %, due to the competitive flux of other native anions in the broth (Figure 5.5A). Acetic acid was extracted at a consistent rate over the course of the experiment, albeit with high variability. Figure 5.5B demonstrates a continuously fed catholyte with accumulation in the anolyte in batch, followed by a biphasic esterification experiment with xylene. As the acetic acid concentration approached 12 g L^{-1} the net flux began to decrease as the acetic acid product accumulated to a final concentration of 14 g L^{-1} prior to esterification.

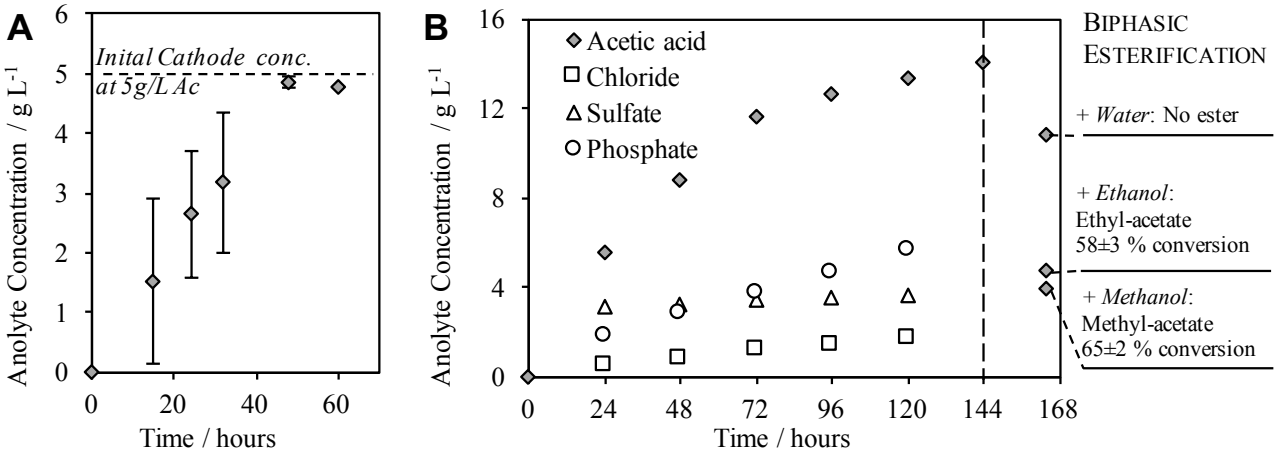

Figure 5.5. A. Batch extraction of acetic acid from thin stillage stream at 5 g L^{-1} acetic acid, with equal volumes of catholyte and anolyte. **B.** Continuously fed 5 g L^{-1} acetic acid stream to the catholyte, with batch operation of the anolyte to allow acid concentration, followed by biphasic esterification at 144 h.

5.3.2 Aqueous acetic acid to methyl- and ethyl-acetate. The high salinity and low pH of the anolyte can support a phase transition of the acetic acid to the water-excluding hydrophobic phase where it is esterified with added alcohol and heat. This was tested with both synthetic and real anolyte using xylene as model solvent and vector for ester measurement. Gas chromatography and mass spectrometry confirmed the presence of methyl acetate and ethyl acetate, and the absence of esters in the control test with distilled water. For the synthetic anolyte, acetic acid concentration fell by 26 ± 5 % after esterification with methanol, 10 ± 3 % after addition with ethanol, and no change in acetic acid was observed (0 ± 1 %) where only water was added, after taking dilution and transference to the solvent layer into consideration. The same process was applied to the real anolyte collected at t = 144 of the continuous cathode / batch anode experiment, as shown in Figure 5.5B. The decrease in acetic acid concentration was great for the real extract solution, at 58 ± 3% for the production of ethyl acetate and 65 ± 2% for methyl acetate. This may be due to improved catalysis by the lower pH in the real anolyte, measured at pH 0.94 compared to the synthetic anolyte's pH 2, as the batch was under electrolytic conditions for 144 h prior to the esterification. Acetic acid consumption proceeded rapidly in the initial period, at 2.82 g L^{-1} h^{-1} over the first hour during biphasic esterification with ethanol. This is equivalent to a maximum esterification rate calculated at 4.14 g L^{-1} h^{-1} in the first hour of the reaction (per g of ethyl acetate per L anolyte, assuming complete stoichiometric conversion). The presences of ethyl acetate and methyl acetate in

the respective reactions were confirmed by GC-MS but could not be quantified due to high decomposition in the xylene between sampling and GC-MS measurement.

5.3.3 Screening ionic liquids. Four IL anions were screened for single stage transfer of aqueous acetic acid, esterification of acetic acid with ethanol to ethyl acetate and evaporation of ethyl acetate from the IL (Figure 5.6). The comparison of these four common ILs enables the study of the effect of the anion on the performance of the process.

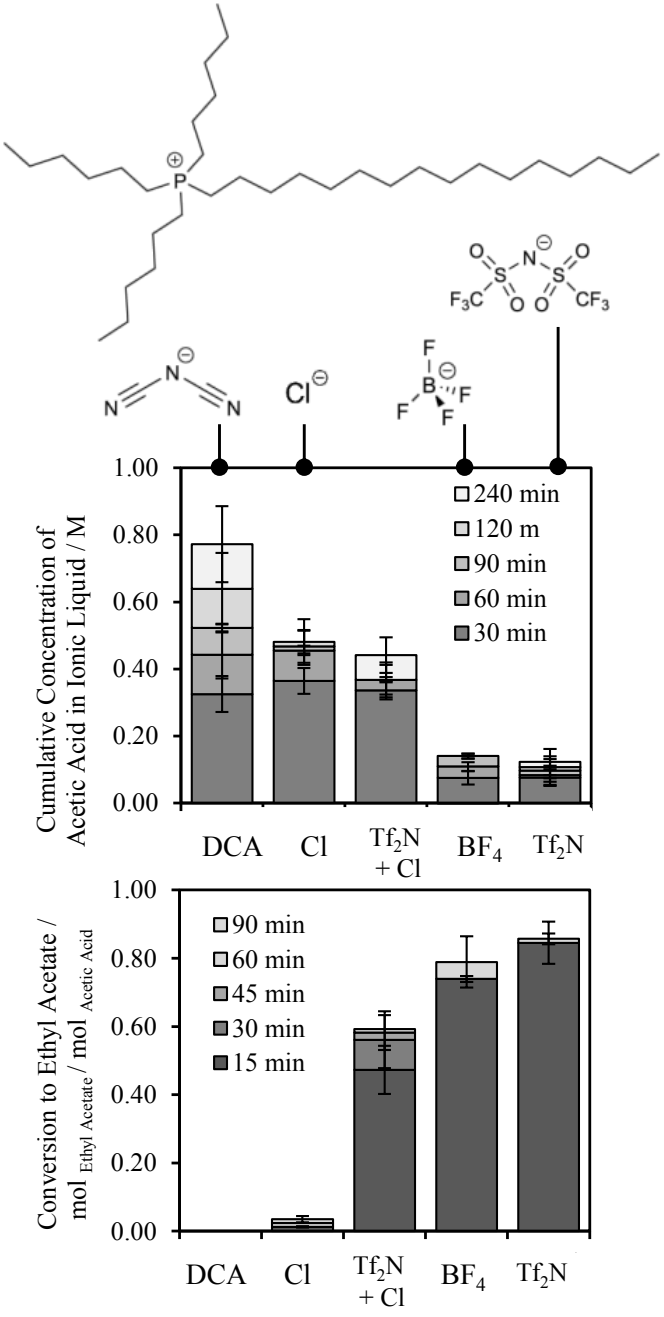

Figure 5.6. Single stage transfer of 330 mM acetic acid to the ionic liquid and esterification to ethyl acetate.

Top (Pictured). Molecular structure of trihexyl(tetradecyl)phosphonium ($P_{666,14}$) cation IL with anions (from left to right) of dicyanamide (DCA), chloride (Cl), tetrafluoroborate (BF_4) and bis(trifluoromethylsulfonyl)imide (Tf_2N).

Middle. Cumulative concentration of acetic acid in the ionic ionic liquid over time, transferred from a 0.3 M acetic acid source.

Bottom. Cumulative molar conversion, expressed as moles of ethyl acetate as a fraction of the initial molar concentration of acetic acid.

Transfer of acetic acid from a 330 mM (19.8 gL^{-1}) aqueous phase (10 mL) into the IL phase (1 mL) was assessed at 75°C. The final acetic acid concentrations were 123 mM in the IL phase for $P_{666,14}$ Tf_2N, 131 mM for $P_{666,14}$ BF_4, up to an apparent 772 mM for $P_{666,14}$ DCA after 240 min (Figure 5.5). At 30 min, the concentration of acetic acid in the $P_{666,14}$ DCA (325 ± 54 mM) and $P_{666,14}$ Cl (364 ± 38 mM) had reached the same concentration at as the aqueous phase (330 mM), i.e. a partition ratio of around 1 ([acetic $acid_{IL}$] / [acetic $acid_{AQUEOUS}$]). $P_{666,14}$ DCA thus achieved a significantly greater apparent concentration of acetic acid at 240 min. This can be attributed to exchange of $acetate^-$ for the $P_{666,14}$ DCA anion, as the DCA anion was found to hydrolyze under these conditions and the $acetate^-$ ion migrated into the IL phase to conserve electroneutrality. The byproduct peaks were detected by ^1H NMR and ^{13}C NMR but could not be successfully identified by LC-MS. The concentration of acetic acetic at 30 min was comparatively low for both $P_{666,14}$ BF_4 (75 ± 20 mM) and $P_{666,14}$ Tf_2N (76 ± 25 mM), with a partition ratio of 0.23. Combining Cl and Tf_2N in a 1:1 mix resulted in a partition ratio of 1 after 30 min (337 ± 28 mM).

Each IL was screened for its ability to mediate esterification by dosing acetic acid and sulfuric acid in the absence of water at 75 °C and a 3 × molar excess of ethanol. $P_{666,14}$ Tf_2N was the most effective IL for esterification with a conversion of 84.5 ± 1.6 % in 15 minutes, with a similar conversion for $P_{666,14}$ BF_4 at 74.5 ± 1.6 %, and a minimal or absent conversion for $P_{666,14}$ Cl and $P_{666,14}$ DCA (Figure 5.6), the inverse order of the acetic acid concentration. The 1:1 $P_{666,14}$ Tf_2N and $P_{666,14}$ Cl mix had a conversion of 47.3 ± 7.1 % at 15 min, and 56.1 ± 8.3 % at 30 min, with no significant conversion following. This highlights the capacity for different anions to bring combined functionality to the same IL in reactive extraction, indicating the critical importance of anion selection. The $P_{666,14}$ Cl IL is lower in cost with good extraction and poor esterification, while $P_{666,14}$ Tf_2N is the opposite: excellent esterification, poor extraction, and costly. This Mixed Anion IL has extraction and esterification properties between that of $P_{666,14}$ Tf_2N and $P_{666,14}$ Cl, which has potential for a multi-stage column in which extraction and esterification could be tailored according to the ratio of ions in the stage. Mixed anionic salts have been explored in battery electrolytes (Kerner et al. 2015), but not in extraction and catalysis.

5.3.4 Ionic liquid esterification heat and substrate efficiency. Heat and substrate efficiency was explored by decreasing the esterification temperature and concentration of ethanol. Esterification in $P_{666,14}$ Tf_2N at 75 °C and a 3:1 stoichiometric ratio was compared against 55 °C and a 1:1 ratio (exact stoichiometric ratio) of reactants (Figure 5.7). The

maximum conversion remained high with 1 ethanol equivalent, at 75.5 ± 2.8 % at 15 min and 85.9 ± 1.3 % at 30 min. Conversion slowed at 55 °C, with 47.6 ± 8.4 % at 15 min, and reached the maximum conversion of 81.4 ± 11.9 % at 60 min. This demonstrates that a milder temperature results in a decreased rate, but the same total conversion is reached within an hour. Ethyl acetate was added to the IL and evaporated for 5 minutes at 55°C while stirring, and reached almost completely recovery in this time (Table 5.1). The efficiency (proportion recovered after 5 min) was inversely related to the IL viscosity.

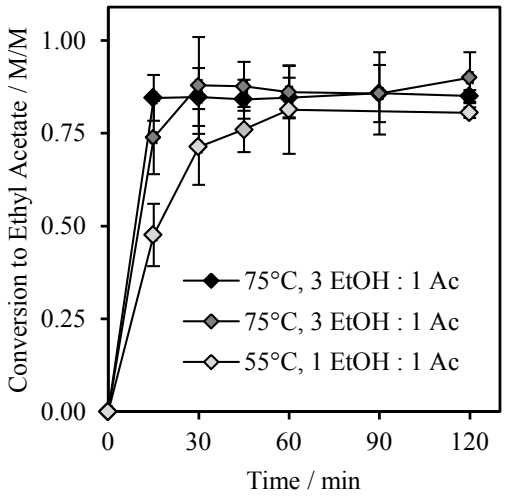

Figure 5.7. Molar conversion to ethyl acetate over two hours at either 75 °C or 55° C and either 3 or 1 moles of ethanol per mol of acetic acid, in $P_{666,14}$ Tf_2N.

Table 5.1. Total amount of ethly acetate evaporated after 5 mins and reported viscosity of the four ILs.

IL	Evaporation efficiency (%)	Viscosity (mPa s)
$P_{666,14}$ DCA	94.9 ± 1.3	256
$P_{666,14}$ Tf_2N	86.7 ± 5.4	312
$P_{666,14}$ Cl	75.3 ± 1.9	1824
$P_{666,14}$ BF_4	77.3 ± 4.2	787

5.3.5 Concentration, recovery and valorization of VFA from CO_2. Acetic acid can be generated through microbial electrosynthesis with CO_2 as the sole carbon source, and Gildemyn et al. (2015) demonstrated that membrane electrolysis extraction can be driven by the same electrical power that drives the bio-production. In this experiment, the acetic acid concentrate reached a concentration of 13.5 g L^{-1} (225 mM).

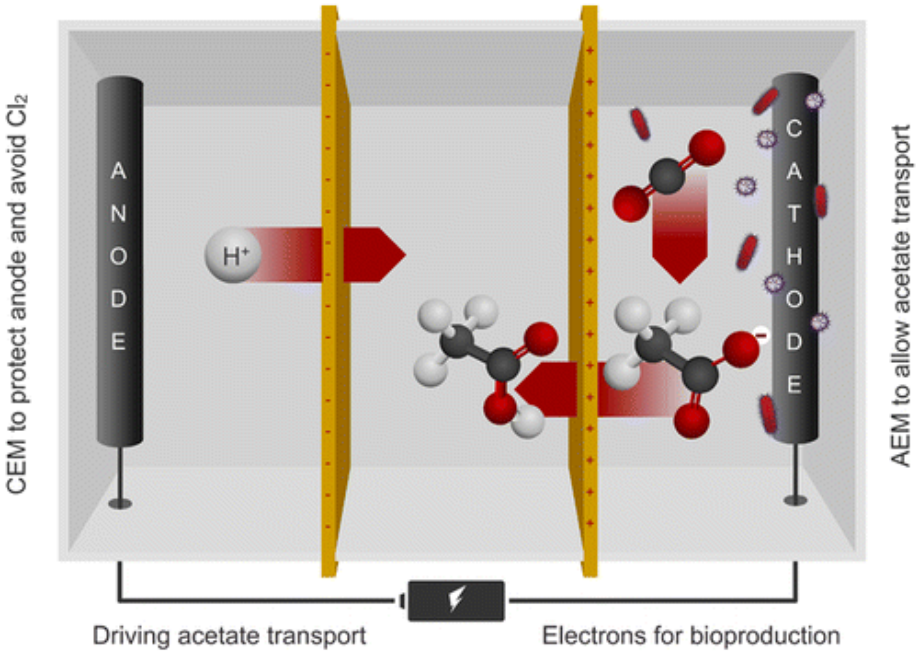

Figure 5.8. An acetic acid concentrate can be generated using CO_2 as the sole carbon source. Image by Tim Lacoere.

From Sylvia Gildemyn, Kristof Verbeeck, Rik Slabbinck, **Stephen J. Andersen**, Antonin Prévoteau and Korneel Rabaey, Integrated Production, Extraction, and Concentration of Acetic Acid from CO_2 through Microbial Electrosynthesis, *Environ. Sci. Technol. Lett.*, 2015, 2 (11), pp 325 - 328

As a proof of concept, IL esterification was executed on the microbial electrosynthesis extract solution from Gildemyn et al. (2015). This acetic acid transferred into the Tf_2N IL to a maximum concentration of 0.08 M, followed by 74 ± 10% conversion to ethyl acetate in 15 min and maximum conversion of 90 ± 7 % after 120 min. This is the first time that ethyl acetate was produced from CO_2 and ethanol. Considering that both methanol and ethanol can be produced from CO_2 (Gao et al. 2012), this approach enables the production and recovery of an energy dense, C4 room temperature liquid product starting from C1 compounds.

5.4 Discussion

Be it hexanoic acid, succinic acid or acetic acid from organic waste or CO_2, a unit operation to increase the concentration of the end-product is critical in the recovery of bio-chemicals from an aqueous broth. Hexanoic acid and other MCFA can be recovered by phase separation due to its hydrophobicity, and similarly succinic acid can be crystalized and precipitated, but in both cases trace contamination of compounds remain, such as VFA including acetic or lactic acid. Targeted, selective extraction is a defining feature of a high performing separation system and this is an issue for both membrane electrolysis and esterification. In its current incarnation, the membrane electrolysis step has not been demonstrated to selectively extract specific molecules, although the flux profile and coulombic efficiency clearly varies for acetic acid compared to hexanoic acid, as shown in Chapter 3. It is possible that selectivity can be manipulated through membrane development and/or applied current scheme relative to the carbon chain length or functional groups. Indeed, it is known that the performance of electrodialysis is highly dependent on the intrinsic properties of the AEM (Strathman 2005), however one anticipates for bulk chemical production it is unlikely that the modifications at the membrane level will result in a single step, high purity product. There exists a similar opportunity for product selectivity in the IL, however this may be complicated due to similar physico-chemical properties of VFA.

Here we established an initial perspective on the application of ILs as a dual extract solution and reaction medium, indicating the importance of ion combination as a process optimization tool. The presence of hydrophilic VFAs in a dilute aqueous stream remains a challenge both for extraction and esterification, but with an apt anion the esterification can proceed fast, even at mild conditions and a 1:1 stoichiometric ratio of reactants. The nature of VFA as weak organic acids gives rise to the duality of their potential and their challenge. The extraction of the polar VFA into a hydrophobic IL remains an issue. The variation in performance, both in extraction and esterification, as it pertains to IL anion is not clear and demands further investigation, but also demonstrates the potential for IL tailoring. Hydrogen bonding between the solute and the IL anion has been shown to influence the partition coefficient of organic acids in an IL, alongside hydrophilicity of the solute (Oliveira et al. 2012). The combination of a hydrophobic cation and an anion that features an increased extraction through hydrogen bonding and effective esterification can substantially increase the overall performance. The exclusion of water is critical to

esterification. A dewatering step vastly improved the conversion to esters. Only 44.2 ± 2.9 % of the acetic acid in the IL phase was converted to ethyl acetate after 2 hours in a single stage biphasic esterification (*i.e.* the aqueous phase remains in the vessel), compared with 84.5 ± 1.6 % without water. Phase separation allows a slightly higher conversion of 49 ± 2 % in 2 hours. Phase separation and centrifugation to remove the aqueous phase resulted in 80.1 ± 6.5 % conversion in 15 minutes. This demonstrates that the presence of water, even in minimal amounts in the highly hydrophobic IL, constrains the esterification and must be carefully considered in engineering a full scale process.

The process proposed here operates with an IL / water interface, and dissolution of the IL can lead to losses of a rather expensive compound. Ion losses could impact process economics and product quality, and may require the IL to be recovered from the product or waste stream, for example with another solvent, or replaced over time. This will require careful attention in future studies, particularly with regards to the environmental impact. Though ILs are often regarded as being more sustainable than classic organic solvents, their 'green solvent' label has led to the misconception that they are non-toxic and biodegradable (Stojanovic et al. 2011), which is not the case for some of the ILs used in this study (Mikkola et al. 2015).

Esters are used in a broad variety of applications with extensive existing markets that face increasing consumer demand for green products. Approximately 4 billion tons of ethyl acetate were produced worldwide in 2015, largely from coal and natural gas, and predominantly used as solvents in chemical processing, adhesives and coatings. There is a clear and present opportunity for a positive environmental impact from the bioproduction of sustainably produced and recovered organic acids and solvents (Philp 2015). While expensive IL precursors restrict capacity from the bench through to the industrial scale, increased production and research of ILs should bring a welcome decrease in price over time. This is critical to the success of ILs in sustainable industrial chemistry, and in bulk chemical production from renewable resources.

CHAPTER 6

Discussion and Outlook

6.0 Major findings

Chapter 2

- The competitive environment of a mixed community MCFA fermentation can lead to the dominance of single species and suppression of critical community members involved in producing intermediate compounds
- *Clostridium* group IV species in a mixed community are capable of generating and tolerating toxic MCFA, with decanoic acid reported here for the first time
- The upper chain-length of MCFA production through reverse β oxidation remains unclear due to interference in analysis, possibly from intracellular fatty acids

Chapter 3

- Membrane electrolysis can drive carboxylic acid extraction through an AEM
- Both transport of the target acid and exclusion of protons are key to effective transport in membrane electrolysis
- Electrochemical Impedance Spectroscopy can reveal some of the major transport parameters and resistances associated with membrane electrolysis, such as electrical mobility, membrane resistance, and polarization resistance

Chapter 4

- Applying membrane electrolysis on a mixed culture fermentation of thin stillage selects for species that are likely to metabolize hydrogen gas, thus driving VFA production towards a greater proportion of MCFA
- Membrane electrolysis can completely replace caustic dosing in an VFA fermentation, and may have an electro-coagulation effect on suspended solids

Chapter 5

- The target products can be concentrated by membrane electrolysis, allowing phase separation in MCFA, precipitation in succinic acid, and accumulation of miscible short chain fatty acids, such as acetic acid
- Acetic acid can be esterified and extracted through evaporation by a novel ionic liquid process with low ethanol and energy input
- Ionic liquid performance can be tailored by mixing anions, with $P_{666,\ 14}$ $(Tf_2N)_{0.5}$ $(Cl)_{0.5}$ demonstrated for the first time to be an effective IL for acetic acid solvent extraction (up to 40 $g_{Acetic\ Acid}$ L^{-1} h^{-1}) and esterification (up to 38.2 $g_{Acetic\ Acid}$ L^{-1} h^{-1})

6.1 Adding value through membrane electrolysis

Membrane electrolysis has been demonstrated through this thesis to add value to the processing requirements for the production and recovery of carboxylic acids. With an emphasis on risk versus value, this chapter will discuss some practical considerations that have arose through Chapters 2 through 5, followed by the implications of membrane electrolysis in terms of recovery of the target product, co-products and unit operations, and the unit itself, in terms of critical materials, operation lifetime and sustainability.

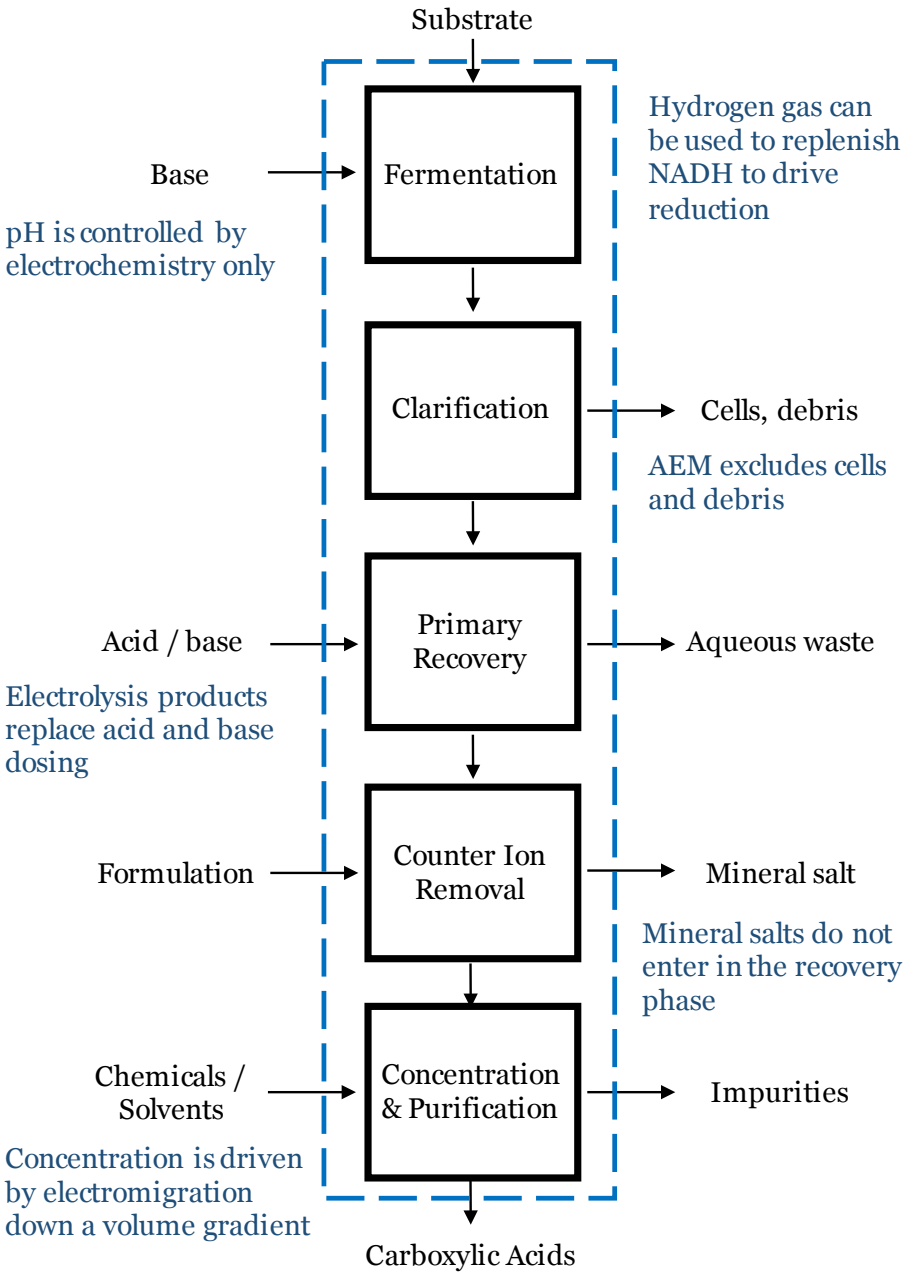

Figure 6.1. The influence of membrane electrolysis (blue) on a general processing scheme for production and recovery of carboxylic acids (adapted from López-Garzón and Straathof 2014)

6.1.1 Operational implications and lessons learned. Beginning in November 2015, the Center of Microbial Ecology and Technology began to work towards a demonstration scale unit (Figure 6.2) based around the findings in this thesis and studies from the Angenent Lab at Cornell University (New York, United States). This project is in collaboration with Paques nv (The Netherlands) as the technology provider, Tereos Starch & Sweeteners Europe (Aalst, Belgium) as a provider of thin stillage and beer for feed, and NuScience Belgium nv (Drongen, Belgium) for product testing, a market leader in supplying MCFA. Unit operations at the experimental scale can imposes boundaries that that can be overcome in scale-up, and some of the operational implications and considerations as the technology moves towards industry will be discussed here.

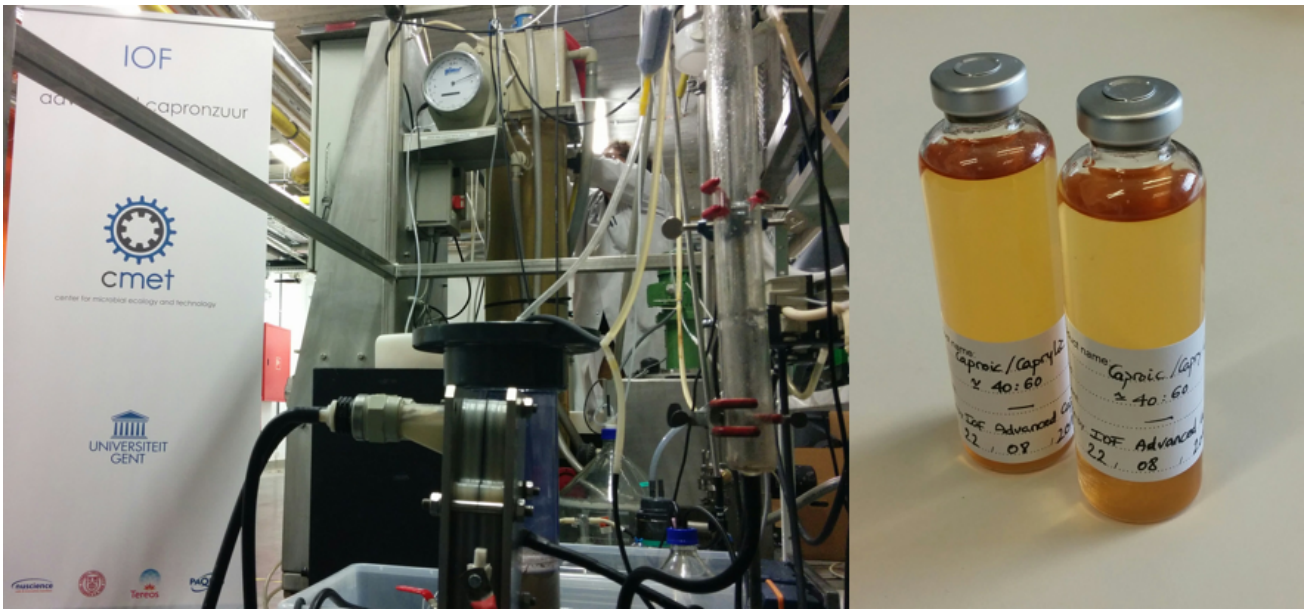

Figure 6.2. The demonstration scale mid chain fatty acid fermentation (60 L fermenter) with membrane electrolysis extraction system, with the product pictured on the right.

MCFA fermentation with a mixed community can lead to the collapse of some species and the domination of others, as demonstrated in Chapter 2. The study by Xu et al (2015), which the demonstration scale fermentation pipeline is modelled after, targets the hydrophobic portion by pertraction followed by a membrane electrolysis extraction from a high pH draw solution. Though effective, this processing pipeline relies upon potentially costly unit operations that must work continuously and effectively to keep the fermenter broth below the toxic concentration threshold. If the extraction unit goes offline, the

fermenter is put at risk of collapse. There exist other methods to avoid product toxicity, including adaption (or engineering) of individual microbial species and/or the community for greater tolerance, changing the physical characteristics fermentation broth such as operating in a neutral pH (Royce et al 2013), and adapting the process for low HRT flow with retained biomass (Grootscholten et al. 2013a). The most effective solution is likely to be some combination of all of the above. The trade-off between toxicity and high concentration MCFA could be balanced with alternative reactor configurations. Extraction with membrane electrolysis is most efficient when the target anion is in far excess in the broth, with extraction from low concentration solutions demonstrated in Chapter 3 but with lower efficiency. Discontinuous or semi-batch fermentations can allow the broth to reach a concentration conducive to effective extraction, followed by membrane electrolysis to deplete the broth of the product, and then recycle into an active fermenter below the toxicity threshold for further conversion. This recycled broth can also be a caustic source for the next fermentation. In Chapter 4, the acidic extract solution was returned to the fermentation solution when the upper pH set-point was exceeded, potentially allowing short chain side products in the extract to be further elongated. As an MCFA fermentation, the experiment executed in Chapter 4 was rather unsuccessful. The proportion of longer chain carboxylic acids increased, but the end product was a concentrated mixed VFA extract broth with the majority having a chain length of C5 and below. If an MCFA product is desired, it may be worthwhile to send the mixed VFA extract to a secondary fermentation for further elongation or return the extract back to the fermenter after the MCFA has phase-separated. For membrane electrolysis to be successful as an *in situ* extraction unit on a single fermenter producing MCFA, some additional strategy for managing toxicity should be used, alongside a valorization strategy for the short chain VFA and the other fermenter salts that were incidentally extracted.

The limitations of low concentration extraction with membrane electrolysis were discussed in Chapter 3, and though electro-migration by an applied current occurs independent of concentration, it is not independent of the other ions present in the system. A fermentation broth will always contain mixed salts (e.g. nitrate, sulfate, phosphate) and side products (e.g. acetic acid) that will compete for transport in the positive direction (cathode to anode), and protons that will compete for transport in the negative direction (anode to cathode). More research is required into competitive ion transport and how this can be managed through membrane development, cross-sectional flow rate, pressure

gradients across the membrane, and optimization of the pH and conductivity on both sides of the AEM. This research can be enabled through analytical techniques such as electrochemical impedance spectroscopy, which can reveal information about the migration parameters of different VFA within and around the membrane. A detailed computational fluid dynamics (CFD) model of membrane electrolysis would be an asset to explore the optimal parameters for highly effective extraction in a complex broth in which many physical and chemical parameters are at play. For example, the difference in osmotic pressure across the AEM will result in the transport of water, most likely towards the concentrated extract. Does this have a positive or negative impact on the flow of charged species in the same direction? How does this affect the resistance across the membrane, and thus the power input? Can the osmotic pressure gradient be exploited or countered by applying a pressure gradient across the membrane? A CFD model could help answer these questions, and to explore the boundaries of membrane electrolysis in application.

Added value and process risks extend beyond the efficacy of membrane electrolysis, beyond unit operations and rector configuration, and beyond the performance – and survival – of the microbial community. Waste streams and co-products must be assessed for recycle within the process or utilized externally, as is discussed further in this chapter in section 6.1.4. Co-products often add stability to a bio-refinery product portfolio, and in MCFA production one must consider trade-off between full conversion of the substrate to MCFA, or alternate routes for valorizing the short chain VFA. In Chapter 5, IL for esterification of short chain VFA were explored, however the dissolution of the IL anion may require attention to process wastewater streams, particularly for molecules such as bis(trifluoromethylsulfonyl)imide (Tf_2N) which may be harmful to aquatic organisms, and phosphonium ILs in general which have some toxicity towards bacteria (Matsumoto et al 2004, Mikkola et al 2015). Membrane electrolysis as performed in the works of this thesis uses an iridium oxide-coated anode, and iridium is a rare earth metal with a tendency towards price fluctuations and governmental stock-piling (U.S. Geological Survey, 2016). As the scale-up process moves forward, it is important to assess the added value and the process risks of MCFA fermentation and membrane electrolysis not only at the biological, electrochemical and physical level, but also within the broader context of sustainability and the environment.

6.1.2 Target Product & Ideal Substrate: two sides of the same coin. Process goals differ for the conversion of a low-value waste stream into a bulk chemical compared to production of specialty chemicals. Bulk Carboxylate Platform products such as mixed VFA (acetic acid, propionic acid, etc) generated by a mixed community have limited added value, with a high potential for a significant positive environmental impact, considering the ubiquity of petrochemically sourced VFA and esters (Philp 2015). MCFA can be generated from wastes with a mixed community at low rates and low titer, or from acetic acid and ethanol with an enriched culture at rates comparable to bioethanol production (Angenent et al. 2016). More functional platform chemicals such as succinic acid are more often produced by a pure culture from a well-defined, higher value substrate such as sugar, or sugar rich wastes. The greater costs of production limit a platform chemical's ability to competitively replace lower cost, petrochemically sourced chemicals. These chemicals tend to require high purity, which dramatically increases processing cost, for example to remove trace lactic or formic acid from a succinic acid extract. For a functional product, trace compounds may interfere with downstream reactions. This is not necessarily an issue for other products, such as bio-degradable polymers of solvents. A mixed ester solvent, for example, may not require a singular, defined ester to retain its properties, thus does not require high energy, high capital distillation to separate its individual components.

Production of bulk chemicals focuses primarily on cost minimization. To extend this to the central costs of membrane electrolysis, this corresponds to (i) minimization of power input per kilogram of product, (ii) long life-time of reactor materials (*i.e.* membrane, electrodes), (iii) minimal transport to the end user; and (iv) targeting the end users' product grade. To minimize cost risks, for example, the anaerobic fermentation of waste may require a solids separation to protect the membrane and electrodes. Alternatively, low cost AEMs could be developed, the cathode could be designed for the exclusion of solids, and units could be designed for high shear (*e.g.* cross sectional flow rate, electrode geometry, etc.), amongst many other permutations. It may be in the interest of the fermentation to disregard conversion of the solids, particularly if the substrate is of sufficiently low value and the solids have value outside the fermentation, as with the example of DDGS (distiller's grains sold as animal feed) in the bioethanol case. Outside of the anaerobic fermentation described at length in this thesis, an example could include extraction from a mixed VFA stream with over 40 g L^{-1}, such as in landfill leachate (Clarke et al. 2015). The membrane electrolysis product of such a stream may be useful as a preservative for animal feed, or as a

substrate in cellulose-acetate-propionate, depending on the market. A mixed VFA stream could be combined with low grade methanol or ethanol to generate a mixed ester solvent. This would need a source of methanol or ethanol, which may be enabled by a reciprocal relationship to an industrial park. Methanol can be generated electrochemically from CO and H_2, and ethanol through fermentations, which can be sourced as co-products from many industrial activities. When the process goal is bulk production from waste, one must take an opportunistic approach to substrates at hand to minimize costs.

Specialty chemical production tends to have a greater margin of profitability, which allows for investment in more expensive substrates and more extensive purification. Membrane electrolysis aligns well with the goals of specialty production, as many specialty acids (*e.g.* succinic acid, malic acid) are generated through fermentation of sugars that do not tend to pass through the AEM, the end product reaches a high molar concentration and the product tends to suppress the fermentation after a certain point, thus opening the possibility for membrane electrolysis to act as an *in situ* extraction for continuous operation. The impact of hydrogen on the fermentation would need to be assessed prior to use as an *in situ* extraction technology, as well as the interaction of the fermenters with the electrode and the applied current. Both MCFA and succinic acid producers can potentially benefit from increased extracellular hydrogen to help replenish intracellular NADH (see Figure 1.1, Chapter 1), but an increased hydrogen gas partial pressure can also suppress chain elongation (Spirito et al. 2014, Angenent et al. 2016). One downside of a pure culture process compared to a mixed culture is the inflexible response of the organism, be it from an applied current, invasive species or complex substrate.

The utility of the substrate is a critical question to production processes. In processing a waste stream, full conversion is rarely an option unless the stream can be unified at the outset (*e.g.* gasification). Targeting reactive fractions of the substrate and/or diverting the unconverted fraction towards downstream processes is more often the case. Membrane electrolysis can support recovery of relatively low concentration VFA, though it is likely that other processes are necessary to drive mixed culture conversions, as discussed in Chapter 2, as VFA tend to inhibit hydrolytic enzymes. On the other hand, the retention of the solids in membrane electrolysis extraction also can contribute to conversion. In CO_2 fixation or the conversion of a costly substrate such as sugar, membrane electrolysis can extract charged products, while assisting in the retention of substrate and the micro-organisms. A greater density of cells often promotes greater conversion of substrate.

6.1.3 Costing and sizing membrane electrolysis. To size a membrane electrolysis unit, the operational boundaries must be assessed. The upper limit of electro-migration through an AEM is dependent on the mass transfer at the surface, charge density in the membrane, diffusion and electro-migration parameters of the target compound and exclusion of the proton, and external factors including temperature and pressure. Manufactures specifications sheets indicate a maximum current, for example the Membrane International AMI 7001 suggests 500 A/m^2, though these only tend to be specified for high concentrations, and only for common salts such as chloride. This must be assessed for target compounds under the operational conditions of the process. Water permeation is also necessary to allow ionic mobility, and according to manufacturer specifications, this tends to be in the vicinity of 3 to 10 ml atm^{-1} m^{-2} hr^{-1} for AEMs. A pressure gradient from the catholyte to the anolyte is likely to improve flux by increasing water permeation. No information is available yet on maximum membrane flux nor the influence of pressure, and thus we will assess membrane electrolysis on the assumption of a maximum current density of 100 Am^{-2} and an assumed 100 % electrical efficiency (*i.e.* one applied electron results in transport of one charged carboxylate group). This corresponds to a flux of 437 g m^{-2} hr^{-1} for hexanoic acid. The maximum hexanoic production rate reported in literature is around 2.4 g L^{-2} hr^{-1}, from a synthetic broth (Grootscholten et al. 2013). 1 m^{-2} of AEM is required for approximately every 200 L of reactor volume at this maximum production rate, with more AEM required for the same amount at a lower efficiency. To produce 1000 kg of hexanoic acid at 2.4 g L^{-2} hr^{-1}, a reactor of around 20 000 L is required, and approximately 100 m^{-2} of AEM. Current state of the art (pictured in Figure 6.3A, the Electro Prod Cell from ElectroCell) fits approximately 16 m^2 of membrane in a 1 m^3 unit, requiring a ratio of almost 1:1 for fermenter to electrochemical cell footprint. To speculate on future designs, the development of a hollow-fibre unit (Figure 6.3B) with fine wire anodes and a tubular cathode has the potential to increase the area of membrane per cubic meter of electrode from 16 $m^2_{memb.}$ / m^3 to 100+ $m^2_{memb.}$ / m^3, and decreases the material usage of iridium oxide coated titanium anode. A voltage balancing control system to connect the anodes may enable the distribution of VFA flux over the broader membrane area.

Table 6.1 and 6.2 contain a summary of comparative product prices and material costs. The price of electricity relative to the value of the products listed in Tables 6.1 only has a significant effect on extraction of acetic acid, with over 10 % of the value of the

product spent on electricity. However, for hexanoic acid one could use six times more electrical energy (*i.e.* an efficiency of less than 20 %) and the cost of electricity still remains only 10 % of the price of the product. Hexanoic acid transport at 100 A m^{-2} from a clean broth at 170 mM (19.8 g L^{-1}) was shown (Chapter 3, Figure 3.5) to have an efficiency of around 40 %. Table 6.2 prices a 100 m^2 unit at 551 000 EUR based on the cost of the Electro Prod Cell (Figure 6.3 A). At this price, 503 EUR d^{-1} is required for a payback time of three years. Acetic acid does not meet this margin when all of the co-products are summed together and costs are extracted. As pumping, staff and other operational costs are also excluded from this analysis, this makes for a hard case for acetic acid, but the comparatively high value of caustic could make an argument for using additional current to generate excess caustic if it can be recycled or sold to a neighboring facility. Ethyl acetate could also add value through IL esterification, which will be discussed in the following section. For succinic acid and hexanoic acid, the payback rate is 37 % and 24 % of the product income, respectively, giving good margin for other expenses.

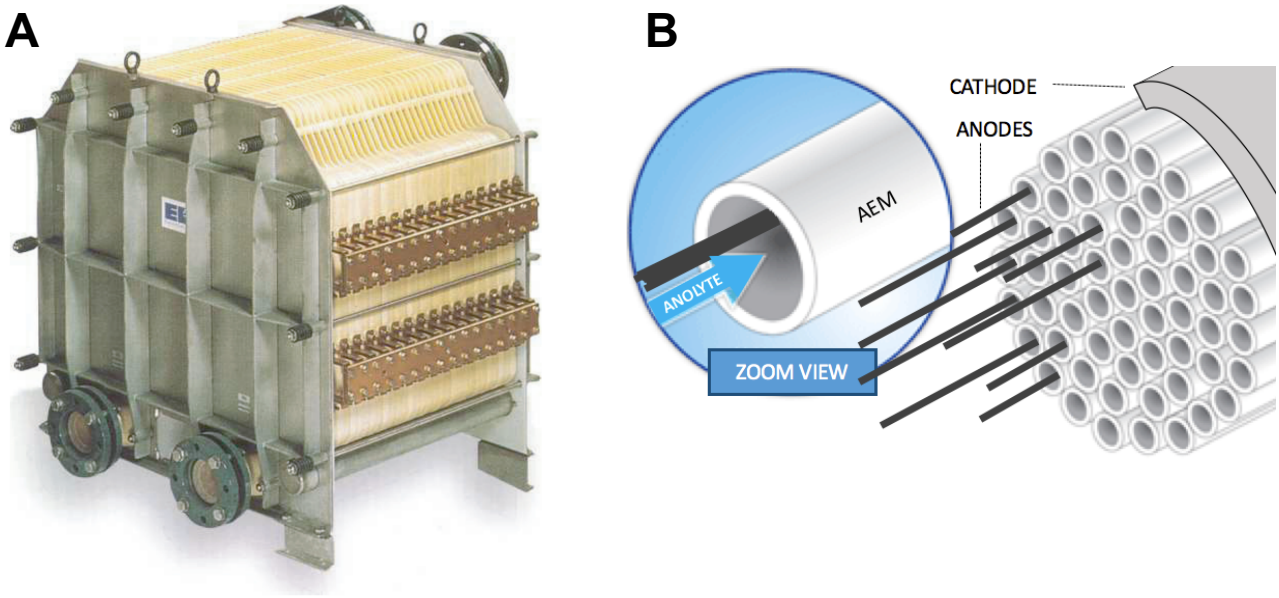

Figure 6.3 A. Current state of the is modified off-the-shelf electrochemical cells, e.g. Electro Prod Cell, ElectroCell AB, Denmark (From http://www.electrocell.com/fileadmin/pdf/EPC-brochure.pdf)

B. Hollow fibre membrane electrolysis cell concept to minimize anode material and maximize membrane area. Fermentation broth passes in between the cathode exterior and the AEM hollow fibers. (Adapted from https://www.freshwatersystems.com/images/Ultra-Filtration-Flow.gif)

Table 6.1 A comparative costing summary of major products, co-products and costs for membrane electrolysis based on a 100 m^2 unit and 100 A m^{-2} applied current.

	Rate	Value/Price	Income/Expense	Efficiency
Products				
Acetic acid	528 kg d^{-1}	0.6 EUR kg^{-1}	+317 EUR d^{-1}	Mid to high
Hexanoic acid	1049 kg d^{-1}	2.0 EUR kg^{-1}	+2098 EUR d^{-1}	Low to mid
Succinic acid	519 kg d^{-1}	2.6 EUR kg^{-1}	+1349 EUR d^{-1}	High
Co-products				
Caustic soda*	358 kg d^{-1}	0.3 EUR kg^{-1}	+107 EUR d^{-1}	High
Sulfuric acid*	877 kg d^{-1}	0.1 EUR kg^{-1}	+87 EUR d^{-1}	Mid to high
Hydrogen	4.5 kg d^{-1}	537 MJ d^{-1}	+7.5 EUR d^{-1}***	High
Costs				
Electricity	720 kWh	0.05 EUR kWh^{-1}	-36 EUR d^{-1}	High
Anode**	0.0014 m^2 d^{-1}	500 EUR m^{-2}	-68 EUR d^{-1}	
AEM**	0.024 m^2 d^{-1}	10 EUR m^{-2}	-24 EUR d^{-1}	

Assumptions:
At 100 A m^{-2}, 100 m^2 installed membrane area, assuming 100 % efficiency. Product prices are approximate market values based on discussions with industry partners. Efficiency refers to confidence that input energy will contribute to the output.
* Electrolysis generates aqueous OH^- and H^+, caustic soda and sulfuric acid are used as a pricing proxy
** Anode costs are calculated on assumed lifetime of 2 y, AEM costs are calculated on an assumed lifetime of 1000 h
*** No consumption in the reactor of H_2 gas, no losses, complete conversion to electricity at 0.05 EUR kWh^{-1}

Table 6.2 A simplified capital cost summary of the major features of membrane electrolysis

	Value/Price	Cost
Capital		
Anode	500 EUR m^{-2}	50 000 EUR
AEM	10 EUR m^{-2}	1 000 EUR
Other (cathode, rig, etc.)	50 000 EUR m^{-2} ****	500 000 EUR
Total		**551 000 EUR**
		503 EUR d^{-1} for 3-year payback

Assumptions:
At 100 A m^{-2}, 100 m^2 installed membrane area
**** Approximation based on the Electro Prod Cell (ElectroCel AS, Denmark)

Anion exchange membrane. Quarternary ammonium groups on a polymer backbone at varying degrees of charge density, membrane thickness and hydrophobicity. Most research centers around transport of salts in relatively clean streams, fouling minimization and selectivity in transport, with a focus on reverse osmosis and wastewater treatment (Mikhaylin and Bazinet 2016).

Cost: Low, in the vicinity of 100 EUR m^{-2}. Fujifilm Membranes (The Netherlands) anticipates the price to reach < 10 EUR m^{-2} with a target of 2 EUR m^{-2}.

Risks: The fouling issue may require consistent replacement, or moving to ceramic membranes that can be cleaned, which may incur the risk of process shut-downs or modular cycling. Electrical resistance must be tracked and managed over time, as one of the major contributions to costs, and may result in transport limitations. Tailored AEMs are a nascent field, and there is potential for technology development in surface modification to improve selectivity towards one species (Kim et al. 2014).

Anode. Dimensionally stable anodes (titanium with iridium oxide coating) were used in this study to target water oxidation and prevent chloride oxidation. Research centers on alternative, lower cost materials, for example nickel cobalt, lead, tin and others (Fabbri et al. 2014).

Cost: Planar IrOx-MMA electrodes at 0.5 to 1 m^2 size are approximately 500 EUR m^{-1}, and at 1 $m^2_{memb.}$: 1 m^2_{anode}, 100+ m^2 is required for 1000 kg d^{-1} hexanoic acid. No information was found on potential costing for wire-style anodes, nor whether this geometry may be practical.

Risks: The anode is the most expensive capital expenditure and the greatest cost in the membrane electrolysis units, and material minimization and optimization is critical here to de-risk investment in the technology. IrOx-MMA electrodes can tolerate the acidic, hydrophobic environment and relatively mild current densities of membrane electrolysis (Owe 2011), with an expected lifetime of two years from constant use, or five to seven years under normal use. Stability and performance of the electrodes under novel geometries is critical to minimizing the risks associated with the anode, which also affects resistance and power input, and mass and energy transfer (*e.g.* gas generation at the electrode surface).

Ionic liquid. ILs are nascent in technological development and industrial deployment, but are beginning to be applied as solvents and catalysts (Plechkova and Seddon 2008, Ratti 2014).

Cost: Current estimates for industrial quantities of ILs used in this study are approximately 50 to 200 EUR kg^{-1}, with projections aiming for < 10 EUR kg^{-1}. Using the maximum extraction and esterification rates of the Mixed Anion IL from Chapter 5, 0.7 m^3 (*i.e.* 700+ kg) of IL is required to generate 1000 kg d^{-1} of ethyl acetate from 681 kg d^{-1} acetic acid and 522 kg d^{-1} ethanol is required.

Risks: Though a large investment is required for both the IL and the liquid-liquid contactor, the low chemical and energy operational requirements combined with physical separation from up-stream processes decrease the risk of IL esterification recovery. The largest risks are involved in dewatering and IL dissolution, however more information will come with continued research, which is likely to decreases the associated risks over time.

6.1.4 Membrane electrolysis co-products: decreasing risk & adding value

Membrane electrolysis, as with other electrochemical and membrane process units, can in principle operate effectively in a modular arrangement. This is advantageous in marketing to risk-averse industrial production processes, as a small demonstration unit can be installed and the product can be tested within the context of the process. The greatest risks associated to a full-scale investment, such as fouling, power input, operator training, can be assessed through the demonstration unit and scaled-up as appropriate. Following is a list of the products and services associated with the installation of a modular membrane electrolysis unit in decreasing order of process risk, with a brief description of the competitive value that it brings the client:

Low-grade caustic. The stream from which the anionic product is extracted will rise in pH from the electrolysis of water. Many fermentation processes are acidogenic, and many recovery strategies require extensive acidification of the product before it is recovered, thus requiring a constant supply of caustic soda (López-Garzón and Straathof 2014). Sodium hydroxide in Europe tends to be priced around 250 to 300 EUR/t (ICIS 2014), and comes with many health, safety and transport issues. Similar issues face potassium hydroxide, and to a lesser extent calcium carbonate. Depending on its use within the process, the high-pH

stream generated within the catholyte electrolytic reduction could be used to manage acidogenesis in the fermentation reactor. If the stream is also sourced from the reactor, then no additional salts (sodium, potassium, calcium) are introduced into the process, which adds savings in wastewater treatment, as there is no need to dilute or recover the added salts. Similarly, if a production pipeline requires extensive acidification to recover the product, the low-grade caustic stream could be used to neutralize this stream.

Integrating low-grade caustic into either up- or down-stream processes is a low-risk opportunity and presents an immediate cost saving on caustic purchasing. The value of this stream is compounded by the decreased risk to workers from caustic exposure, avoiding the need for dealing with salts added to wastewater streams, and the sustainability argument surrounding chemical transport. Depending on the source, however, the low-grade stream may contain solids or other contaminants.

Low-grade acids. The acidic fraction that accumulates in the extract alongside the product was observed to contain a high concentration of mixed VFA and chloride, sulfate and phosphate (Chapter 4 and 5). Some mixed VFA may be appropriate for recycle (*e.g.* solutions of acetic and lactic acid recycled into a MCFA fermentation) or reactive extraction. The remaining acids could be targeted for recovery by precipitation (*e.g.* ferrous iron or ammonium precipitation of phosphates), adsorption, dewatering, etc, or used in pH control or as an acid replacement within the process. Phosphoric acid is also effective at attacking lignocellulosic polymers (Vasconcelos et al. 2013).

Membrane electrolysis extract solution often contained interesting compounds including phenolic compounds and phosphoric acid concentrate. This has potential for value when more is known about the extent of their transport and accumulation, and the potentially negative affect they might have on extraction of the target product. Recycling these products within the process lowers the risk and adds value.

Hydrogen. Many wastewater treatment facilities, particularly those dealing with large volumes of organic waste, use anaerobic digestion technology to generate biogas, which can then be recovered as heat and energy. Hydrogen gas generated during membrane electrolysis can be of a high quality, particularly if recovered from periods of high current density, and could be integrated into existing heat and power infrastructure (*e.g.* boiler), or the hydrogen gas can be captured and utilized by neighboring facilities. Bio-refineries already tend to generate large quantities of high grade carbon dioxide and hydrogen during fermentation processes.

Hydrogen can be a complicated molecule to deal with, and not all biorefineries have the existing infrastructure to valorize it, which places hydrogen as a higher risk, lower value co-product. In some fermentations, hydrogen can be valorized within the fermentation itself to increase intracellular NADH, as mentioned.

Electro-coagulation. There was an indication that some electro-coagulation occurred during electro-fermentation, in which the suspended solids in the fermenter were 42 ± 1 % of the control (Chapter 4), likely due to an electro-coagulation effect. Membrane electrolysis and electro-coagulation are compatible technologies, and in principle could share some reactor elements, such as the cathode, electrical infrastructure and the reactor vessel.

Integrated electro-coagulation and membrane electrolysis is currently untested, but electro-coagulation is a well-established technology, and offered as a service by many water technology companies. Pending further analysis, this is a higher risk co-product, but the concept is rather straight forward (Figure 6.4). Current could simply be switched between the anode of the membrane electrolysis cell and the anode of the electro-coagulation unit, as necessary. The added value is very stream dependent, and enables colloidal solids to be separated from the bulk, and increases biodegradability (Naje and Abbas 2013). Removing the charged colloidal solids is likely to improve membrane flux as the colloidal particles can foul the AEM (Mikhaylin and Bazinet 2016).

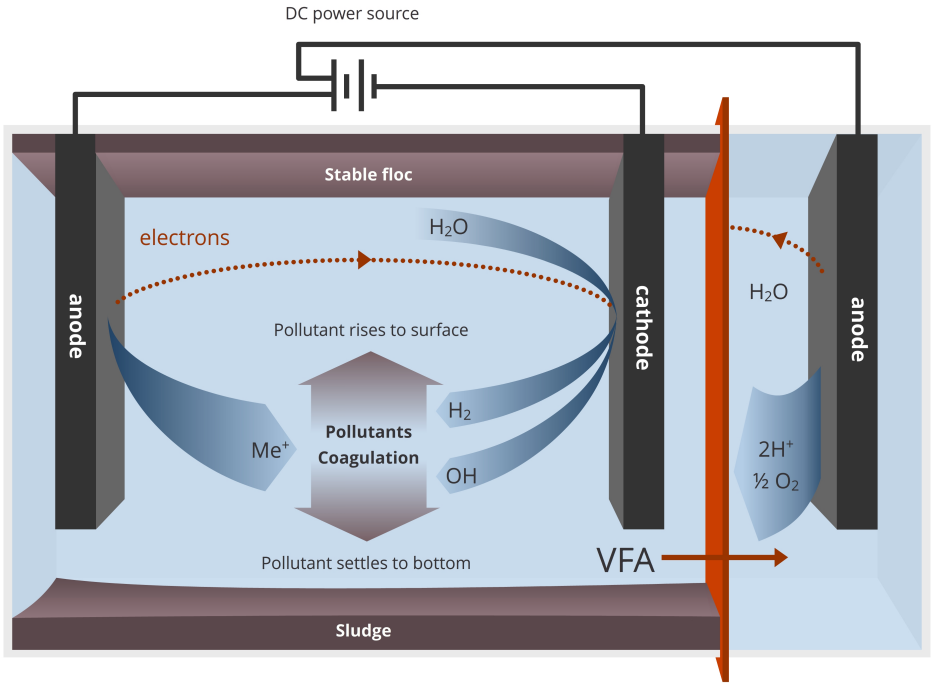

Figure 6.4 Concept art of combined Electrocoagulation / Membrane Electrolysis. Image by Tim Lacoere.

High pH solids. If membrane electrolysis sits on a complex waste stream or down-stream from a fermentation step, any solids that have not been removed will be subject to the increase of pH inherent to the catholyte. High pH treatment has been demonstrated to improve the degradability of lignocellulose and is often used as a pre-treatment prior to bio-ethanol fermentation (Taherzaden and Karimi 2008). Solids passing through the catholyte, depending on pH and residence time, may have an improved degradation profile in a recycled stream or in anaerobic digestion. Unconverted solids from an MCFA fermentation from waste, for example, may be able to be recycled into the reactor after some exposure to an alkaline treatment. The pH can be adjusted based on residence time in the membrane electrolysis unit, and potentially be coupled to an electro-coagulation step. An additional opportunity here lies in the potential to extract VFA and phenolic acids, both of which suppress hydrolysis of cellulose (Siegert and Banks 2005, Tejirian and Xu 2011).

The pH adjustments of the solids are low risk but also low value, unless it can be demonstrated that the pH shift significantly improves the conversion of substrate which is then recycled. The pH is likely to be limited to around pH 12 to 13, as at this point the molar concentration of hydroxide anions becomes dominant and will flux across the AEM. However, as this stream will have a low concentration of VFA, this stream is likely to be highly degradable.

Secondary product recovery. The central feature of membrane electrolysis is product recovery, and the possibility for membrane electrolysis to operate at relatively low concentrations allows a modular unit to be used as a secondary recovery step on wastewaters, on problem or fouled streams, or simply as an economic balance against, for example, extensive dewatering or distillation. Platform chemicals already in industrial production such as succinic acid and malic acid often use extensive acidification and dewatering to increase the concentration of highly involatile products, and some portion of the product is invariably lost to wastewaters. Some streams, such as wash-out from the reactors, can be high in concentration. The concentration of wastewaters are proprietary information, so one can only speculate at the normal concentration lost, but if it is in the vicinity of 0.1 to 0.2 M (around 10 to 20 gL^{-1} for MCFA and succinic acid) where membrane electrolysis has been demonstrated to be highly efficient (Chapter 3), then membrane electrolysis could effectively recover the product, alongside an acid and base co-product. If

the extraction is shown to be very effective, the primary recovery step could be optimized against the membrane electrolysis step, thus potentially allowing a heat or chemical fueled primary recovery (acidification, dewatering, distillation) to be scaled back with the sustainably sourced electricity taking up the balance.

As a waste-treatment step, this use of membrane electrolysis is low risk as it has little impact on downstream processes, and requires minimal installation and adaptation of downstream units. This application will be stream dependent, with lower concentration streams less attractive. Valuable information on electrode and membrane lifetime could be established at this level with a view of an in situ production installation. Membrane electrolysis will change the pH of the streams, and products such as low-grade caustic and low-grade acid could also be utilized.

6.2 From the biorefinery to the market

A new technology is only successful if used by the right people. This section contains a brief discussion on the implications of membrane electrolysis and IL esterification on engineers and operators, followed a summary of the current state of the markets in which membrane electrolysis could play a role.

6.2.1 Operations and health & safety. Membrane electrolysis is a multi-disciplinary platform that connects biotechnology, electrochemistry and chemical engineering. Operators will need a core skill set in industrial fermentation, electrochemistry and membrane processes. Electrochemistry represents the greatest risk in terms of safety and process sensitivity. For a single unit of 100 m^2 and applied currents of up to 100 A m^{-2}, this amounts to 10 000 A, approximately one third of an average bolt of lightning, thus careful health and safety consideration should accompany the scale-up of a membrane electrolysis system. With respect to process sensitivity, if the unit size is minimized in the style of hollow fibre membranes, down time of a single unit of 100 m^2 or more of AEM could result in a rapid concentration increase in the products in the reactor, and a toxic shock to the fermenting community. As mentioned earlier in the chapter, this risk can be managed by controlling membrane electrolysis relative to a carefully managed feeding scheme, or by extracting from the effluent of a low HRT / high throughput system, and recycling the unconverted fraction.

Processing downstream of membrane electrolysis relies more conventional unit operations. Recovery strategies that utilize phase separation and precipitation have analogues in petro-chemistry and chemical production, and present little challenge in design and operation. As with membrane electrolysis, the IL question is more complex, as reactive extraction technologies operated at the industrial scale are rare. Skills in industrial chemistry will be critical to an IL based process, alongside the electrochemistry and an industrial fermentation skill set. Any IL that is brought forward must be assessed for the impacts on human health and safety, as it is inevitable that the liquid will come in contact with an operator. ILs are not anticipated to present a great health hazard, however the IL will need to be tracked over time for degradation, quality and loss, particularly in wastewaters. ILs are likely to represent a large capital investment, and potentially have critical importance in product valorization and process economics.

The multi-disciplinary nature of membrane electrolysis and downstream valorization strategies, such ionic liquid esterification, results in a broad range of engineering challenges, and requires a diverse skill set in engineering and operation. This presents a argument for membrane electrolysis processes integrated into a greater industrial park where skills and expertise can be shared amongst the industrial ecology.

6.2.2 A booming bio-based chemicals market. Sustainable carboxylic acids are beginning to enter the market through syngas fermentation and biomass conversion, with others focusing on carboxylic acids as an intermediate to other chemicals. LanzaTech (United States) is establishing a syngas fermentation on steel-mill syngas using a proprietary *Clostridium* species to convert CO and hydrogen to ethanol, via acetic acid. Avantium (The Netherlands) in partnership with BASF aim to generate the bio-plastic precursor furandicarboxylic acid. Genomatica (United States) generates adipic acid as part of a platform of sustainable nylon production. Zeachem (United States) is developing short to mid-chain carboxylic acid products from sugars, while ChainCraft (The Netherlands) is developing technology towards MCFA from agricultural and food wastes. Infinity Fuels (Germany), which will be discussed in greater detail below, aims to generate fuels from carboxylic acids through an electrochemical process. In the platform chemical sector, Succinity GmbH (Germany), Reverdia (The Netherlands) and Bio-Amber Inc. (United States) generates succinic acid from sugars.

Despite a clear market-side pull in bio-based chemical intermediates, the technology platform and corporate support must be robust. Information is scarce on the common traps that cause bio-based chemical companies to fail, but understanding this is key to minimizing risk and bringing a technology forward. One example includes the bankruptcy of Terrabon (United States), a company focused on generating MCFA through the Mix Alco process, followed by a conversion to fuels. Terrabon failed to secure financial backing to move to a full-scale conversion process despite reportedly meeting demonstration scale technical milestones (BiofuelsDigest 2012). This could be interpreted as a failure of process to link effectively with the end market and consumers, though without more information this is speculation. Greater transparency on such business failures would greatly improve our ability to de-risk new products and technologies.

This section will cover a market outlook on MCFA, carboxylic acid platform chemicals and fuel derivatives, and mixed methyl- and ethyl-esters, including an assessment on market sustainability and risk.

MCFA. The MCFA market currently focusses on food and medical applications, produced from petrochemical and vegetable oils. NuScience Group (Belgium) for example markets an Aromabiotic MCFA animal feed additive, consisting of hexanoic, octanoic, decanoic and dodecanoic acid, to be used as anti-microbial growth promoters. Decanoic acid makes up the largest portion of the MCFA market, representing about 60 000 t y^{-1} (Zion Research 2016). Different reports place the projected compound annual growth of the MCFA market at 6.5 to 12.7 % (Zion Research 2016, Allied Market Research 2016, Brisk Insights 2016). This strong projected growth and stable market makes for a very attractive field. Current production methods of MCFA are not viewed as environmentally friendly, particularly those recovered from vegetable and palm oil plantations. A shift to fermentation processes is likely to be seen favorably, particularly if the carbon can be sourced from waste organics and syngas. Octanoic or decanoic acid production may be suitable to produce with a sugar substrate, however the robustness of *Clostridium spp*. to perform with a variety of substrates makes low grade mixed VFA and ethanol or lactic acid attractive.

Carboxylic acid platform chemicals. VFA have value in their independent markets as bulk chemicals, but can also be converted to other chemicals, such as ketones, aldehydes, alcohols and alkanes (Agler et al. 2011). Acetic acid has a global market of 3 700 000 t y^{-1}, and is mostly used as a precursor to vinyl acetate monomers and terephthalic acid, a precursor to polyester polyethylene terephthalate (PET) polymers (Grand View Research 2015). Unless additional functional groups can be added to acetic acid in the recovery phase, the aqueous acetic acid concentrate is unlikely to be sustainably funneled towards this market, considering the costs associated with purification. Other short chain VFA such as propionic and butyric acid also have added value and more niche markets, with the same technical drawbacks as acetic acid in purification.

Higher value, more functional platform chemicals are presently being developed, generally as products of sugar fermentation. Bio-Succinic acid is the most mature of the platform chemicals, currently produced industrially by the market leaders Succinicity GmbH (Germany), Reverdia (The Netherlands) and BioAmber Inc (United States). The market for succinic acid is currently in the vicinity of 50 000 t y^{-1} and optimistically expected to grow to 600 000 t y^{-1} by 2020. Production of succinic acid, similar to other fermentation based platform chemicals, is constrained by large recovery costs and has resulted in a market price of around 3 000 EUR t^{-1}, compared to around 2 400 EUR t^{-1} for petrochemically produced succinic acid (Pateraki et al. 2016).

The expanse of the acetic acid market and its heavy reliance on the petrochemical substrate for production makes acetic acid a very attractive candidate in terms of environmental impact, however the low price and technological hurdles add significant risk. The growth and broader function of succinic acid makes for a low risk product, and improved recovery technologies and sustained consumer demand for sustainable products minimize the risks associated with bio-succinic production, as well as targeting low value sugars and wastes as a substrate. Sugar based fermentations has been viewed very negatively in the ethanol case, and can sway public and legislative opinion against the technology. An attractive feature of some carboxylic acid fermentations is the potential for CO_2 fixation in the substrate, such as in acetic acid (Gildemyn et al. 2016), and succinic acid (Pateraki et al. 2016). Utility of waste carbon in these fermentations can be a technical challenge, but improves the sustainability and public image of the production process.

MCFA as a fuel precursor. MCFA, and some shorter chain carboxylic acids, can be converted through Kolbe electrolysis to fuels (Kolbe 1849). Kolbe electrolysis involves the removal of two carboxylate functional groups as carbon dioxide, and the dimerization of the two chains to form a single chain. For example, pentanoic (valeric) acid can be converted to octane, and hexanoic acid can be converted to decane (Nilges et al. 2011, dos Santos et al. 2015). Jet fuels mostly consist of heptane and isooctane, both of which are possible products through Kolbe electrolysis.

Transportation fuels account for approximately one third of all greenhouse gas emissions, and remains a critical point in the carbon economy. In a process currently under development, colleagues at the Center of Microbial Ecology and Technology are developing a fermentation pipeline that uses waste grass clippings as feed in a conversion pipeline. The grass is converted by a mixed community through lactic acid to caproic acid, extracted by membrane electrolysis and converted to decane by Kolbe electrolysis. In a similar process, Infinite Fuels GmbH (Germany) is aiming to take the electrochemical conversion carboxylic acid to jet fuels to the industrial scale, and if this can be executed sustainably and effectively this represents the biggest market for carboxylic acids as an intermediate, and the greatest potential for a disruptive industrial bio-chemical technology. The principle risks here are associated with the availability and efficiency of conversion of the source carbon.

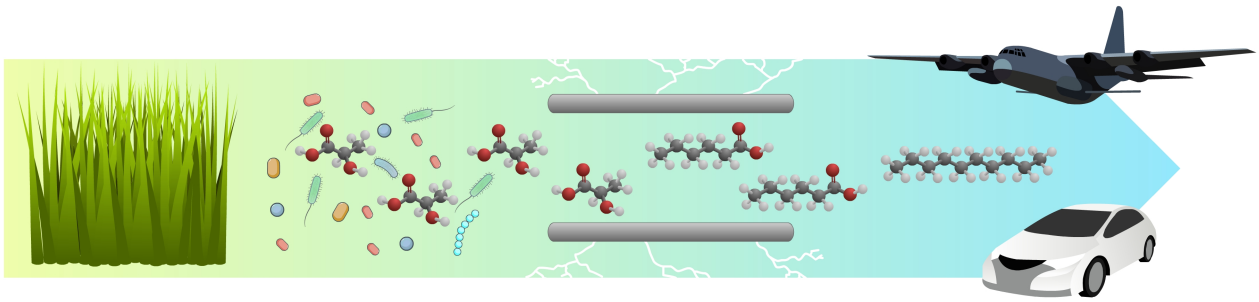

Figure 6.5 Processing pipeline for the grass to fuel pipeline. Grasses are degraded and fermented by lactic acid and caproic acid producing communities, which is then extracted and converted to decane, an energy dense alkane, through Kolbe electrolysis. Image by Tim Lacoere.

From Way Cern Khor, **Stephen J. Andersen**, Han Vervaeren, Korneel Rabaey, **2016** (*Manuscript in preparation*)

6.5 Next Generation Chemical Industry

The chemical industry is in the midst of a shift to sustainable products and processes. It is estimated that replacing the global chemical demand would require only 5 % of the worlds agricultural biomass production, and growth in the fermentation and renewable chemicals market is observed across the globe (Deloitte 2014). Growth in the renewable chemical sector is currently driven by regulatory restrictions on environmentally harmful processes (Brisk Insights 2016), as entrenched petrochemical processes still economically outcompete bio-refinery processes. Technological lock-in pushes against industrial bio-technology, pitting bio-based products against petrochemical alternatives produced from an established technology, knowledge and asset base (Deloitte 2014). Technically sound processes that merge sustainability and profit are few and far between, particularly in fermentation. Fermentation occurs through biological conversion that requires conditions amenable to life, while petrochemical conversions are only bound by chemical engineering. This gulf between aqueous biochemistry and industrial chemistry can attributed to the power-chemical relationship, and the single-substrate pure-product bias of petrochemical processes. There exist many technical challenges in driving towards the next generation of the chemical industry, and here we will discuss some of the global changes that can drive the shift towards renewable chemicals, and how membrane electrolysis and IL processes can play a role.

Oil and gas are not only carbon-rich substrates, but are also energy dense. A petrochemical refinery has access to both substrate and energy from the same source while a bio-refinery relies on gas and fuels as a source of heat and power in contrast to the bio-base substrates. Aqueous conversions and side products compound this, requiring energy intensive dewatering strategies and trace removal of products with similar physico-chemical properties. For example, bioethanol's sustainability argument is wounded in the energy intensive distillation from water, while in succinic acid fermentation the evaportation or distillation of formic, acetic, and lactic acids contributes extensive costs in (López-Garzón et al. 2016). Sustainably separating the power-chemical relationship is one of the greatest hurdles in a transition to carbon sustainability, and critical in minimizing energy investment and emissions. In this thesis electrochemistry has been presented as an alternative, however electrochemistry is only a sustainable alternative if the power is sourced from renewable energy. Solar and wind power capacity is growing in Europe, projected to grow between 4 and 10 GW y^{-1} for solar, and between 7 and 16 GW y^{-1} for wind

(eHighway2050, 2015). This transition to an expanded sustainable electricity grid can enable the application of membrane electrolysis through sites in Europe, as long as expanded industrial capacity is taken into consideration. Electricity cannot replace all energy requirements in a process, but an emphasis on process integration for utility of heat, power and products can minimize the need for oil and gas fuels, particularly between neighboring facilities.

While heat and energy can often be successfully integrated across the borders of facilities, the flow of co-products from a bio-refinery is often limited to gases like CO, CO_2 and H_2. The myriad of other complex biological side products; such as cellulose, phenolic acids, proteins, etc.; require a targeted recovery strategy in a complex medium, with relatively low concentration compounds. There is ongoing research in the valorization of side streams and wastes from bio-refineries, however there is little to no research from industrial processes to explore production from lower grade feed stocks (Raguskas et al. 2014; Fava et al. 2015). In order to participate in the existing infrastructure, most bio-refinery successes center around drop-in chemicals that fit the chemical process without too much adaption. Bio-ethanol's success can partly be attributed to the fact that after the distillation column, biological complexity no longer impacts the product. In order to achieve a pure bio-chemical product, a great deal of research focusses on conversion strategies to unify a substrate, such as gasification of waste, followed by, for example, a genetically modified species to unify a product output (Zhang et al. 2009). This places all the technological burden on the front end, whereas industrial chemistry could serve the transition to the bio-economy by exploring an adaption to aqueous, mixed or so co-called low grade inputs. ILs hold an intriguing place in bridging biological and chemical processes. Mixed methyl- or ethyl- esters of VFAs can be generated from a mixed VFA extract esterification, and the ability of ILs to be tailored as a solvent opens up a range of opportunities as a combined solvent/catalytic site for other chemicals, particularly if a chemical process can utilize a low-grade input. This could extend through the esterification of cellulose, the addition of cyclic groups, polymerization and more (Plechkova and Seddon 2007).

The market is the core driver of industrial up-take, and this relates both to the biochemical products and the unit operation products that enable them. Ethyl acetate produced from CO_2 and other wastes is attractive as a product, but a new product purported to display similar properties, such as a solvent of mixed ethyl acetate and ethyl propionate,

will often be met with skepticism until it has been thoroughly demonstrated. This is as true for processes as it is for products. Demonstration plants are often run for at least four to five years before the technology can be translated into a mainstream process. As discussed earlier, explicit details on the failures of a company, process or product are rarely reported, hindering our ability to de-risk new technologies, and accurately assess when a technology is approaching the valley of death between demonstration scale and industrial scale.

6.6 More Research Required

Bio-production and fermentation is a dynamic research area, both in academia and industry. One of the greatest challenges of this sector lies in generating an effective substrate for biological conversion, be it in CO/CO_2 capture, hydrolysis of woody biomass, or unifying organic wastes. In the context of Chapters 2 and 4, more research into the mechanisms that promote and suppress hydrolysis of solid substrates may allow the MCFA fermentation to be adapted to optimize substrate conversion, MCFA concentration and production rate. There is a great deal of energy that can be saved if we can improve a fermenting community's access to the carbon in wastes, be it from lignocellulose, polymers or gasses.

As mentioned at the start of the chapter, MCFA fermentation and membrane electrolysis is currently being brought to demonstration scale from biorefinery stillage and beer. This will bring more information on power input per kg product, and AEM lifetime and flux limitations. Unit design and CFD modelling that incorporates ion and mass transfer is critical to assess the boundaries of membrane electrolysis. Membrane (e.g. anti-fouling, decreased resistance, product selectivity) and electrode (e.g. alternate materials for cost limitation, prevention of oxidation and chlorination of VFA) development will also allow a smoother transition to industry. There is often an industry side focus on decreasing the costs of AEM and dimensionally stable anodes, but in the context of membrane electrolysis research into extending the effective lifetime is much more attractive.

Extraction, recovery and valorization of the products, be it MCFA, mixed esters or succinic acid, and co-products such as low-grade base and acids, can be powered by membrane electrolysis, and this now must be demonstrated and critically analyzed at a greater scale with renewable energy so that a greener path for industrial biochemistry can be paved with sustainable bio-electrochemistry.

Abstract

Abstract

During fermentations of complex streams, microbial communities are engaged in a carbon and energy economy that includes competition for substrate, the consumption of intermediates and the suppression of species intolerant to MCFA. In chapter 2 this interaction was explored, which revealed the impact MCFA had on carbon efficiency, the relative abundance of different species and the occurrence of other products. Hexanoic acid was sustained in one fermentation at 5.2 ± 1.5 g L^{-1} for 32 days, but in a twin reactor fed from the same source, the production of octanoic acid resulted in a 32 ± 2 % decrease in carbon conversion to VFA after 6 days. This was associated with the collapse of species capable of fermenting glycerol, such as *Lactobacillus spp*. An uncultured species implicated in the production of MCFA was *Clostridium sp*. BS-1_{sec}, which dominated the reactors with a relative abundance of more than 50 % when octanoic acid was present. Even a closely related species similar to *Clostridium sp*. CPB-6 – also implicated in MCFA production – appeared to be suppressed by the presence of octanoic acid. For the first time decanoic acid was also implicated as a microbial product from reverse β oxidation, a compound that is also known to be highly toxic at low concentrations.

In situ extraction is valuable in MCFA fermentation to suppress toxicity and recover the product, but it is also a challenging task considering the relatively low concentrations typical to many fermentations, particularly those from mixed communities and waste streams. In chapter 3 membrane electrolysis was explored using acetic acid as a model acid in concentrations up to 170 mM (10 g L^{-1}). High molar concentrations of acetic acid were shown to approach almost 100 % efficiency, though comparative extractions with 170 mM hexanoic acid did not high efficiency, at around 50 % at 50 A m^{-2} and 40 % at 100 for A m^{-2}, demonstrating the need for high-current extraction optimization. A mathematical model for transport was proposed for acetic acid transport in membrane electrolysis and characterized with EIS. The analysis demonstrated the (pseudo-) capacitance and (pseudo-) resistance of both acetic acid transport and proton exclusion (and transport), and it was shown that the electrical mobility of a species in the membrane can be deduced from EIS parameters. For acetic acid through an AMI-7001 Membrane International AEM, this value was found to be (1.40 ± 0.30) × 10^{-8} m^3 V^{-1} s^{-1}. Further research is required to validate this across existing and new membranes with other carboxylic acid fermentation products, and to develop this method in to a tool for screening AEM properties.

Beyond the transport of acids from the broth, membrane electrolysis also generates H_2 and OH^- in the fermentation broth. Chapter 4 explored the influence of these products on a VFA fermentation of biorefinery stillage, and demonstrated that membrane electrolysis can completely replace chemical pH control with electrolysis products and create a shift in the product outcome, likely through the metabolism of H_2 by the fermenting community. Contrary to Chapter 2, the predominant elongating species in this study was a *Megasphaera sp.*, also likely to be elongating VFA through lactic acid. *Lactobacillus spp.* were more relatively abundant in the applied current fermentation than the control without current. Further research is required to confirm that *Megasphaera sp.* and *Lactobacillus spp.* can metabolize hydrogen, though it was implied in this work by the shift in the product outcome to more reduced, longer chain VFA with applied current, however the concentrations of MCFA were consistently low and the extract solution consisted mostly of shorter chain VFA.

SCFA such as acetic acid are valuable bulk products and can be accumulated in a membrane electrolysis extract solution. Hexanoic acid phase separates under acidic conditions and succinic acid precipitates, but acetic acid remains miscible in water. Moreover, when hexanoic acid and succinic acid are recovered from these extracts, a concentrated mixed VFA acid is likely to remain. Accumulation and esterification of acetic acid was demonstrated in Chapter 5, alongside a screening of ILs to establish which anions may be best suited as a solvent, catalytic site for esterification, and involatile vector for recover by vaporization of the ester. Trihexyl(tetradecyl)phosphonium cation ILs with different anions were screened, demonstrating a range of capabilities. For the first time we demonstrated that a mixed anion IL $P_{666,\ 14}$ $(Tf_2N)_{0.5}$ $Cl_{0.5}$ was effective as an acetic acid solvent, extracting at up to 40 $g_{Acetic\ Acid}\ L^{-1}\ h^{-1}$, and esterification, converting acetic acid to ethyl acetate at up to 38.2 $g_{Acetic\ Acid}\ L^{-1}\ h^{-1}$.

One might balk at increasing the electricity load of the chemical sector to drive the production of bulk chemicals, particularly when it comes to watery, complex biological conversions, however electricity is an excellent and increasingly sustainable energy vector, projected to have extensive growth in wind and solar output over the coming decades. Membrane electrolysis sourced from renewable energy has potential to bring energy sustainability to the chemical industry through the electrochemical extraction, recovery and valorization of carboxylic acids from biorefineries.

Bibliography

Bibliography

Abels C, Carstensen F, Wessling M, Membrane processes in biorefinery applications; *J. Mem Sci* **2013;** 444: 285–317, DOI:10.1016/j.memsci.2013.05.030

Arce A, Earle MJ, Rodriguez H, Seddon KR, Separation of aromatic hydrocarbons from alkanes using the ionic liquid 1-ethyl-3-methylimidazoliumbis{(trifluoromethyl) sulfonyl}amide, *Green Chem*., **2007**; 9, 70-74; DOI:10.1039/B610207G

Agler MT, Spirito CM, Usack JG, Werner JJ, Angenent LT, Chain elongation with reactor microbiomes: upgrading dilute ethanol to medium-chain carboxylic acids. *Energ Environ Sci* **2012**; 5(8):8189-8192; DOI:10.1039/C2EE22101B

Agler MT, Wrenn BA, Zinder SH, Angenent LT, Waste to bioproduct conversion with undefined mixed cultures: the carboxylate platform. *Trends Biotechnol* **2011**; 29(2):70-8; DOI:10.1016/j.tibtech.2010.11.006

Andersen SJ, Berton JKET, Naert P, Gildemyn S, Rabaey K, Stevens CV, Extraction and esterification of low-titer short chain volatile fatty acids from anaerobic fermentation with ionic liquids; *ChemSusCem* **2016**, *Accepted*

Andersen SJ, Candry P, Basadre T, Khor WC, Roume H, Hernandez Sanabria E, Coma M, Rabaey K, Electrolytic extraction drives volatile fatty acid chain elongation through lactic acid and replaces chemical pH control in thin stillage fermentation; *Biotechnol Biofuels* **2015**, 8:221 DOI:10.1186/s13068-015-0396-7

Andersen SJ, Hennebel T, Gildemyn S, Coma M, Desloover J, Berton J, Tsukamoto J, Stevens C, Rabaey K, Electrolytic Membrane Extraction Enables Production of Fine Chemicals from Biorefinery Sidestreams. *Environ Sci Technol* **2014**; 48(12):7135-7142; DOI:10.1021/es500483w

Angenent LT, Richter H, Buckel W, Spirito CM, Steinbusch KJJ, Plugge CM, Strik DPBTB, Grootscholten TIM, Buisman CJN, Hamelers HVM, Chain Elongation with Reactor Microbiomes: Open-Culture Biotechnology To Produce Biochemicals, *Environ Sci Technol* **2016**; 50 (6), 2796–2810; DOI:10.1021/acs.est.5b04847

Angenent LT, Rosenbaum MA, Microbial electrocatalysis to guide biofuel and biochemical bioprocessing, *Biofuels*, **2013**; 4(2):131–134; DOI:10.4155/bfs.12.93

Anton JE, Llobet-Brossa E, Rodriguez-Valera F, Amann R, Fluorescence in situ hybridization analysis of the prokaryotic community inhabiting crystallizer ponds, *Environ Microbiol* **1999**; 1:517-523

Antony A, Chilcott T, Coster H, Leslie G, In situ structural and functional characterization of reverse osmosis membranes using electrical impedance spectroscopy; *J. Mem Sci* **2013**; 425–426, 89–97; DOI:10.1016/j.memsci.2012.09.028

APHA, Standard Methods for the Examination of Water and Wastewater, American Public Health Association, Washington DC, USA. **2005**

Arnold S, Becker T, Delgado A, Emde F, Enenkel A, Optimizing high strength acetic acid bioprocess by cognitive methods in an unsteady state cultivation, *J. Biotechnol* **2002**; 97:133–145

Awad HA, Diaz R, Malek RA, Othman NZ, Aziz RA, El Enshasy HA, Efficient Production Process for Food Grade Acetic Acid by Acetobacter aceti in Shake Flask and in Bioreactor Cultures, *E-Journal of Chemistry* **2012**; 9(4): 2275-2286; DOI:10.1155/2012/965432

Bard AJ, Faulkner LR. Electrochemical Methods: Fundamentals and Applications (2nd ed.), New York, Gänle MG, Follador R. Metabolism of Oligosaccharides and Starch in Lactobacilli: A Review. *Front Microbiol* **2012**; 3:340; DOI:10.3389/fmicb.2012.00340

Baker RW, *Ion Exchange Membrane Processes – Electrodialysis, in Membrane Technology and Applications*, Third Edition, John Wiley & Sons, Ltd.: Chichester, U.K., **2012**

Barker HA, Taha SM. Clostridium kluyverii, an Organism Concerned in the Formation of Caproic Acid from Ethyl Alcohol. *J Bacteriol* **1942**; 43(3):347-363

Bechtold I, Bretz K, Kabasci S, Kopitzky R, Springer A, Succinic Acid: A New Platform Chemical for Biobased Polymers from Renewable Resources, *Chem Eng Technol* **2008**; 31 (5): 647-654, DOI:10.1002/ceat.200800063

Becker J, Reinefeld J, Stellmacher R, Schäfer R, Lange A, Meyer H, Lalk M, Zelder O, Von Abendroth G, Schröder H, Haefner S, Wittmann C, Systems-wide analysis and engineering of metabolic pathway fluxes in bio-succinate producing Basfia succiniciproducens, *Biotechnol Bioeng* **2013**; 110: 3013–3023, DOI:10.1002/bit.24963

Berezina NP, Kononenko NA, Dyomina OA, Gnusin NP, Characterisation of ion-exchange membrane materials: Properties vs structure, *Adv. Colloid Interface Sci* **2008**; 139: 3–28, DOI:10.1016/j.cis.2008.01.002

Beijerink MW. Sur les ferments lactiques de l'industrie. Arch Neerl Sci **1901**; II(7): 212–243

BiofuelsDigest, Advanced biofuels pioneer Terrabon files for chapter 7 bankruptcy: One-off or trend? by Jim Lane; **2012** http://www.biofuelsdigest.com/bdigest/2012/09/10/advanced-biofuels-pioneer-terrabon-files-for-chapter-7-bankruptcy-one-off-or-trend/ (Accessed 10th June 2016)

Blundell RK, Licence P, Quaternary ammonium and phosphonium based ionic liquids: a comparison of common anions, *Phys Chem Chem Phys* **2014**; 16 (29): 15278-88, DOI:10.1039/c4cp01901f

Bibliography

Brisk Insights, Renewable Chemical Manufacturing Market By Materials (Corn, Sugarcane, Sugar Beet, Wheat, Cassava, Vegetable Oils, Coconut, Palm Oil, & Palm Kernel Oil), By Product Type (Bio-Based Chemicals, Platform Chemicals, Biopolymers), By Application, Industry Size, Growth, Share And Forecast To 2022, **2016;** http://www.briskinsights.com/report/renewable-chemical-manufacturing-market (Accessed 11th June 2016)

Brodeur G, Yau E, Badal K, Collier J, Ramachandran KB, Ramakrishnan S, Chemical and Physicochemical Pretreatment of Lignocellulosic Biomass: A Review, *Enzyme Res* **2011**; Article ID 787532. DOI: 10.4061/2011/787532

Caldwell JM, Juvonen R, Brown J, Breidt F. Pectinatus sottacetonis sp. nov., isolated from a commercial pickle spoilage tank, *Int J Syst Evol Microbiol* **2013**; 63:3609–3616; DOI:10.1099/ijs.0.047886-0

Cantoni C, Molnar MR, Investigations on the Glycerol Metabolism of Lactobacilli, *J Appl Microbiol* **1967**, 30(1):197-205, DOI:10.1111/j.1365-2672.1967.tb00289.x

Castresana J, Selection of conserved blocks from multiple alignments for their use in phylogenetic analysis. *Mol Biol Evol* **2000**; 17: 540-552

Cen J, Vukas M, Barton G, Kavanagh J, Coster HGL, Real time fouling monitoring with electrical impedance spectroscopy, *J Mem Sci* **2015,** 484: 133–139 DOI:10.1016/j.memsci.2015.03.014

Chaturvedi V, Verma P, An overview of key pretreatment processes employed for bioconversion of lignocellulosic biomass into biofuels and value added products, *3 Biotech*. **2013**; 3(5): 415–431 DOI:10.1007/s13205-013-0167-8

Chevenet F, Brun C, Bañuls A-L, Jacq B, Christen R, TreeDyn: towards dynamic graphics and annotations for analyses of trees, *BMC Bioinformatics* **2006**; 7: 439

Choi K, Jeon BS, Oh MK, Sang BI. In situ biphasic extractive fermentation for hexanoic acid production from sucrose by Megasphaera elsdenii NCIMB 702410. *Appl Biochem Biotechnol* **2013**; 171(5):1094-107; DOI:10.1007/s12010-013-0310-3

Coster HGL, Chilcott TC, Coster ACF, Impedance spectroscopy of interfaces, membranes and ultrastructures, *Bioelectrochem Bioenerg* **1996**, 40 (2): 79-98

Coma M, Vilchez-Vargas R, Roume H, Jauregui R, Pieper DH, Rabaey K, Product Diversity Linked to Substrate Usage in Chain Elongation by Mixed-Culture Fermentation, *Environ Sci Technol* **2016**, (Article ASAP) DOI:10.1021/acs.est.5b06021

Clarke WP, Xie S, Patel M, Rapid digestion of shredded MSW by sequentially flooding and draining small landfill cells, *Waste Manag* **2015**, 15, 30232-4, DOI:10.1016/j.wasman.2015.11.050

Cleenwerck I, Vandemeulebroecke D, Janssens D, Swings J, Re-examination of the genus Acetobacter, with descriptions of Acetobacter cerevisiae sp. nov. and Acetobacter malorum sp. nov. *Int J Syst Evol Microbiol* **2002**, 52: 1551–1558

Deloitte, Opportunities for the fermentation-based chemical industry: An analysis of the market potential and competitiveness of North-West Europe, **2014**; http://www2.deloitte.com/global/en/pages/manufacturing/articles/opportunities-for-fermentation-based-chemical-industry.html; (Accessed 8th June 2015)

Desloover J, Woldeyohannis AA, Verstraete W, Boon N, Rabaey K, Electrochemical Resource Recovery from Digestate to Prevent Ammonia Toxicity during Anaerobic Digestion, *Environ Sci Technol* **2012**; 46 (21): 12209-12216; DOI:10.1021/es3028154

Demler M, Weuster-Botz D, Reaction Engineering Analysis of Hydrogenotrophic Production of Acetic Acid by Acetobacterium woodii, *Biotech Bioeng* **2010**; 108 (2): 470-474; DOI 10.1002/bit.22935

Denis PG, Harnisch F, Yeoh YK, Tyson GW, Rabaey K. Dynamics of Cathode-Associated Microbial Communities and Metabolite Profiles in a Glycerol-Fed Bioelectrochemical System, *Appl Environ Microbiol* **2013**; 79 (13): 4008-4014; DOI:10.1128/AEM.00569-13

Dereeper A, Guignon V, Blanc G, Audic S, Buffet S, Chevenet F, Dufayard JF, Guindon S, Lefort V, Lescot M, Claverie JM, Gascuel O, Phylogeny. fr: robust phylogenetic analysis for the non-specialist, *Nucleic Acids Res* **2008**; 36: W465-W469

Devos O, Gabrielli C, Tribollet B, Simultaneous EIS and in situ microscope observation on a partially blocked electrode application to scale electrodeposition, *Electrochim Acta* **2006**; 51: 1413–1422

De Vrieze J, Saunders AM, He Y, Fang J, Nielsen PH, Verstraete W, Boon N, Ammonia and temperature determine potential clustering in the anaerobic digestion microbiome. *Water Res* **2015**; 75(0), 312-323; DOI:10.1016/j.watres.2015.02.025:

Disabb-Miller ML, Johnson ZD, Hickner MA, Ion Motion in Anion and Proton-Conducting Triblock Copolymers; *Macromol* **2013;** 46: 949–956; dx.DOI.org/10.1021/ma301947t

Długołecki P, Anet B, Metz SJ, Nijmeijer K, Wessling M, Transport limitations in ion exchange membranes at low salt concentrations, *J Membr Sci* **2010a** 346:163 – 171; DOI:10.1016/j.memsci.2009.09.033

Bibliography

Długołecki P, Ogonowski P, Metz SJ, Saakes M, Nijmeijer K, Wessling M, On the resistances of membrane, diffusion boundary layer and double layer in ion exchange membrane transport, *J. Membe Sci* **2010b,** 349, 369–379; DOI:10.1016/j.memsci.2009.11.069

Dohno R, Azumi T, Takashima S, Permeability of mono-carboxylate ions across an anion exchange membrane, *Desal* **1975**; 16 (1), 55-64

Dominguez-Benetton X, Sevda S, Vanbroekhoven K, Pant D, The accurate use of impedance analysis for the study of microbial electrochemical systems, *Chem Soc Rev* **2012**; 41 (21): 7228-46. DOI:10.1039/c2cs35026b

Edgar RC, Haas BJ, Clemente JC, Quince C, Knight R. UCHIME improves sensitivity and speed of chimera detection. *Bioinformatics* **2011**; 27(16): 2194–2200; DOI:10.1093/bioinformatics/btr381

Edwards J, Othman M, Burn S, A review of policy drivers and barriers for the use of anaerobic digestion in Europe, the United States and Australia, *Renew Sustainable Energy Rev* **2015**; 52: 815-828, DOI:10.1016/j.rser.2015.07.112

Eflingenir A, Fievet P, Déon S, Salut R, Characterization of the isolated active layer of a NF membrane by electrochemical impedance spectroscopy, *J Membr Sci* **2015**; 477, 172–182 DOI:10.1016/j.memsci.2014.12.044

eHighway2050, Europe's future secure and sustainable electricity infrastructure, **2015**; http://www.e-highway2050.eu/fileadmin/documents/e_highway2050_booklet.pdf (Accessed 11th June 2016)

EIA (U.S. Energy Information Administration), International Energy Outlook, **2016**; http://www.eia.gov/forecasts/ieo/ (Accessed 9th June 2016)

European Commission, Horizon 2020: On to second-generation bioethanol, **2015**; https://ec.europa.eu/programmes/horizon2020/en/news/second-generation-bioethanol (Accessed: 9th June 2016)

European Parliament, EU biofuels policy: dealing with indirect land use change, **2015,** http://www.europarl.europa.eu/RegData/etudes/BRIE/2015/545726/EPRS_BRI(2015)545726_REV1_EN.pdf (Accessed: 9th June 2016)

Fabbri E, Habereder A, Waltar K, Kötz R, Schmidt TJ, Developments and perspectives of oxide-based catalysts for the oxygen evolution reaction, *Catal Sci Technol* **2014**; 4: 3800-3821 DOI:10.1039/C4CY00669K

Fava F, Totaro G, Diels L, Reis M, Duarte J, Carioca OB, Poggio-Varaldo HM, Ferreira BS. Biowaste biorefinery in Europe: opportunities and research & development needs, *Biotechnol* **2015**; 32(1): 100-108; DOI:10.1016/j.nbt.2013.11.003

Gänle MG, Follador R. Metabolism of Oligosaccharides and Starch in Lactobacilli: A Review, *Front Microbiol* **2012**; 3: 340; DOI:10.3389/fmicb.2012.00340

Gao Y, Li W, Lay WCL, Coster HGL, Fane AG, Tang CY, Characterization of forward osmosis membranes by electrochemical impedance spectroscopy; *Desal* **2013**; 312: 45–51; DOI:10.1016/j.desal.2012.03.006

Gao Z, Zhao H, Li Z, Tan X, Lu X, Photosynthetic production of ethanol from carbon dioxide in genetically engineered cyanobacteria, *Energy Environ Sci* **2012**; 5: 9857-9865

Gavrilescu M, Chisti Y, Biotechnology – a sustainable alternative for chemical industry. *Biotech Adv* **2005**, 23:471–499; DOI:10.1016/j.biotechadv.2005.03.004

Ge S, Usack JG, Spirito CM, Angenent LT, Long-Term n-Caproic Acid Production from Yeast-Fermentation Beer in an Anaerobic Bioreactor with Continuous Product Extraction, *Environ Sci Technol* **2015**; 49(13): 8012–8021, DOI:10.1021/acs.est.5b00238

Gerbrandt K, Chu PL, Simmonds A, Mullins KA, MacLean HL, Griffin WM, Saville BA, Life cycle assessment of lignocellulosic ethanol: a review of key factors and methods affecting calculated GHG emissions and energy use, *Curr Op Biotechnol* **2016**; 38: 63–70 DOI:10.1016/j.copbio.2015.12.021

Gildemyn S, Verbeeck K, Slabbinck R, Andersen SJ, Prevotéau A, Rabaey K. Integrated production, extraction and concentration of acetic acid from CO_2 through microbial electrosynthesis. *Environ Sci Technol Lett* **2015**; 2 (11): 325–328; DOI:10.1021/acs.estlett.5b00212

Gohil GS, Trivedi GS, Rangarajan R, Nagarale RK, Thampy SK, Shahi VK, Studies on transport properties of short chain aliphatic carboxylic acids in electrodialytic separation, *Desalination* **2004**, 171,195-204

Grand Vuew Research, Acetic Acid Market By Application (VAM, Acetic Anhydride, Acetate Esters, PTA) Is Expected To Reach USD 13.31 Billion By 2022, **2015**, https://www.grandviewresearch.com/press-release/global-acetic-acid-market-analysis (Accessed 11th June 2016)

Grootscholten TIM, Steinbusch KJJ, Hamelers HVM, Buisman CJN, Chain elongation of acetate and ethanol in an upflow anaerobic filter for high rate MCFA production, *Bioresour Technol* **2013a**; 135:440-5; DOI:10.1016/j.biortech.2012.10.165

Bibliography

Grootscholten TIM, Steinbusch KJJ, Hamelers HVM, Buisman CJN. High rate heptanoate production from propionate and ethanol using chain elongation. *Bioresour Technol* **2013b**; 136:715-718; DOI:10.1016/j.biortech.2013.02.085

Guettler MV, Jain MK, Rumler D, Method for making succinic acid, bacterial variants for use in the process and methods for obtaining variants, **1996**, US Patent 5,573,931.

Guindon S, Dufayard J-F, Lefort V, Anisimova M, Hordijk W, Gascuel O, New algorithms and methods to estimate maximum-likelihood phylogenies: assessing the performance of PhyML 3.0. *Syst Biol* **2010**; 59: 307-321.780

Heaviside O, The Electrician, p. 212, **1886** (reprinted as Electrical Papers, p64, AMS Bookstore, ISBN 0821834657)

Hino T, Shimada K, Maruyama T, Substrate preference in a strain of Megasphaera elsdenii, a ruminal bacterium, and its implications in propionate production and growth competition, *Appl Environ Microbiol* **1994**; 60(6): 1827-1831

Hirschorn B, Orazem ME, Tribollet B, Vivier V, Frateur I, Musiani M, Constant-Phase-Element Behavior Caused by Resistivity Distributions in Films, *J Electrochem Soc* **2010**; 157: C458-C463

Hirschorn B, Orazem ME, Tribollet B, Vivier V, Frateur I, Musiani M, Determination of effective capacitance and film thickness from constant-phase-element parameters, *Electrochim. Acta*. **2010** 55, 6218–6227

Holtzapple MT, Granda CB, Carboxylate Platform: The MixAlco Process Part 1: Comparison of Three Biomass Conversion Platforms, *Appl Biochem Biotechnol* **2009**, 156: 525–536; DOI:10.1007/s12010-008-8466-y

Huang HJ, Ramaswamy S, Tschirner UW, Ramarao BV, A review of separation technologies in current and future biorefineries, *Sep Purif Technol,* **2008**; 62 (1): 1-21

Huddleston JG, Visser AE, Reichert WR, Willauer HD, Broker GA, Rogers RD, Characterization and comparison of hydrophilic and hydrophobic room temperature ionic liquids incorporating the imidazolium cation, *Green Chem* **2001;** 3: 156–164

ICIS, European chloralkali output hit as growth slows, Ukraine volumes drop; Chemicals & The Economy with Paul Hodges, **2014** http://www.icis.com/blogs/chemicals-and-the-economy/2014/08/european-chloralkali-output-hit-growth-slows-ukraine-volumes-drop/ (Accessed 11th June 2016)

Izak P, Mateus NMM, Afonso CAM, Crespo JG, Enhanced esterification conversion in a room temperature ionic liquid by integrated water removal with pervaporation, *Sep Pur Tech* **2005**; 41 (2), 141 – 145

Jeon BS, Kim BC, Um Y, Sang BI, Production of hexanoic acid from D-galactitol by a newly isolated Clostridium sp. BS-1, *Appl Microbiol Biotechnol* **2010**; 88:1161–1167, DOI:10.1007/s00253-010-2827-5

Jorcin J, Orazem ME, Nadine P, Tribollet B, CPE analysis by local electrochemical impedance spectroscopy, *Electrochim Acta* **2006**; 51: 1473–1479

Jönsson LJ, Alriksson B, Nilvebrant NO, Bioconversion of lignocellulose: inhibitors and detoxification, *Biotechnol Biofuels* **2013**; 6: 16, DOI: 10.1186/1754-6834-6-16

Joyce, B.L; Stewart Jr, C.N; Designing the perfect plant feedstock for biofuel production: Using the whole buffalo to diversify fuels and products, *Biotechnol. Adv.* **2012**, 30 (5), 1011-1022

Jumas-Bilak E, Hélene JP, Carlier JP, Teyssier C, Bernard K, Gay B, Calpos J, Morio F, Marchandin H, Dialister micraerophilus sp. nov. and Dialister propionicifaciens sp. nov., isolated from human clinical samples; *Int J Syst Evol Microbiol* **2005**; 55: 2471-2478; DOI 10.1099/ijs.0.63715-0

Kerner M, Plylahan N, Scheers J, Johansson P, Ionic liquid based lithium battery electrolytes: fundamental benefits of utilising both TFSI and FSI anions?, *Phys Chem Chem Phys* **2015**, 17: 19569-19581; DOI:10.1039/c5cp01891a

Kennelly, A. *Impedance*. IEEE, **1893**

Kim BC, Seung Jeon B, Kim S, Kim H, Um Y, Sang BI, Caproiciproducens galactitolivorans gen. nov., sp. nov., a bacterium capable of producing caproic acid from galactitol, isolated from a wastewater treatment plant, *Int J Syst Evol Microbiol* **2015**; 65(12): 4902-8; DOI:10.1099/ijsem.0.000665

Kim DH, Park HS, Seo SJ, Park JS, Moon SH, Choi YW, Jiong YS, Kim DH, Kang MS, Facile surface modification of anion-exchange membranes for improvement of diffusion dialysis performance, *J Colloid Interface Sci* **2014**; 416: 19-24; DOI:10.1016/j.jcis.2013.10.013

Kim S, Dale BE, Global potential bioethanol production from wasted crops and crop residues*, Biom Bioenerg* **2004**; 26(4): 361–375; DOI:10.1016/j.biombioe.2003.08.002

Kim Y, Mosier NS, Hendrickson R, Ezeji T, Blaschek H, Dien B, Cotta M, Dale B, Ladisch MR, Composition of corn dry-grind ethanol by-products: DDGS, wet cake and thin stillage. *Biores Technol* **2008**; 99: 5165-5176; DOI:10.1016/j.biortech.2007.09.028

Kolbe H, Untersuchungen über die Elektrolyse organischer Verbindungen, *Justus Liebigs Ann Chem* **1849**; 69: 257–294, DOI:10.1002/jlac.18490690302

Kracke F, Krömer JO, Identifying target processes for microbial electrosynthesis by elementary mode analysis, *BMC Bioinformatics* **2014**; 15(1): 410; DOI:10.1186/s12859-014-0410-2

Kucek LA, Nguyen M, Angenent LT, Conversion of L-lactate into n-caproate by a continuously fed reactor microbiome, *Water Res* **2016;** 93: 163-71; DOI:10.1016/j.watres.2016.02.018

Kurzrock T, Weuster-Botz D, Recovery of succinic acid from fermentation broth, *Biotechnol Lett* **2010**; 32 (3): 331-339

Kwak R, Guan G, Peng WK, Han J, Microscale electrodialysis: Concentration profiling and vortex visualisation; *Desalination* **2013**, 308, 138 – 146; DOI:10.1016/j.desal.2012.07.017

Lagi M, Bar-Yam Y, Bertrand KZ, Bar-Yam Y, Accurate market price formation model with both supply-demand and trend-following for global food prices providing policy recommendations, *Proc Natl Acad Sci USA* **2015**, 112(45): E6119–E6128.

Lai IK, Liu YC, Yu CC, Lee MJ, Huang HP, Production of high-purity ethyl acetate using reactive distillation, *Chem Eng Process* **2008**; 47: 1831-1843

Latif H, Zeidan AA, Nielsen AT, Zengler K, Trash to treasure: production of biofuels and commodity chemicals via syngas fermenting microorganisms, *Cur Op Biotech* **2014**, 27 (0): 79-87; DOI:10.1016/j.copbio.2013.12.001

Lee SY, Mabee MS, Jangaard NO, Pectinatus, a new genus of the family Bacteroidaceae. *Int J Syst Bacteriol* **1978**; 28: 582–594

Li Y, He D, Niu D, Zhao Y, Acetic acid production from food wastes using yeast and acetic acid bacteria micro-aerobic fermentation, *Bioprocess Biosyst Eng* **2015**; 38(5): 863-9, DOI:10.1007/s00449-014-1329-8

Lindemann SR, Bernstein HC, Song HS, Fredrickson JK, Fields MW, Shou W, Johnson DR, Beliaev AS, Engineering microbial consortia for controllable outputs, *The ISME Journal* **2016** (advance online publication); DOI:10.1038/ismej.2016.26

Liu Y, Lotero E, Goodwin Jr JG, Effect of carbon chain length on esterification of carboxylic acids with methanol using acid catalysis, *J Mol Catal A Chem* **2006**; 243 (2): 132-140

Liu K, Rosentrater KA, Distillers grains: production, properties and utilization, CRC Press, **2012;** Boca Raton, FL

Logan BE, Rabaey K, Conversion of Wastes into Bioelectricity and Chemicals by Using Microbial Electrochemical Technologies, *Science* **2012**; 337:(6095): 686-690, DOI: 10.1126/science.1217412

López-Garzón CS, Straathof AJJ, Recovery of carboxylic acids produced by fermentation. *Biotech Adv* **2014**; 32(5): 873–904; DOI:10.1016/j.biotechadv.2014.04.002

Lopetuso LR, Scaldaferri F, Petito V, Gasbarrini A, Commensal Clostridia: leading players in the maintenance of gut homeostasis, *Gut Pathog*. **2013**; 5 (1): 23; DOI:10.1186/1757-4749-5-23

Lovley D, Nevin KP, Electrobiocommodities: powering microbial production of fuels and commodity chemicals from carbon dioxide with electricity, *Curr Op Biotech* **2013**, 24 (3): 1-6; DOI:10.1016/j.copbio.2013.02.012

Lupitskyy R, Staff C, Satyavolu J, Towards integrated biorefinery from dried distillers grains: Evaluation of feed application for Co-products, *Biom Bioenerg* **2015**; 72: 251-255; DOI:10.1016/j.biombioe.2014.10.029

Lyko H, Deerberg G, Weidner E, Coupled production in biorefineries - Combined use of biomass as a source of energy, fuels and materials, *J Biotechnol* **2009**, 142 (1), 78-86; DOI:10.1016/j.jbiotec.2009.03.016.

Macdonald DD, Reflections on the history of electrochemical impedance spectroscopy, *Electrochim Acta* **2006**, 51: 1376–1388; DOI:10.1016/j.electacta.2005.02.107

Martak J, Schlosser S, Extraction of lactic acid by phosphonium ionic liquids, *Sep Purif Technol* **2007**, 57, 483–494; DOI:10.1016/j.seppur.2006.09.013

Market Reasearch Store, Global Medium-chain Triglycerides Market Set for Rapid Growth, To Reach Around USD 1,250 Million By 2020, **2016**; http://www.marketresearchstore.com/news/global-medium-chain-triglycerides-market-155 (Accessed 11th June 2016)

Matsumoto M, Mochiduki K, Fukunishi K, Kondo K, Extraction of organic acids using imidazolium-based ionic liquids and their toxicity to Lactobacillus rhamnosus, *Sep Purif Technol* **2004**; 40: 97–101; DOI:10.1016/j.seppur.2004.01.009

Maurya DP, Singla A, Negi S, An overview of key pretreatment processes for biological conversion of lignocellulosic biomass to bioethanol, *3 Biotech* **2015**; 5(5): 597–609. DOI: 10.1007/s13205-015-0279-4

Mikhaylin S, Bazinet L, Fouling on ion-exchange membranes: Classification, characterization and strategies of prevention and control, *Adv Colloid Interface Sci* **2016**; 229: 34–56 DOI:10.1016/j.cis.2015.12.006

McFarlane J, Ridenour WB, Luo H, Hunt RD, DeOaoli DW, Ren RX, Room temperature ionic liquids for separating organics from produced water. *Sep Sci Technol* **2005**, 40, 1245 – 1265 DOI:10.1081/SS-200052807

Mikkola SK, Lokajova RA, Holding AJ, Lämmerhofer M, Kilpeläinen I, Holopainen JM, King AW, Wiedmer SK, Impact of amphiphilic biomass-dissolving ionic liquids on biological cells and liposomes, *Environ Sci Technol* **2015**, 49, 1870-1878; DOI:10.1021/es505725g

Mollah MYA, Morkovsky P, Gomes JAG, Kezmez M, Parga J, Cocke DL, Fundamentals, present and future perspectives of electrocoagulation. *J Hazard Mater B* **2004**; 114: 199–210; DOI:10.1016/j.jhazmat.2004.08.009

Moore LVH, Moore WEC, Oribaculum catoniae gen. nov., sp. nov.; Catonella morbi gen. nov., sp. nov.; Hallella seregens gen. nov., sp. nov.; Johnsonella ignava gen. nov., sp. nov.; and Dialister pneumosintes gen. nov., comb. nov., nom. rev., Anaerobic Gram-Negative Bacilli from the Human Gingival Crevice. *Int J Syst Evol Microbiol* **1994**; 44: 187-192, DOI:10.1099/00207713-44-2-187

Moya AA, Study of the electrochemical impedance and the linearity of the current–voltage relationship in inhomogeneous ion-exchange membranes, *Electrochim Acta* **2010**; 55: 2087–2092 DOI:10.1016/j.electacta.2009.11.038

Moya AA, Electrochemical impedance of ion-exchange membranes in asymmetric arrangements; Journal of Electroanalytical Chemistry **2011**, 660, 153–162 DOI:10.1016/j.jelechem.2011.06.025

Moya AA, Sistat P, Chronoamperometric response of ion-exchange membrane systems, *J Membr Sci* **2013**; 444: 412–419; DOI:10.1016/j.memsci.2013.05.059

Moya AA, Electrochemical Impedance of Ion-Exchange Membranes in Ternary Solutions with Two Counterions, *J Phys Chem C* **2014**; 118: 2539–2553; DOI:10.1021/jp4108238

Moya AA, Theory of the formation of the electric double layer at the ion exchange membrane–solution interface *Phys Chem Chem Phys* **2015**; 17: 5207; DOI:10.1039/c4cp05702c

Naje AS, Abbas SA, Electrocoagulation Technology in Wastewater Treatment: A Review of Methods and Applications, *Civil and Environmental Research* **2013;** 3(11), 29-42

Neves CMSS, Granjo JFO, Freire MG, Robertson A, Oliveira NMC, Coutinho JAP, Separation of ethanol–water mixtures by liquid–liquid extraction using phosphonium-based ionic liquids, *Green Chem* **2011**; 13: 1517; DOI:10.1039/C1GC15079K

Newman J, Thomas-Alyea KE, Electrochemical Systems 3rd Edition, **2004**, John Wiley & Sons, Inc., Hoboken, NJ, USA.

Nikonenko V, Zabolotsky V, Larchet C, Auclair B, Pourcelly G, Mathematical description of ion transport in membrane systems, *Desalination* **2002**; 147: 369-374; DOI:10.1016/S0011-9164(02)00611-2

Nikonenko VV, Kozmai AE, Electrical equivalent circuit of an ion-exchange membrane system, *Electrochim Acta* **2011,** 56: 1262–1269; DOI:10.1016/j.electacta.2010.10.094

Nilges P, dos Santos TR, Harnisch F, Schröder U, Electrochemistry for biofuel generation: Electrochemical conversion of levulinic acid to octane, *Energy Environ Sci* **2012**; 5: 5231-5235; DOI:10.1039/C1EE02685B

OECD, Biobased chemicals and plastics. Finding the right policy balance. OECD Science, Technology and Industry Policy Papers No. 17. **2014**; OECD Publishing, Paris, France

Oksanen J, Blanchet FG, Kindt R, Legendre P, Minchin PR, O'Hara RB, Simpson GL, Solymos P, Henry M, Stevens M, Wagner H, vegan: Community Ecology Package. R package version 23-0. **2015**

Oliveira FS, Araújo JMM, Ferreira R, Rebelo LPN, Marrucho IM, Extraction of I-Iactic, I-malic, and succinic acids using phosphonium-based ionic liquids, *Sep Purif Technol* **2012;** 85: 137 – 146; DOI:10.1016/j.seppur.2011.10.002

Orazem ME, Tribollet B, Electrochemical Impedance Spectroscopy, **2008**, John Wiley & Sons, Inc., Hoboken, NJ, USA. doi: 10.1002/9780470381588

Owe LE, Characterisation of Iridium Oxides for Acidic Water Electrolysis (Thesis), **2011**, Norwegian University of Science and Technology, Trondheilm, Norway

Palmqvist E, Grage H, Meinander NQ, Hahn-Hägerdal B, Main and interaction effects of acetic acid, furfual, and p-hydroxybenzoic acid on growth and ethanol productivity of yeasts, *Biotechnol Bioeng* **1999**; 63(1): 46 – 55

Palmqvist E, Hahn-Hägerdal B, Fermentation of lignocellulosic hydrolysates. I: inhibition and detoxification, *Biores Technol* **2000** 74: 17 – 24

Park J, Jung Y, Kusumah P, Le J, Kwon K, Lee CK, Application of Ionic Liquids in Hydrometallurgy, *Int J Mol Sci* **2014**; 15(9): 15320-15343; DOI:10.3390/ijms150915320

Percival Zhang YH, What is vital (and not vital) to advance economically-competitive biofuels production, *Process Biochem* **2011**; 46(11): 2091-2110; DOI:10.1016/j.procbio.2011.08.005

Philp J; Balancing the bioeconomy: supporting biofuels and bio-based materials in public policy *Energ Environ Sci* **2015**, 8, 3063-3068 DOI:10.1039/C5EE01864A

Plechkova NV and Seddon KR., Applications of ionic liquids in the chemical industry, *Chem Soc Rev* **2008**; 37: 123-150; DOI:10.1039/B006677J

Poole CF, Poole, SK, Extraction of organic compounds with room temperature ionic liquids, *J Chromatog A* **2010**; 1217 (16), 2268-2286; DOI:10.1016/j.chroma.2009.09.011

Pratt S, Liew D, Batstone DJ, Werker AG, Morgan-Sagastume F, Lant PA, Inhibition by fatty acids during fermentation of pre-treated waste activated sludge, *J Biotechnol* **2012**; 159 (1-2): 38-43; DOI: 10.1016/j.jbiotec.2012.02.001

Rabaey K, Ronzendal RA. Microbial electrosynthesis – revisiting the electrical route for microbial production. *Nat Rev Microbiol* **2010**; 8:706-716; DOI:10.1038/nrmicro2422

Raguskas AJ, Beckham GT, Biddy MJ, Chandra R, Chen F, Davis MF, Davison BH, Dixon RA, Gilna P, Keller M, Langan P, Naskar AK, Saddler JN, Tshaplinski TJ, Tuskan GA, Wyman CE, Ligin Valorization: Improving Lignin Processing in the Biorefinery, *Science* **2014**; 344: 1246843, DOI:10.1126/science.1246843

Ramaswamy S, Huang HJ, Ramarao BV. Separation and Purification Technologies in Biorefineries. Hoboken, New Jerssey: John Wiley & Sons **2013**; DOI:10.1002/9781118493441

Ratti R, Ionic Liquids: Synthesis and Applications in Catalysis, **2014**, *Advances in Chemistry*, Article ID 729842, DOI:10.1155/2014/729842

Rogosa M, Transfer of Peptostreptococcus elsdenii Gutierrez et al. to a new genus, Megasphaera [M. elsdenii (Gutierrez et al.) comb. nov.]. *Int J Syst Bacteriol* **1971,** 21:187–189

Roume H, Muller EEL, Cordes T, Renaut J, Hiller K, Wilmes P, A biomolecular isolation framework for eco-systems biology. *ISME J* **2013**, 7: 110-121; DOI: 10.1038/ismej.2012.72

Royce LA, Liu P, Stebbins MJ, Hanson BC, Jarboe LR, The damaging effects of short chain fatty acids on Escherichia coli membranes, *Appl Microbiol Biotechnol* **2013**; 97: 8317–8327; DOI:10.1007/s00253-013-5113-5

Rubinstein I, Zaltzman B, Extended space charge in concentration polarization; *Adv Colloid Interface Sci* **2010,** 159, 117–129; DOI:10.1016/j.cis.2010.06.001

Santaella MA, Orjuela A, Narváez PC, Comparison of different reactive distillation schemes for ethyl acetate production using sustainability indicators, *Chem Eng Process* **2015**; 96: 1-13; DOI:10.1016/j.cep.2015.07.027

Sauer M, Porro D, Mattanovich D, Branduardi P, Microbial production of organic acids: expanding the markets, *Trends Biotechnol*, **2008** 26 (2), 100-108

Saxena A, Gohil GS, Shahi VK, Electrochemical Membrane Reactor: Single-Step Separation and Ion Substitution for the Recovery of Lactic Acid from Lactate Salts, *Ind Eng Chem Res* **2007**, 46, 1270-1276; DOI: 10.1021/ie060423v

Schloss PD, Westcott SL, Ryabin T, Hall JR, Hartmann M, Hollister EB, Lesniewski RA, Oakley BB, Parks DH, Robinson CJ, Sahl JW, Stres B, Thallinger GG, Van Horn DJ, Weber CF. Introducing mothur: Open-Source, Platform-Independent, Community-Supported Software for Describing and Comparing Microbial Communities. *Appl Environ Microbiol* **2009**; 75(23):7537–7541; DOI:10.1128/AEM.01541-09

Seerdorf H, Fricke WF, Veith B, Brüggemann H, Liesegang H, Strittmatter A, Miethke M, Buckel W, Hinderberger J, Li F, Hagemeier C, Thauer RK, Gottschalk G, The genome of Clostridium kluyveri, a strict anaerobe with unique metabolic features, *PNAS* **2007**; 105 (6), 2128–2133, DOI:10.1073/pnas.0711093105

Sgorbati B, Biavati B, Palenzona D. The genus Bifidobacterium. The Genera of Lactic Acid Bacteria; The Lactic Acid Bacteria Volume 2, pp 279-306. Springer US, **1995**; DOI:10.1007/978-1-4615-5817-0_8

Shafaat HS, Rüdiger O, Ogata H, Lubitz W. [NiFe] hydrogenases: A common active site for hydrogen metabolism under diverse conditions. *BBA-Bioenergetics* **2013**; 1827 (8-9): 986-1002; DOI:10.1016/j.bbabio.2013.01.015

Shah HN, Collins DM, Prevotella, a New Genus To Include Bacteroides melaninogenicus and Related Species Formerly Classified in the Genus Bacteroides, *Int J Syst Bacteriol* **1990**; 40(2):205-208

Siegert I, Banks C, The effect of volatile fatty acid additions on the anaerobic digestion of cellulose and glucose in batch reactors, *Process Biochem* **2005,** 40 (11): 3412-3418; DOI:10.1016/j.procbio.2005.01.025

Sikora A, Zielenkiewicz U, Blaszczyk M, Jurkowki M, Lactic Acid Bacteria in Hydrogen-Producing Consortia: On Purpose or by Coincidence?, Lactic Acid Bacteria - R & D for Food, Health and Livestock Purposes, Dr. J. Marcelino Kongo (Ed.), InTech, **2013** DOI:10.5772/50364

Sistat P, Kozmai A, ïsmenskaya N, Larchet C, Pourcelly G, Nikonenko V, Low-frequency impedance of an ion-exchange membrane system; *Electrochimica Acta* **2008**, 53, 6380–6390; DOI:10.1016/j.electacta.2008.04.041

Sluiter A, Hames B, Ruiz R, Scarlata C, Sluiter J, Templeton D; Determination of Sugars, Byproducts, and Degradation Products in Liquid Fraction Process Samples: Laboratory Analytical Procedure **2006**; National Renewable Energy Laboratory; U.S. Department of Energy; NREL/TP-510-42623

Spirito CM, Richter H, Rabaey K, Stams AJM, Angenent LT, Chain elongation in anaerobic reactor microbiomes to recover resources from waste, *Curr Opin Biotechnol* **2014**; 27:115-122; DOI:10.1016/j.copbio.2014.01.003

Steinbusch KJJ, Hamelers HVM, Buisman CJN. Alcohol production through volatile fatty acids reduction with hydrogen as electron donor by mixed cultures, *Water Res* **2008**; 42 (15): 4059-4066, DOI:10.1016/j.watres.2008.05.032

Steinbusch KJJ, Hamelers HVM, Plugge CM, Buisman CJN. Biological formation of caproate and caprylate from acetate: fuel and chemical production from low grade biomass. *Energ Environ Sci* **2011**; 4 (1): 216-224; DOI:10.1039/C0EE00282H

Stewardson AJ, Gaïa N, François P, Malhotra-Kumar S, Delémont C, Martinez de Tejada B, Schrenzel J, Harbarth S, Lazarevic V, SATURN WP1 and WP3 Study Groups. Collateral damage from oral ciprofloxacin versus nitrofurantoin in outpatients with urinary tract infections: a culture-free analysis of gut microbiota. *Clin Microbiol Infect* **2015**; 21(4):344.e1-344.e11; DOI:10.1016/j.cmi.2014.11.016.

Stojanovic AC, Morgenbesser D, Kogelnig R, Krachler R, Keppler BK, Quaternary Ammonium and Phosphonium Ionic Liquids in Chemical and Environmental Engineering; "Ionic Liquids: Theory, Properties, New Approaches (Ed. Kokorin, A)," **2011**, 657–681.

Strathmann H, Ion-Exchange Membrane Separation Processes, **2004**, Elsevier, The Netherlands

Strathmann H, Membranes and Membrane Separation Processes, Ullmann's Encylcopeadia of Industrial Chemistry, **2005,** Wiley Publishing, Germany

Swain T, Goldstein JL, Chapter 11 – The Quantitative Analysis of Phenolic Compounds. In: Methods in Polyphenol Chemistry, Proceedings of the Plant Phenolics Group Symposium, Oxford, **1964**

Taherzaden MJ, Karimi K, Pretreatment of Lignocellulosic Wastes to Improve Ethanol and Biogas Production: A Review, *Int J Mol Sci* **2008** 9(9): 1621–1651 DOI: 10.3390/ijms9091621

Tejirian A, Xu F, Inhibition of enzymatic cellulolysis by phenolic compounds, *Enzyme Microb Technol* **2011**, 48 (3): 239-47, DOI:10.1016/j.enzmictec.2010.11.004

Temudo MF, Muyzer G, Kleerbezem R, van Loosdrecht MC, Diversity of microbial communities in open mixed culture fermentations: impact of the pH and carbon source, *Appl Microbiol Biotechnol* **2008**; 80 (6), 1121-1130

Tenenbaum DJ, Food vs. Fuel: Diversion of Crops Could Cause More Hunger, *Environ Health Perspect* **2008**; 116(6): A254–A257

Tribollet B, Newman J, Smyrl WH, Determination of the Diffusion Coefficient from Impedance Data in the Low Frequency Range, *J Electrochem Soc*, **1988**; 135(1); DOI:10.1149/1.2095539

U.S. Geological Survey, Mineral Commodity Summaries, January 2016: Platinum-Group Metals, **2016**, http://minerals.usgs.gov/minerals/pubs/commodity/platinum/mcs-2016-plati.pdf (Accessed 5th October 2016)

Vasconcelosa SM, Pinheiro Santos AM, Moraes Rochac GJ, Souto-Maior AM, Diluted phosphoric acid pretreatment for production of fermentable sugars in a sugarcane-based biorefinery, *Biores Tech* **2013**; 135, 46–52; DOI:10.1016/j.biortech.2012.10.083

Van Eerten-Jansen MCAA, Ter Heijne A, Grootscholten TIM, Steinbusch KJJ, Sleutels THJA, Hamelers HVM, Buisman CJN. Bioelectrochemical poduction of caproate and caprylate from acetate by mixed cultures. *ACS Sustain. Chem. Engin.* **2013**; 1: 513–518

Vanwonterghem I, Jensen PD, Rabaey K, Tyson G. Temperature and solids retention time control microbial population dynamics and volatile fatty acid production in replicated anaerobic digesters, *Sci Rep* **2015**; 5: 8496; DOI:10.1038/srep08496

Velt A, Akhtar MK, Mizutani T, Jones PR. Constructing and testing the thermodynamic limits of synthetic NAD(P)H:H2 pathways, *Microb Biotechnol* **2008**;1(5):382–394; DOI:10.1111/j.1751-7915.2008.00033.

Wagemann, K. Herstellung von Grundchemikalien auf Basis nachwachsender Rohstoffe als Alternative zur Petrochemie? / Production of Basic Chemicals on the Basis of Renewable Resources as Alternative to Petrochemistry? *Chelie Ingenieur Technik*, **2014**; 86(12): 2115-2134; DOI:10.1002/cite.201400108

Wang Y, Naumann U, Wright ST, Warton DI, mvabund- an R package for model-based analysis of multivariate abundance data. *Methods in Ecology and Evolution* **2012** 3: 471-474

Weast RC, CRC handbook of chemistry and physics. 60th ed. CRC Press; **1979**, Boca Raton, FL, United States

Weimer PJ, Moen GN, Quantitative analysis of growth and volatile fatty acid production by the anaerobic ruminal bacterium Megasphaera elsdenii T81. *Appl Microbiol Biotechnol* **2013**; 97(9): 4075-81; DOI:10.1007/s00253-012-4645-4

Weimer PJ, Stevenson DM, Isolation, characterization, and quantification of Clostridium kluyveri from the bovine rumen, *Appl Microbiol Biotechnol.* **2012**; 4(2):461-6. DOI:10.1007/s00253-011-3751-z

Bibliography

Windholz M, The Merck Index. 9th ed. Merck & Co., **1976**; Rahway, NJ, United States

Xu J, Guzman JJ, Andersen SJ, Rabaey K, Angenent LT, In-line and selective phase separation of medium chain carboxylic acids using membrane electrolysis, *Chem Comm* **2015**; 51: 6847-6850; DOI:10.1039/C5CC01897H

Yang J, Hou X, Mir PS, McAllister TA, Anti-Escherichia coli O157:H7 activity of free fatty acids under varying pH. *Can J Microbiol* **2010**; 56(3): 263–267; DOI:10.1139/w09-127

Yang ST, Bioprocessing for Value-Added Products from Renewable Resources: New Technologies and Applications, **2011**; Elsevier BV, The Netherlands; DOI:10.1016/B978-044452114-9/50001-3

Zhang Y, Zhu Y, Zhu Y, Li Y, The importance of engineering physiological functionality into microbes, *Trends Biotechnol* **2009** 27 (12), 664-672; DOI: 10.1016/j.tibtech.2009.08.006

Zhou M, Chen J, Freguia S, Rabaey K, Keller J. Carbon and Electron Fluxes during the Electricity Driven 1,3-Propanediol Biosynthesis from Glycerol, *Environ Sci Technol* **2013**; 47: 11199–11205; DOI:10.1021/es402132r

Zhu X, Tao Y, Liang C, Li X, Zhang W, Zhou Y, Tank Y, Bo T. The synthesis of n-caproate from lactate: a new efficient process for medium-chain carboxylic acids production, *Sci Rep* **2015**; 5:14360; DOI:10.1038/srep14360

List of contributions

List of contributions

Stephen J Andersen, Tom Hennebel, Sylvia Gildemyn, Marta Coma, Joachim Desloover, Jan Berton, Junko Tsukamoto, Christian Stevens and Korneel Rabaey, Electrolytic Membrane Extraction Enables Production of Fine Chemicals from Biorefinery Sidestreams; *Environmental Science & Technology,* **2014**; 48 (12), pp 7135–7142; DOI: 10.1021/es500483w

SJA, TH, CS and KR designed the experiments and interpreted the results. SG, MC and JD designed and executed aspects of the experiments in the membrane electrolysis portion, while JB and JT designed and executed aspects of the experiments in the ionic liquid esterification portion. SJA and TH wrote the paper.

Stephen J Andersen, Pieter Candry, Thais Basadre, Way Cern Khor, Hugo Roume, Emma Hernandez Sanabria, Marta Coma and Korneel Rabaey, Electrolytic extraction drives volatile fatty acid chain elongation through lactic acid and replaces chemical pH control in thin stillage fermentation; *Biotechnology for Biofuels* **2015**, 8:221 DOI: 10.1186/s13068-015-0396-7

SJA designed the experiments, interpreted the results and wrote the paper. PC and TB executed the experiments. WCK contributed to stream analysis and data interpretation. HR and EHS contributed to microbial community analysis and interpretation. MC contributed to guidance of students and interpretation of results.

Stephen J Andersen, Jan Berton, Pieter Naert, Sylvia Gildemyn, Korneel Rabaey, Christian Stevens, Extraction and esterification of low-titre short chain volatile fatty acids from anaerobic fermentation with ionic liquids; *ChemSusChem*, 2016; 9 (16), pp 2059 – 2063; DOI: 10.1002/cssc.201600473

SJA, JB and PN contributed to the design of the experiments, interpreted the results and wrote the paper. SG contributed to the design of an experiment. KR and CS guided the work and contributed to data interpretation.

Stephen J Andersen, Korneel Rabaey and Xochitl Dominguez-Benetton, An Electrochemical Impedance Spectroscopy Characterization of the Membrane Electrolysis of Acetic Acid, (*Manuscript in preparation*).

SJA and XDB designed the experiments, interpreted the results and wrote the paper. KR contributed to the interpretation of the results.

Co-authorships

Andrea Schievano, Tommu Pepé Sciarria, Korolien Vanbroekhoven, Heleen De Wever, Sebastia Puig., **Stephen J. Andersen,** Korneel Rabaey, Deepak Pant, D. Electro-fermentation - Merging electrochemistry with fermentation in industrial applications. *Trends in Biotechnology*, **2016,** pii: S0167-7799(16)30026-9. DOI: 10.1016/j.tibtech.2016.04.007

SJA contributed to the text

Sylvia Gildemyn, Kristof Verbeeck, Rik Slabbinck, **Stephen J. Andersen**, Antonin Prévoteau and Korneel Rabaey, Integrated Production, Extraction, and Concentration of Acetic Acid from CO_2 through Microbial Electrosynthesis, *Environ. Sci. Technol. Lett.*, 2015, 2 (11), pp 325 – 328

SJA contributed to the experimental design and assisted in interpreting results

Jiajie Xu, Juan J.L. Guzman, **Stephen J. Andersen**, Korneel Rabaey and Largus T. Angenent, In-line and selective phase separation of medium-chain carboxylic acids using membrane electrolysis, *Chem. Commun.*, 2015, 51, 6847.

SJA contributed to the experimental design and assisted in interpreting results

Way Cern Khor, **Stephen J. Andersen**, Han Vervaeren, Korneel Rabaey, 2016 (*Manuscript in preparation*)

SJA contributed to the experimental design, assisted in interpreting results, and contributed to the text

Chrysanthi Pateraki, **Stephen J. Andersen**, et al.. (*Manuscript in preparation*)

SJA contributed to the experimental design and assisted in interpreting results

Curriculum Vitae

Stephen John Andersen, 20th July 1983; Brisbane, AUSTRALIA

Center of Microbial Ecology and Technology

Faculty of Bioscience Engineering, Department of Biochemical and microbial technology

Coupure Links 653 (A0.092), 9000 Ghent, BELGIUM

Education

PhD Candidate in Applied Biological Sciences

Centre of Microbial Ecology and Technology, Ghent University, BELGIUM, 2012 – present

VITO nv, BELGIUM, 2013 – present

Bachelor of Chemical Engineering (Hon. II)

University of Queensland, AUSTRALIA, 2006 – 2009

University of Illinois, Urbana-Champaign, UNITED STATES, 2008 (exchange program)

Bachelor of Science in the fields of Biochemistry and Neuroscience

University of Queensland, AUSTRALIA, 2001 – 2003

Professional experience

Project Engineer; IOF Adv. Capronzuur Project, Ghent University, BELGIUM 2015 – 2016

Project Engineer; Bilexys Pty Ltd, AUSTRALIA, 2010 – 2012

Roughneck & Drilling Assistant, Ensign Drilling, CANADA, June – August 2008

Laboratory Technician, Australian Red Cross Blood Service, AUSTRALIA, 2006 - 2007

Voluntary experience

B-FAST Water Purification System Team, BELGIUM, 2014 – present

Queensland State Emergency Services, AUSTRALIA, 2009 – 2011

Engineers Without Borders, University of Illinois, U.-C. Chapter, UNITED STATES, 2008

Engineers Without Borders, University of Qld Chapter, AUSTRALIA, 2007 – 2010

Refugee Claimants Support Center, Brisbane, AUSTRALIA, 2006 – 2007

A1 Publications

Stephen J Andersen, Jan Berton, Pieter Naert, Sylvia Gildemyn, Korneel Rabaey and Christian Stevens, Extraction and esterification of low-titre short chain volatile fatty acids from anaerobic fermentation with ionic liquids; *ChemSusCem,* **2016**, 9 (16), pp 2059 – 2063; DOI: 10.1002/cssc.201600473

Stephen J Andersen, Pieter Candry, Thais Basadre, Way Cern Khor, Hugo Roume, Emma Hernandez Sanabria, Marta Coma and Korneel Rabaey, Electrolytic extraction drives volatile fatty acid chain elongation through lactic acid and replaces chemical pH control in thin stillage fermentation; *Biotechnology for Biofuels* **2015**, 8:221 DOI: 10.1186/s13068-015-0396-7

Stephen J Andersen, Tom Hennebel, Sylvia Gildemyn, Marta Coma, Joachim Desloover, Jan Berton, Junko Tsukamoto, Christian Stevens and Korneel Rabaey, Electrolytic Membrane Extraction Enables Production of Fine Chemicals from Biorefinery Sidestreams; *Environmental Science & Technology,* **2014**; 48 (12), pp 7135–7142; DOI: 10.1021/es500483w

Stephen J Andersen, Ilje Pikaar, Stefano Freguia, Brian C Lovell, Korneel Rabaey and René Rozendal; A dynamically adaptive control system for bioanodes in serially stacked bioelectrochemical systems; *Environmental Science & Technology,* **2013**, 47 (10), pp 5488–5494; DOI: 10.1021/es400239k

Articles intended for publication

Stephen J Andersen, Vicky De Groof, Way Cern Khor, Hugo Roume, Ruben Props, Marta Coma and Korneel Rabaey, *Clostridium* Group IV species dominates and suppresses a mixed culture fermentation by mid-chain fatty acids production and tolerance; *Submitted*, **2016**

Stephen J Andersen, Korneel Rabaey and Xochitl Dominguez-Benetton, An Electrochemical Impedance Spectroscopy Characterization of the Membrane Electrolysis of Acetic Acid; *Submitted,* **2016**

Publications, as a co-author

Schievano, A., Sciarria, T.P., Vanbroekhoven, K., De Wever, H., Puig., S. **Andersen, S.J.,** Rabaey, K., Pant, D. Electro-fermentation - Merging electrochemistry with fermentation in industrial applications. *Trends in Biotechnology*, **2016,** In Press, DOI: 10.1016/j.tibtech.2016.04.007

Gildemyn, S., Verbeeck, K., Slabbinck, R., **Andersen, S.J.,** Prevotéau, A., Rabaey, K. Integrated production, extraction and concentration of acetic acid from CO2 through microbial electrosynthesis. *Environmental Science & Technology Letters*, **2015**, 2 (11), 325-328, DOI: 10.1021/acs.estlett.5b00212

Xu J, Guzman J.J., **Andersen, S.J.,** Rabaey K., and Angenent L.T. In-line and selective phase separation of medium chain carboxylic acids using membrane electrolysis. *Chemical Communications*, **2015**, 51, 6847-6850, DOI: 10.1039/C5CC01897H

Gildemyn, S., Luther, A., **Andersen, S.J.,** Desloover, J., Rabaey, K. Electrochemically and Bioelectrochemically Induced Ammonium Recovery. *Journal of Visualized Experiments*, **2015,** http://www.jove.com/video/52405/electrochemically-and-bioelectrochemically-induced-ammonium-recovery

Articles, as a co-author, intended for publication

Khor, W.C., **Andersen, S.J**., Vervaeren, H., Rabaey, K. (Untitled grass fermentation combined with Kolbe electrolysis study), **2016**

Pateraki, C., **Andersen, S.J**., et al. (Untitled succinic acid fermentation and membrane electrolysis study), **2016**

Patent Contributions

Contributor (5%); Electrochemical processes to separate products from biological conversions - US20150014169 A1

Conference Presentations

Stephen J Andersen, Pieter Candry, Marta Coma and Korneel Rabaey, Electro-Fermentation: Production and Recovery of Volatile Fatty Acids from Thin Stillage with Zero Chemical Input, *Oral Presentation,* 11th International Conference on Renewable Resources & Biorefineries, 3 - 5 June 2015, York, UK

Stephen J Andersen, Thais Basadre Castro, Marta Coma and Korneel Rabaey, Electro-fermentation: membrane electrolysis drives the rapid valorisation of biorefinery thin stillage, *Oral Presentation,* EU-ISMET 2014, 3 - 5 September 2014, Alcala, SPAIN

Stephen J Andersen, Tom Hennebel, Sylvia Gildemyn, Marta Coma, Joachim Desloover, Jan Berton, Junko Tsukamoto, Christian Stevens and Korneel Rabaey; Electrolytic Membrane Extraction Enables Fine Chemical Production From Biorefinery Sidestreams

Oral Presentation

1 - 11th IWA Leading Edge Technology Conference on Water and Wastewater Technology, 26 – 29 May 2014, Abu Dhabi, UNITED ARAB EMIRATES

2 - Francqui Symposium: Recent advances in microbial and enzymatic electrocatalysis, 22 November 2013, Ghent, BELGIUM

Poster Presentation

1 - 11th Intl. Con. on Renewable Resources & Biorefineries, 3 - 5 June 2015, York, UK

2 - EU-ISMET 2014*,* 3 - 5 September 2014, Alcala, SPAIN

Stephen J Andersen, Ilje Pikaar, Stefano Freguia, Brian C Lovell, Korneel Rabaey and René Rozendal; An effective control system for serially stacked bioelectrochemical systems, *Oral Presentation*, European International Society for Microbial Electrochemistry and Technology, 2012, Ghent, BELGIUM

Stephen J Andersen, René Rozendal and Korneel Rabaey; Continuous production of caustic soda from synthetic and real wastewater, *Oral Presentation*, 3rd International Microbial Fuel Cell Conference, 2011, Leeuwarden, THE NETHERLANDS

Conference presentations, as a collaborator

Vanoppen, M., Criel, E., **Andersen, S.J.**, Prévoteau, A., Verliefde, A.R.D. (2016) Assisted reverse electrodialysis: a novel technique to decrease reverse osmosis energy demand, AMTA/AWWA 2016 Membrane Technology Conference & Exposition, 1 - 4 February 2016, San Antonio, TX, USA.

Desloover, J., **Andersen, S.J.**, *Rabaey, K.* Improving Anaerobic Digestion with Electrochemistry, 14th World Congress on Anaerobic Digestion, 15 - 18 November 2015, Viña Del Ma, CHILE

Xu, J, Guzman, J.J., Spirito, C.M., **Andersen, S.J**., Rabaey, K., *Angenent, L.T.* Oil Production From Complex Substrates With Microbiomes At Ambient Temperatures And Pressures, 14th World Congress on Anaerobic Digestion, 15 November - 18 November, Viña Del Ma, CHILE

Gildemyn, S., Verbeeck, K., Slabbinck, R., **Andersen, S.J.,** Prevotéau, A., Rabaey, K. Integrated production, extraction and concentration of acetic acid from CO2 through microbial electrosynthesis, 5th International Meeting on Microbial Electrochemistry and Technologies, 1 - 4 October 2015, Arizona, UNITED STATES

Naert P., **Andersen S.J.**, Berton J., Rabaey K. and Stevens C.V.; Valorisation of volatile fatty acids by ionic liquid biphasic esterification, 1st IWA Resource Recovery Conference, 3 August - 2 September 2015, Ghent, BELGIUM

Gildemyn S., Slabbinck R., Prévoteau A., Verbeeck K., **Andersen S.J.,** and Rabaey K.; Integrated production, extraction and concentration of acetic acid from CO2 through microbial electroynthesis, 1st IWA Resource Recovery Conference, August 30th - September 2nd 2015, Ghent, BELGIUM

Coma M., **Andersen S.J.,** Candry P., Acosta N.K. and Rabaey K.; Potential for chemicals recovery from thin stillage, 1st IWA Resource Recovery Conference, August 30th - September 2nd 2015, Ghent, BELGIUM

Rabaey K., **Andersen S.J**., Coma, M; Combining mixed culture fermentation with electrochemistry for simultaneous production and extraction of carboxylates, Water Research Conference, January 11 – 15, 2015, Shenzhen, CHINA

Andersen S.J., Angenent L.T., *Rabaey K.* Electrolytic extraction of high value products from mixed microbial fermentation broth. IWA, 26-30 October 2014, Kathmandu, NEPAL

Xu J., Guzman J. J., **Andersen S.J**., Rabaey K., Angenent L. T. Continuous production of an oily stream of medium-chain carboxylic acids with a microbial electrochemical technology. North American regional meeting of the International Society for Microbial Electrochemistry and Technology (NA-ISMET meeting), May 13-15 2014, Penn State University, University Park, PA., UNITED STATES

Gildemyn, S., Verbeeck, K., **Andersen, S.J**, Rabaey, K. Microbial electrosynthesis - electricity driven bioproduction and extraction. 2nd AP-ISMET International Society for Microbial Electrochemistry and Technology Meeting, July 21st-23rd 2014, SINGAPORE.

Rabaey K., Guo K., Dennis P., Gildemyn S., Tyson G., **Andersen S.J.** Operational and technical aspects for microbial electrosynthesis. Microbial Fuel Cells, 4th International Conference, September 1 - 4 2013, Cairns, Queensland, AUSTRALIA

Rabaey K., **Andersen S.J.,** Voulis N., Hennebel, T. Combined fermentation and extraction in a bioelectrochemical system. North American regional meeting of the International Society for Microbial Electrochemistry and Technology (NA-ISMET meeting), October 9-10 2012, Cornell University, Ithaca, NY, UNITED STATES

Acknowledgements

I'd like to acknowledge my father, this work is dedicated to him. Dr John Andersen taught me the importance of visualization to learn, to understand, and to communicate a concept. He was a radiologist, his work was in nuclear medicine, so visualization was his bread and butter. He said that his ability to draw and label a diagram of the human eye got him through medical school, and now my ability to draw and label an electrochemical cell has got me through an engineering PhD, just don't ask me to which terminal I'm supposed to hook up the anode and cathode on the power supply unless I've pen and paper. My father told me he would've done engineering if he was smarter, but he was smart, he worked hard and he was good to the people around him. I hope I lived up to his example. And so I acknowledge my father, and pieces of scrap paper, white boards, black boards, other people's lab note books, the skin on the back of my hand, dirty surfaces and, to a lesser extent, the blank slate that's rattling around in my mind's eye.

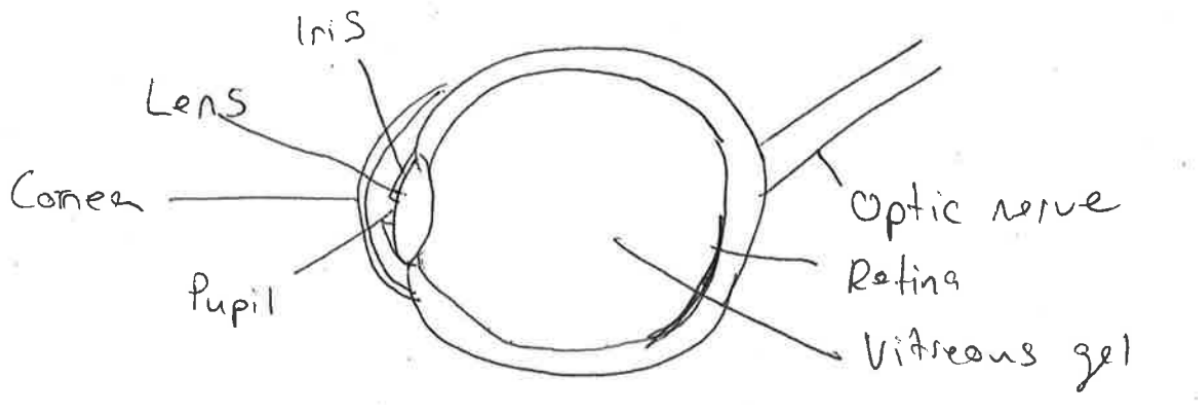

Figure A.1. Diagram of a human eye

I'd like to acknowledge online applications for engineering jobs, and I'd like to acknowledge their position somewhere between the eighth and ninth circles of hell. I had no interest in following an academic career, but these applications also made me realize that I had no interest in trading my sanity to a big engineering firm one tedious form at a time, whether they wanted me or not. At the end of 2009 after graduating from Chemical Engineering, I invested months and months in filling them out, before I gave up and thought I should try out some networking within my non-existent network. I went to a talk at UQ on "Bioenergy production using microbial fuel cell technologies" by Prof. Bruce Logan, my first exposure

to bio-electrochemical systems, and through that went on to work a little with Tom Seviour, a great scientist and top bloke, who inadvertently coaxed me into dipping my toes into research. Tom introduced me to Korneel Rabaey and René Rozendal, who then hired me and sent me down this research road, which I've walked with excitement and trepidation. I'd like to acknowledge Tom, YingYu Law and Ilje Pikaar, three excellent researchers that I met in this time who I'm lucky to count as friends. Tom, Ying and Ilje showed me how to simultaneously do good work and live a good life, which can be surprisingly complicated in science. I'd like to acknowledge Carol Kistler, Mark Howes and Richard Gilbert, three of the smartest people I've known from my formative science and engineering days. Each of them walked away from academic research for better things. I ask myself what would Tom, Ying, Ilje, Carol, Mark and Richard would do before I make any big decisions in life and science. I'd like to acknowledge these great minds and great friends. I'd like to acknowledge Korneel and René for giving me a chance and hiring me. I learned a lot simply by being present in meetings and listening to them argue and bicker with each other like brothers, and although I didn't realize it at the time, your future battles tend to go smoothly if you're accidentally following a couple of titans.

I'd like to acknowledge the Flemish. While I was studying in Illinois I met Jozefien, my first personal exposure to the Flemish. Jozefien warned me that her people were a little frigid, and hard to crack through into a close friendship. There might even be a scouts badge for that. As a foreignate in a foreign land, you come to know that everyone lives their own lives. Flanders is a small community of small communities, and sometimes frigidity and solidarity can overlap. I'd like to acknowledge Tom Hennebel and Joachim Desloover who brought me in from the cold, as if I was a little Flemish dog lost in the world for a few decades. Tom, who apparently is only ever referred to as Tom Hennebel as if he's a general leading a horde of elephants down the E17, invited me into his home and his often Italian, always exquisite dinner table. Tom trusted my scientific input before he probably should have, which makes an incredible difference early in the PhD. I'd like to acknowledge Joey and the full Desloover clan, and in particular the one night of Ename fest 2012 that lasted for three days. I'd like to acknowledge that I remember great people, great Enameans, and great stories about Joachim that I wish I didn't remember. I remember the indomitable Yvan and the Liefmans, a good name for a Viking rock band, and I remember a very affectionate retriever, Blanche, who thought she was pregnant, but was just well loved. Another Flemish stalwart

is Joeri Coppens, an escapee from the Final Destination franchise with a remarkably malleable accent that switches between Aalst, Bri'ish and Indonesian depending on who he's talking to, and a good friend from the start. It was a great pleasure to find someone such as myself who was happy to escalate an argument, scientific or otherwise, and will always listen to my advice and do the opposite (which has admittedly got him far). When you can't return to the devastating heat of the Australian Christmas, it's great to be warmly welcomed into the Coppenses for a dinner from a world-class chef and bemused glances from Poncho. Finally, I'd never gotten this far, personally and professionally, without Sylvia Gildemyn, who has always been a close friend and confidant, and has provided a much needed counter-weight to my chaotic approach to science and life. I'd like to acknowledge that it's not always easy to be a foreignate in Flanders, but with my typical Andersen good fortune, I've been lucky to have the pleasure to get to know the people and meet the families of many of my friends and colleagues in Lab-/CMET.

The change from Lab to C doesn't fully encompass the differences between LabMET 2012 and CMET 2016, and thus I'd like to acknowledge the arrow of time. When I first arrived, I was the only foreignate in the Rotonde. All I would hear was "Echt? Ja maar ja, flemish flemish flemish flemish 't Huis flemish, flemish flemish," plus some other things best not transcribed in acknowledgements, thanks very much Willem. The 'Old Rotonde' was a great place to work alongside some truly excellent minds, Haydee is particularly memorable, and some equally excellent characters, like the devious, deadpan De Corte. Back then when all I would hear was Flemish, I started to understand a little, but I do wish that I'd been recording some of the conversations because I was never able to figure out why everyone would explode in laughter when Joachim would incoherently mumble out a joke. Since then the Rotonde has lost a wall, tripled in size and embraced the more international research body. Whereas in the past you'd mostly be limited to the frustrated Flemish exclamations of Coppens, Desloover, De Muynck, et al, now you can hear more multilingual catharsis, French, Greek, maybe some Mandarin if you are lucky, but to honest most likely Italian. I'd like to acknowledge that CMET has done something wonderful by now having a majority female and majority international research staff, and I hope in time that the Belgian boys-club of Professors starts to reflect the people that drive their success. While much changes, somethings stay the same, and I'd like to acknowledge Christine Graveel and Regine Haspelagh, and the early learned lesson that the shortest distance from A to B is via

Christine and Regine. They've both long been keystones in the lab, and their warmth and support in the lab sets the tone for the rest of us. The secretariat and the technical staff are amongst the hardest working people in the lab, and I very much appreciate all the support they have given me in my time here. You'll notice that 'Image by Tim Lacoere' appears around ten times in this thesis, and you could just as easily put 'Labwork held together by Jana De Bodt,' or 'Blood, sweat and tears care of Mike Taghon' after each methods section. I hope I wasn't too much of a problem, and if I was, I hope you take revenge lightly.

I'd like to acknowledge my sanity, and by extension some more of the friends and colleagues that have kept that fire burning. I'd like to acknowledge alphabetically arranging lists by first names, because that is very convenient. Alberto Scoma is an exercise in predictable unpredictability which always keeps conversations entertaining and illuminating, except if you make the mistake of talking about basketball. Antonin Prevoteau technically goes here, even though he could also be filed under S. I've said it once and I'll say it again, Soupy is the strongest scientist in CMET and makes great duck. Baharak Hosseinkhani, my Persian sister, helped bring me into the international Gent life, and I'm still sorry about killing her fish. Cristina Cagnetta somehow transformed from a terrified science squirrel into a vicious research lion, heaven protect any of the goats that get in her way. Ekin Dalak was my conduit into the Boeretang Kingdom, and a great friend. Emma Hernandez-Sanabria was responsible for the majority of my refined sugar intake over the last four years, and was always a pleasure when I needed to bring my microbiology knowledge into focus. Giovannai Ganendra is an infinite source of relaxation and stability, and I'll still see Gio even when ASIO stops paying me to spy on him. Hugo Roume is a character that escaped from a work of literary fiction, and one day I will figure out how he managed to do that. Marta Coma is a thoughtful scientist and a patient teacher, and her example changed the way I work with my students. Nina Murvandize, ნინა, შენთან გატარებული დრო ძალიან სასიამოვნო იყო. ველოდები კიდევ ერთხელ როდის დავლევ ღვინოს, ჯინს, ტონიკს და შევჭამ ხაჭაპურს შენთან ერთად. ასევე, ნებისმიერ დროს ვუპასუხებ ყველა იმ შეკითხვას რომელიც გაინტერესებს. Pieter Candry and Pieter Naert are annoyed that I lumped them together, but I'm just starting to get to know them. They taught me that sometimes when you have excellent scientists as your students, you should do your best to power them up then get out of their way. I'd like to acknowledge that as much as I'd like to I can't thank everyone who has had an input, such as Amanda Luther,

Ackowmedgements

Eleni Vaiopoulou, the indestructible Jan B.A. “Johnny Eagles” Arends, Jo De Vrieze, Kun Guo, José M. Carvajal Arroyo, Ralph Lindeboom, Ramon Gangiué, Ruben Props, Way Cern Khor, et al., so please excuse me if I’ve not mentioned you and I’ll do my best to thank you personally. I wish I could’ve worked with more of you more often, it’s hard to cast a line around here without hooking a great scientist.

I’d like to thank my family for being happy and healthy, and I’d like to thank the matriarch Anna Andersen for helping me stay a part of the family while being absent, and being quick with a camera, whether to point at human, dog or the deep blue sky. Thanks to Peter and Kelly for making some adorable babies that tempt me back to Australia now and again, thanks to Meliss and Dave for being Europhilic, and thanks to Jane for missing missing me while we travelled through France. Think it was a good trip? Well it was. I’d like to acknowledge the few brave Australians that have ventured to the dark heart of Europe to visit me during my PhD, such as Pelham Vaughn, Callum Mahoney and Peter Binnington. Good on you all.

Korneel Rabaey and Xochitl Dominguez-Benetton, thank you for giving me this opportunity, and connecting me with other great scientists. Particular thanks to Chris Stevens and his team at SynBioC, with whom I worked with closely through the thesis. Thanks to the team at VITO who supported my time at Mol, it was a steep learning curve but a valuable one. I’d also like to thank Chrysanthi Pateraki and Apostolis Koutinas for inviting me to their lab at the Agricultural University of Athens, and I hope the collaboration we started can lead to plenty of fermentations and extractions.

These years have been an incredible learning experience, and I’m looking forward to putting the skills I’ve learnt to good use, to working hard and trying to be good to the people around me.